Determination and use of scatter correction factors of megavoltage photon beams

Measurement and use of collimator and phantom scatter correction factors of arbitrarily shaped fields with a symmetrical collimator setting

NEDERLANDSE COMMISSIE VOOR STRALINGSDOSIMETRIE

Report 12 of the Netherlands Commission on Radiation Dosimetry

Netherlands Commission on Radiation Dosimetry

March 1998

Determination and use of scatter correction factors of megavoltage photon beams

Measurement and use of collimator and phantom scatter correction factors of arbitrarily shaped fields with a symmetrical collimator setting

NEDERLANDSE COMMISSIE VOOR STRALINGSDOSIMETRIE

Report 12 of the Netherlands Commission on Radiation Dosimetry

Authors:
J.J.M. van Gasteren
S. Heukelom
H.N. Jager
B.J. Mijnheer
R. van der Laarse
H.J. van Kleffens
J.L.M. Venselaar
C.F. Westermann

Netherlands Commission on Radiation Dosimetry

March 1998

Preface

The Nederlandse Commissie voor Stralingsdosimetrie (NCS, Netherlands Commission on Radiation Dosimetry) was officially established on 3 September 1982 with the aim of promoting the appropriate use of dosimetry of ionizing radiation both for scientific research and practical applications. The NCS is chaired by a board of scientists, installed upon the suggestion of the supporting societies, including the Nederlandse Vereniging voor Radiotherapie en Oncologie (Netherlands Society for Radiotherapy and Oncology), the Nederlandse Vereniging voor Klinische Fysica (Netherlands Society for Clinical Physics), the Nederlandse Vereniging voor Radiobiologie (Netherlands Society for Radiobiology), the Nederlandse Vereniging voor Stralingshygiëne (Netherlands Society for Radiological Protection), the Nederlandse Vereniging van Radiologisch Laboranten (Netherlands Society of Radiographers and Radiological Technologists), and the Ministry of Health, Welfare and Sports.
To pursue its aims, the NCS accomplishes the following tasks: participation in dosimetry standardisation and promotion of dosimetry intercomparisons, drafting of dosimetry protocols, collection and evaluation of physical data related to dosimetry. Furthermore, the commission shall maintain or establish links with national and international organisations concerned with ionizing radiation and promulgate information on new developments in the field of radiation dosimetry.

Current members of the board of the NCS:

J.J. Broerse, chairman
W. de Vries, secretary
J. Zoetelief, treasurer
A.J.J. Bos
W.C.A.M. Buijs
R.B. Keus
J.L.M. Venselaar
F.W. Wittkämper
D. Zweers

Determination and use of scatter correction factors of megavoltage photon beams

Measurement and use of collimator and phantom scatter correction factors of arbitrarily shaped fields with a symmetrical collimator setting

Prepared by the Task Group on Dose Calculations for External Beam Radiotherapy of the Netherlands Society on Radiation Dosimetry (NCS).

Members of the Task Group:

J.J.M. van Gasteren
S. Heukelom
H.N. Jager
B.J. Mijnheer
R. van der Laarse
H.J. van Kleffens
J.L.M. Venselaar
C.F. Westermann

For further copies of this report see last page.

Contents

0.1 Abstract

For each radiation treatment machine, the dose per monitor unit must be known at a reference point in a water-phantom under reference conditions. It varies with field size, due to: (1) changes in radiation scattered from the head of the treatment machine to the reference point and into the monitor chamber and (2) changes in the radiation scattered from the irradiated part of the phantom to the reference point. The field size dependence is usually described by the *total scatter correction factor*, S_{cp}. If the field size defined by the collimator setting at the reference source-surface distance (SSD) does not correspond with the field size at the phantom surface, S_{cp} must be separated into two factors, the head or *collimator scatter correction factor*, S_c, and the *phantom scatter correction factor*, S_p. This is the case when a source-surface distance different from the SSD of the reference condition is used, when tissue is missing in the beam, or when shielding blocks are applied. The factor S_c describes the influence of the setting of the collimator on the total scatter correction factor; S_p describes the influence of the field size at the phantom surface, and thus of the irradiated volume on this correction factor.

In this report, recommendations are given for the measurement of S_{cp}, S_c and S_p in a photon beam at a reference depth of 10 cm. The *reference field* is defined as the open field, with a collimator setting yielding a 10 cm x 10 cm field when the SSD is set equal to the source-axis distance (SAD). For the determination of S_c, the use of a narrow cylindrical beam-coaxial phantom (the mini-phantom) is recommended. In this way, measurements can be performed in small fields and the disturbance of contaminating electrons, reaching the point of interest from the head of the treatment machine, becomes negligible. Construction details of the mini-phantom are described.

Furthermore, a consistent set of relations is presented for the use of these factors in dose calculations for symmetrically collimated square, rectangular and arbitrarily shaped fields, at an arbitrary SSD. These include blocked and wedged fields. A procedure to use S_c and S_p data in the calculation of monitor units is presented. Relations are given to calculate the collimator and phantom scatter data for the reference situation from already available data, measured at a non-reference depth and at a non-reference SSD. The influence of asymmetric set-up of the collimating jaws or multi-leaf collimators on the scatter correction factors is, however, *not* yet considered.

S_{cp}, S_c and S_p data sets are presented in this report for different types of treatment machines and for a wide range of photon beams, with beam qualities ranging from ^{60}Co to 25 MV. S_p is shown to be a smooth function of the beam quality if the same reference depth of 10 cm and an SSD of 100 cm is chosen for all beam qualities. However, S_c is shown to depend on the design of the head of the linear accelerator.

0.2 List of symbols and abbreviations

CEE	collimator exchange effect
C_{fx}, C_{fy}	parameters used in an expression for determination of S_c of rectangular fields
C_x, C_y	parameters used in the decision criterion whether or not $S_{c,blocked}$ can be taken equal to $S_{c,open}$
d	depth in the phantom
d_m	*depth of maximum absorbed dose at the central axis of the beam
d_{ref}	*reference depth
D	absorbed dose
D_{cal}	absorbed dose per monitor unit at the depth of calibration of the treatment machine
D_{presc}	dose prescribed at the dose prescription point
D_{ref}	absorbed dose per monitor unit in the *reference irradiation set-up
f	source-surface distance (SSD)
f_{ref}	source-surface distance in the reference irradiation set-up
F	geometrical factor, correcting field size v_p with changing SSD
iso	(in superscripts) isocentric irradiation set-up
N	number of monitor units
PDD	*percentage depth dose
QI	*quality index
r	radius of circular field
r_{eq}	radius of equivalent circular field
R	reading of an electrometer connected to an ionization chamber
RDD	*relative depth dose
ref	*(in subscripts) reference irradiation set-up
RTF	*relative tray transmission factor
RWF	*relative wedge transmission factor
S_{cp}	*total scatter correction factor
S_c	*collimator scatter correction factor
S_p	*phantom scatter correction factor
SAD	source-axis distance
SDD	source-detector distance
SSD	source-surface distance (f)
T	distance from focus to additional shielding blocks
TF	*tray transmission factor
TF_{ref}	*reference tray transmission factor
TPD	tray-phantom distance
TPR	*tissue-phantom ratio
U_x, U_y	distance from focus to X or Y collimator jaw, respectively
v_{eq}	*equivalent field size
v_c	*collimator defined field size, at SAD
$v_{c,ref}$	*reference collimator defined field size, at SAD

v_p	*phantom field size defined at the phantom surface; used in this notation when source-surface distance is equal to SAD
$v_{p,f}$	*phantom field size defined at the phantom surface; used in this notation when source-surface distance is *not* equal to SAD
$v_{p,ref}$	*reference field size defined at the phantom surface, with source-surface distance equal to SAD
v(d)	field size defined at depth d in the phantom
WF	*wedge transmission factor
WF_{ref}	*reference wedge transmission factor
X	setting of X-collimator
Y	setting of Y-collimator
Ω	*solid angle, defined by the point of measurement and that part of the surface of the flattening filter that can be seen from that point

(*) See section 0.3 for a more complete definition.

0.3 Glossary of terms

In this section definitions are given of quantities used in this report as far as they are important for understanding or if they deviate in one or more respects from the definitions given in the 'Glossary of terms' of the British Journal of Radiology Supplement 17, pp 143-147 [8] and Supplement 25, pp 183-188 [9].

collimator scatter correction factor S_c
The collimator scatter correction factor S_c (also called the head scatter correction factor) is defined as the electrometer reading per monitor unit of an ionization chamber measured in a mini-phantom at the reference depth and the reference source-surface distance for a specified collimator defined field size v_c, normalized to unity for the reference field size $v_{c,ref}$: $S_c(v_c) = R(v_c) / R(v_{c,ref})$. This factor describes the relative energy fluence per monitor unit due to photons originating in the head of the treatment machine only.

collimator defined field size v_c
The field size v_c is determined by the adjustable collimator jaws in the head of the treatment machine. The setting of the jaws defines a field of size v_c at a distance from the source *equal to SAD*. In most clinical cases, v_c defines the solid angle Ω. In the text, often the term collimator setting is used for v_c.

depth of maximum dose d_m
The depth d_m of maximum absorbed dose is the depth along the beam axis at which maximum dose occurs. For a given beam quality this depth will vary with field size and source-surface distance. However, percentage depth doses for all field sizes are normalized to 100% at the *fixed depth* d_m of the 10 cm x 10 cm reference field size. The actual maximum depth dose for some field sizes may therefore slightly exceed 100%.

equivalent field v_{eq}
The equivalent field is defined as that square field which yields for a given physical quantity (e.g., phantom scatter correction factor at d_{ref}, or PDD), the same value as the field under consideration. Note that for quantities, which are primarily related to phantom scatter (e.g., S_p, PDD, TPR), the sizes of the equivalent fields may mutually differ from those which are primarily related to collimator scatter.

percentage depth dose PDD
The percentage depth dose is the absorbed dose per monitor unit at a given depth d at the central beam axis, normalized to 100% at a depth which is equal to d_m of the reference field size. $PDD(v_p) = 100\% \times D(v_p,d) / D(v_p,d_m)$.

phantom field size v_p

For a photon beam impinging perpendicularly on a flat phantom surface, the field size v_p is defined as the size of the field at the *surface* of the phantom with a source-surface distance equal to SAD. v_p is one of the variables that determine the phantom scatter dose contribution to the point of measurement. Furthermore, the presence of shielding blocks in the beam or missing tissue influences the actual field size v_p, and therefore the phantom scatter contribution. Whenever the source-surface distance f is *not* equal to SAD, the notation $v_{p,f}$ is used.

phantom field size $v_{p,f}$

The definition of the field size $v_{p,f}$ is the same as for v_p, but now the source-surface distance f differs from SAD.

phantom scatter correction factor S_p

The phantom scatter correction factor S_p is defined as the phantom scatter dose contribution for a specified collimator defined field size and a specified field size at the phantom surface, normalized to unity for the reference irradiation set-up. It is derived from the total scatter correction factor S_{cp}, divided by the collimator scatter correction factor S_c for the same collimator defined field size. The phantom scatter correction factor describes the influence of the scatter originating in the phantom only.

quality index QI

The quality index QI is defined as the ratio of the electrometer reading per monitor unit with the ionization chamber at a depth of 20 cm in a water phantom, R_{20}, to the reading at a depth of 10 cm, R_{10}, for a source-detector distance SDD equal to SAD and for a collimator setting v_c of 10 cm x 10 cm. It is used as an indicator of the photon beam quality:
$QI = R(v_{c,ref}, d = 20, SDD = SAD) / R(v_{c,ref}, d = 10, SDD = SAD)$.

reference collimator defined field size $v_{c,ref}$

The reference field size $v_{c,ref}$ is that field size defined by the collimator setting which yields a field of 10 cm x 10 cm at SAD.

reference depth d_{ref}

d_{ref} is the reference depth, taken in this report equal to 10 cm irrespective of the radiation beam quality. In this way, uniformity of algorithms and continuity of beam data acquisition are obtained. For all clinically used megavoltage photon beams, d_{ref} is beyond the range of contaminating electrons.

reference field size $v_{p,ref}$

The reference phantom field size $v_{p,ref}$ is the phantom field size in the reference irradiation set-up. $v_{p,ref}$ = 10 cm x 10 cm.

reference irradiation set-up; ref (in subscripts)
The reference irradiation set-up is defined as that irradiation geometry for which $d = d_{ref}$ (=10 cm), $v_p = v_{p,ref}$ (=10 cm x 10 cm) and $v_c = v_{c,ref}$ (=10 cm x 10 cm). As a consequence, $f = f_{ref}$ = SAD.

reference tray transmission factor TF_{ref}
The reference tray transmission factor TF_{ref} is the tray transmission factor, determined in the reference irradiation set-up. TF_{ref} can be measured in a full scatter phantom or in a mini-phantom.

reference wedge transmission factor WF_{ref}
The reference wedge transmission factor WF_{ref} is the wedge transmission factor, determined in the reference irradiation set-up. WF_{ref} should be measured in a full scatter phantom.

relative depth dose RDD
The relative depth dose is the absorbed dose per monitor unit for a given depth at the central beam axis, normalized to unity at the reference depth d_{ref}, $RDD(v_p,d,f) = D(v_p,d,f) / D(v_p,d_{ref},f)$.

relative tray transmission factor RTF
The relative tray transmission factor is the tray transmission factor, determined at the reference depth for a given field size and tray-phantom distance, relative to the tray transmission factor for the reference irradiation set-up: $RTF(v_c,TPD) = TF(v_c,TPD) / TF_{ref}$. The relative tray transmission factor describes the variation of the tray transmission factor with variations of field size and tray-phantom distance. RTF can be measured in a full scatter phantom or in a mini-phantom.

relative wedge transmission factor RWF
The relative wedge transmission factor is the wedge transmission factor, determined at the reference depth for a given field size and SSD, relative to the wedge transmission factor for the reference irradiation set-up: $RWF(v_c,f) = WF(v_c,f) / WF_{ref}$. The relative wedge transmission factor factor describes the variation of the wedge transmission factor with variations of field size and source-surface distance. RWF can be measured in a full scatter phantom as well as in a mini-phantom.

solid angle Ω
The solid angle Ω is the angle which is geometrically defined by the point of measurement in the phantom and the surface of the flattening filter as observed from that point. The solid angle determines the amount of photons which is scattered in the flattening filter of the treatment machine in the direction of that point of measurement.

tissue-phantom ratio TPR

The tissue-phantom ratio TPR at a point in a phantom irradiated by a photon beam is the total absorbed dose per monitor unit at that point, divided by the absorbed dose per monitor unit in the same point, but with the surface of the phantom moved in such a way that the point is at a specified reference depth.

total scatter correction factor S_{cp}

The total scatter correction factor is defined as the absorbed dose per monitor unit measured in a full scatter water phantom at the reference depth and the reference source-surface distance for a specified collimator defined field size v_c and a specified field size at the phantom surface v_p, normalized to unity for the reference irradiation set-up.

$S_{cp}(v_c,v_p) = S_{cp}(v_c,v_p,d_{ref},f_{ref}) = D(v_c,v_p,d_{ref},f_{ref}) / D(v_{c,ref},v_{p,ref},d_{ref},f_{ref})$.

The total scatter correction factor describes the influence on the dose of both the collimator setting and the phantom field size.

tray transmission factor TF

The tray transmission factor is the ratio of the dose per monitor unit at the reference depth in a given field *with* a tray, to the dose per monitor unit in the same field *without* a tray in the beam. For a given tray, this ratio is slightly dependent on the field size and on the distance from the tray to the phantom surface, TPD: $TF(v_c,v_p,d_{ref},TPD) = D_{tray}(v_c,v_p,d_{ref},TPD) / D_{open}(v_c,v_p,d_{ref},TPD)$.

wedge transmission factor WF

The wedge transmission factor is the ratio of the dose per monitor unit at the reference depth in a specified field *with* a wedge present in the beam, to the dose per monitor unit in the same field *without* a wedge. $WF(v_c,v_p,d_{ref},f) = D_{wedge}(v_c,v_p,d_{ref},f) / D_{open}(v_c,v_p,d_{ref},f)$. The wedge transmission factor is dependent on field size and SSD.

0.

1. Introduction

The determination of the dose delivered to a patient receiving radiotherapy consists of several steps, each one introducing uncertainties in the reported dose value. To obtain an optimal dose with respect to tumour control and damage to normal tissues, the overall uncertainty in the dose has to be small. A value of about 3.5% (1 SD) has been proposed by several authors [7,19,48]. This can not always be achieved in clinical practice [16]. However, each source of error in the dose delivery has to be minimized. The calculation of the dose at a specified point, or the determination of the number of monitor units necessary to deliver a given dose, is one of the sources of uncertainty, especially when non-square, blocked, wedged or asymmetric fields are involved or a source-surface distance different from the reference one is applied.

One of the essentials in preparing a radiation treatment is the transformation of the prescribed dose into the appropriate radiation units of the treatment machine. In the case of a linear accelerator, these radiation units are measured by a monitor, which has to be calibrated in a predefined standard set-up, described as the reference condition. The dose at a particular point in a water phantom in a non-reference treatment set-up will be different. Scatter correction factors that mathematically describe these differences are used to translate the prescribed dose into a number of monitor units. This report describes the determination and use of these scatter correction factors for megavoltage photon beams.

In general, the output of a linear accelerator is adjusted in such a way that 100 monitor units (MU) correspond to a dose delivery of 1 Gy at a calibration point in a water-phantom under reference irradiation conditions: usually a symmetrical open field of 10 cm x 10 cm, defined at the phantom surface and at an SSD equal to the source-axis distance. The calibration point is usually chosen on the central beam axis at the depth of maximum absorbed dose d_m in the 10 cm x 10 cm field.

Note: for ^{60}Co therapy machines the output is expressed in units of dose per unit of time, e.g. Gy.min^{-1} at the date of calibration for specified calibration conditions.

The ratio of Gy to MU or time units depends on several parameters such as field size, depth, and SSD. The magnitude of the change with field size can be taken into account in dose calculations by applying the *total scatter correction factor*, which is defined as the absorbed dose per monitor unit, measured at the reference depth and reference SSD for a specified collimator setting and a specified field size at the phantom surface, normalized to unity for the reference collimator setting and a reference field size at the phantom surface. If the

reference depth is taken equal to d_m, the total scatter correction factor is equal to what is commonly called the *field size correction factor* or *output factor* [8].

Recently, the influence of the geometry of the field size and the presence of blocks on the total scatter correction factor has been discussed by a number of authors [14,25,27,33-34,36-39,43-46,54,64]. It is generally agreed that the total scatter correction factor has to be separated into a *collimator* and a *phantom scatter correction factor* in order to improve the accuracy of dose calculations. These factors are related to the contributions of the collimator and phantom scatter to the output (in Gy/MU) of the treatment machine at a certain reference depth [1,25,34,45,51,54,64]. Several authors proposed a reference depth of 5 or 10 cm, depending on whether the quality index QI [17,47] of the photon beam is smaller or larger than 0.75 [1,64], because then these depths are beyond the range of contaminating electrons. These electrons, originating in the head of the treatment machine, can influence the dose to superficial tissues in a rather unpredictable way. At larger depths, the influence of these electrons on the scatter correction factors is negligible. These reference depth values correspond to the phantom depth for the calibration, as proposed in a number of dosimetry protocols [10,28,47]. Furthermore, a high accuracy of the absorbed dose at the reference depth of 5 or 10 cm is clinically more relevant than at depth d_m. However, the use of two different reference depths for different beam qualities leads to a discontinuity in the description of the behaviour of the scatter factors as a function of beam quality. This discontinuity is eliminated by using a single reference depth of 10 cm, irrespective of the photon beam quality.

Several methods to separately measure the phantom and collimator scatter components of the total scatter correction factor have been described [42,64]. This report adopts the use of a *narrow cylindrical beam-coaxial phantom* (mini-phantom) for the measurement of the collimator scatter contribution. In combination with measurements in a full scatter phantom, the phantom scatter contribution can be derived.

The determination of these scatter correction factors is time consuming, due to the large number of possible field sizes in combination with beam modifiers. Limitation of the number of measurements can be obtained by expressing the scatter correction factors as a function of a limited set of parameters such as treatment machine and beam quality. A further reduction can be obtained if interpolation algorithms are applied.

The aim of this report is to describe the separation of the total scatter correction factor into its component parts. A coherent system of expressions is presented for the use of these scatter factors in the calculation of monitor units in clinical situations. The report considers the use of shielding blocks and wedges in a symmetrical set-up of the collimating jaws. Field sizes are defined and used for beams directed perpendicularly to the surface. Oblique incidence and the use of asymmetric collimating jaws and multi-leaf collimator set-ups are not considered.

Measured data are presented for photon beam qualities ranging from ^{60}Co to 25 MV, for a large number of treatment machines. The reference depth is taken equal to 10 cm, irrespective of the quality index of the photon beam.

The report recommends performing measurements and the handling of beam data in such a way that the uncertainty in the calculation of the number of monitor units for clinical situations is considerably smaller than 3.5% (1 SD), preferably smaller than 1% (1 SD). Whenever possible, reference is made to interpolation algorithms with which a user can reduce the number of measurements necessary to obtain the required accuracy.

Section 2 of this report discusses the basic definitions and principles of this approach and the applicability of the methods to calculate the dose in megavoltage beams for square fields at arbitrary depths and SSDs. The influence of field elongation and the presence of a tray, blocks or wedges is discussed in section 3. Experimental methods and the results of a large number of measurements are given in sections 4 and 5, respectively. The recommendations are summarized in section 6. Additional information is presented in the Appendices.

In this report the definitions of beam parameters and the reference geometry are based on a beam set-up involving *a fixed SSD* technique, and not on *an SAD or isocentric* approach. In a water phantom, percentage depth dose data can be more easily measured than, for example, tissue-phantom ratio data, because the water level can be kept constant during the measurements. If TPR data are required for the calculations, the generally applied procedure is to perform PDD measurements and convert them into TPR data using conversion rules. Conversion rules have been published for this purpose [8,9]. Because the reference conditions are different for both approaches, care must be taken not to confuse the data. The definitions of the quantities and the relations between them in the fixed SSD (or PDD) approach and the isocentric (or TPR) approach are discussed in more detail in [71]. A brief summary is presented in Appendix 8.3. Whenever the quantities with definitions in the isocentric approach are used, the superscript ^{iso} is added.

The formalism presented in this report for the determination and use of scatter correction factors is similar to the procedure recommended in a recent ESTRO booklet "Monitor unit calculation for high energy photon beams" [18]. In that report, all the measurements and calculations needed for the determination of absorbed dose along the central axis per monitor unit are listed. Output factors are also defined at 10 cm depth and both the isocentric set-up and the fixed SSD approach are allowed. Consequently, the use of tissue-phantom ratios as well as relative depth doses are recommended and both formalisms are described. The ESTRO booklet gives an extensive description of the number of intermediate steps for the calculation of the number of monitor units for open beams, blocked beams, wedged beams, and beams at other distances than the

reference distance. Apart from differences in nomenclature, other differences with the ESTRO booklet are that in the present report no introduction is needed of a new quantity, the *volume scatter ratio*, and that in this report a wide variety of measured data is presented.

2. Collimator and phantom scatter correction factors for square fields

2.1 Definitions and principles

Principles of separation and measurement of scatter correction factors

In the concept adopted in this report, the dose at a certain point in an irradiated phantom is attributed to two different origins.

First, there is the energy fluence of primary, unscattered photons which originate from the target, and of photons scattered somewhere in the head of the treatment machine. For practical reasons, no attempt is made to separate contributions from the various components of the treatment head, such as the flattening filter and collimator parts. It is assumed that the variation of these components with field size can be described with the desired accuracy by using only one factor, the *collimator scatter correction factor*.

Second, there is a contribution to the dose from radiation which is scattered within the phantom. The influence of the field size at the phantom surface on this contribution is described by the *phantom scatter correction factor*.

Scatter correction factors are defined as ratios of dose values, relative to values for a specified reference irradiation condition. The reference situation should reflect a clinically relevant geometry within the phantom, be easily accessible for measurement, and be free of disturbing influences. The use of only one reference situation is recommended, irrespective of photon beam quality or machine type. In this way, uniformity and continuity in presenting data as a function of beam quality is obtained.

Total scatter correction factor S_{cp}

The *total scatter correction factor* $S_{cp}(v_c,v_p,d_{ref},f_{ref})$ is defined as the ratio of the absorbed dose per monitor unit measured at the reference depth d_{ref}, a reference source-surface distance f_{ref} for a specified collimator defined field size v_c and a specified field size at the phantom surface v_p, normalized to unity for the reference collimator setting and reference field size at the phantom surface. v_c sets the field size at the SAD and v_p the field size at the phantom surface. The reference values of the parameters $v_{c,ref}$ = 10 cm x 10 cm and $v_{p,ref}$ = 10 cm x 10 cm, can only be realized if the source-surface distance is equal to SAD (for most megavoltage units SAD is equal to 100 cm). If, in addition, the depth in the phantom is set equal to the reference depth, d_{ref}, the dose measurement set-up is referred to as the *reference irradiation set-up*. The dose, measured under reference conditions, is then $D_{ref} = D(v_{c,ref},v_{p,ref},d_{ref},f_{ref})$ and the total scatter correction factor S_{cp} can be written as:

$$S_{cp}(v_c,v_p,d_{ref},f_{ref}) = D(v_c,v_p,d_{ref},f_{ref}) / D_{ref} \qquad (2.1.1)$$

With respect to the choice of the reference depth it should be noted that at shallow depths the dose is influenced by electrons contaminating the photon beam, of which the contribution varies markedly with the setting of and the distance from the collimator. These electrons originate from the target, the flattening filter, and from the beam defining parts of the treatment head. When hitting the phantom, the electrons are totally absorbed in the first few centimeters. Therefore, contaminating electrons do not contribute to the dose at depths where most tumours are found in clinical practice. Furthermore, prediction of the contribution of contaminating electrons to the dose for a particular irradiation geometry is a complex matter. For these reasons, the reference depth should be chosen in such a way that the effect of the contaminating electrons is negligible.

Note, that the total scatter correction factor is strictly defined for a depth equal to the reference phantom depth and for an SSD equal to the SAD. This definition is more restrictive than the definitions given in earlier publications of this task group [64] and of others [25,34] (see Appendix 8.1). Furthermore, due to the restrictions of the reference conditions of the scatter correction factor, the parameters d_{ref} and f_{ref} in equation (2.1.1) are fixed and can therefore be removed from the notation of S_{cp} without misunderstanding.

The total scatter correction factor $S_{cp}(v_c,v_p)$ is now written as the product of two components: the collimator scatter correction factor $S_c(v_c,v_p)$ and the phantom scatter correction factor $S_p(v_c,v_p)$ [1,25,34,45,51,54,64]. In a general form:

$$S_{cp}(v_c,v_p) = S_c(v_c,v_p) \times S_p(v_c,v_p) \qquad (2.1.2)$$

Collimator scatter correction factor S_c

$S_c(v_c,v_p)$ reflects the change in the energy fluence in air per monitor unit of the scattered photons emitted from the head of the accelerator due to a varying opening of the collimator jaws, relative to the reference irradiation set-up [34,64]. Variation of the collimator setting results, on the one hand, in variable amounts of photons scattered to the point of measurement from the primary collimator, the flattening filter and, on the other hand, in variable amounts of radiation scattered backwards from the collimator jaws into the monitor chamber, situated in the head of the treatment machine [26,33,37-39,45]. The variable amount of scattered radiation reaching the point of measurement is for a large part related to the solid angle Ω, which is the angle geometrically defined by the point of measurement in the phantom and the surface of the flattening filter that can be seen from that point. It is the setting of the collimator jaws, given by v_c, which determines that surface. Thus, v_c is directly related to the solid angle Ω and partly determines the change in the energy fluence in air per

monitor unit. In case of extreme blocking of the field with blocks on a tray, certain parts of the flattening filter may be hidden and the solid angle Ω has to be used as a variable in the calculation procedures instead of v_c (see section 3 and Appendix 8.5).

Like the total scatter correction factor S_{cp}, the collimator scatter correction factor $S_c(v_c,v_p)$ is defined at the reference depth. Concerning the choice of the reference depth, note that the variation of the energy fluence in air per monitor unit is primarily determined by the volume of the primary collimator and the flattening filter within the solid angle Ω. The influence of the depth in the phantom on this volume is almost negligible [64]. S_c can, therefore, be considered to be independent of the choice of d_{ref} as long as d_{ref} is larger than the range of the contaminating electrons. For the same reason, the collimator scatter correction factor is hardly influenced by the choice of the SSD within the clinical useful range [64].

The primary energy fluence in air cannot be measured directly. However, it can be deduced relatively to the energy fluence under reference conditions by using a *mini-phantom*, as proposed by this task group (van Gasteren et al. [64]). In such a mini-phantom, the ionization chamber is placed in an upright position, at a depth of 10 cm. The collimator scatter correction factor S_c is then the ionization reading for the collimator defined field size v_c, normalized to unity for the reference field $v_{c,ref}$.

S_c is a machine related factor, which can be assumed to depend only on the collimator setting which is defined by the field size at SAD. Because S_c is independent of the choice of SSD and depth in the mini-phantom, as long as this depth is larger than the range of contaminating electrons, S_c can be written as a function of v_c only: $S_c(v_c)$.

Phantom scatter correction factor S_p

The phantom scatter correction factor S_p accounts for the contribution of the radiation scattered in the phantom material to the dose at the point at depth d_{ref} on the central axis, relative to the phantom scatter contribution in the reference irradiation set-up. The amount of scattered radiation reaching the point depends on the volume of the irradiated phantom material. Therefore, S_p is a phantom related factor with a dependence on the irradiated volume, which is accounted for by writing S_p as a function of the field size at the surface of the phantom. The increase of phantom scatter with depth makes S_p dependent on the choice of the reference depth. It is, however, important to note that S_p is defined only for one reference depth, d_{ref}, equal to the one chosen for S_{cp} and S_c. For this reason d_{ref} does not need to be given as a parameter of S_p.

Another important factor, influencing the amount of scattered radiation, is the quality of the photon beam, indicated by the quality index, QI. S_p varies with the nominal photon beam energy [64]. For a given beam, some changes in the

photon energy spectrum will occur, when for example beam modifiers such as wedges and heavy metal compensators are used in the field. This may influence to some extent the magnitude of S_p, but these effects are small, even for wedged photon beams [22]. In addition, it can be assumed that the influence of commonly applied blocking trays on the value of S_p can be neglected. Therefore, for a beam with a given QI, S_p will be written as a function of v_p only, that is: $S_p(v_c,v_p) = S_p(v_p)$.

Reference depth, d_{ref}

The reference depth d_{ref} is chosen to be 10 cm for all photon beam qualities addressed in this report, i.e. from ^{60}Co to 25 MV. As indicated previously, the use of a single reference depth ensures continuity of S_p as a function of beam quality. The depth of 10 cm is chosen to obtain the highest accuracy in the calculation of treatment times and monitor units at depths which are clinically most relevant. For the same reason, this reference depth is chosen in most dosimetry protocols to measure the output of treatment machines. Note that the influence of contaminating electrons in the beam on the dose at shallow depths is not ignored, but taken into account by the percentage depth dose or relative depth dose (PDD or RDD; see section 2.2 for the definition of RDD) values at these depths.

Summary

As a result of these considerations, the total scatter correction factor $S_{cp}(v_c,v_p)$ is given by:

$$S_{cp}(v_c,v_p) = S_c(v_c) \times S_p(v_p) \qquad (2.1.3)$$

S_{cp} and S_c data can be obtained by using the measurement method shown in figure 2.1. S_p can be obtained from equation (2.1.3). The measurement conditions are discussed in more detail in section 4 of this report.

In the following sections, the use of the scatter correction terms will be discussed for dose calculations at arbitrary depths and arbitrary SSDs. In most clinical cases, the situation will be more complex, because in addition to an arbitrary depth and SSD, customized blocks and other beam modifying devices are also used. However, it is important to keep in mind that the same methodology can still be applied: a separation of the influence of collimator and phantom related scatter to the dose at the reference point. Factors influencing the energy fluence from the head of the treatment machine to the phantom surface are taken into account by the collimator scatter correction factor S_c, which has to be measured using the mini-phantom as described in this report. For specific cases, individual measurements of S_c may be needed. Factors influencing the phantom volume irradiated by the beam are taken into account by the phantom scatter correction factor S_p. Because the variation of S_p with variations of the mean energy of megavoltage photon beams is slow [56], in

general no further measurements will be needed for the determination of S_p if beam modifying devices are applied.

Some guidelines for the use of the scatter correction factors in more complex cases will be given in section 3.

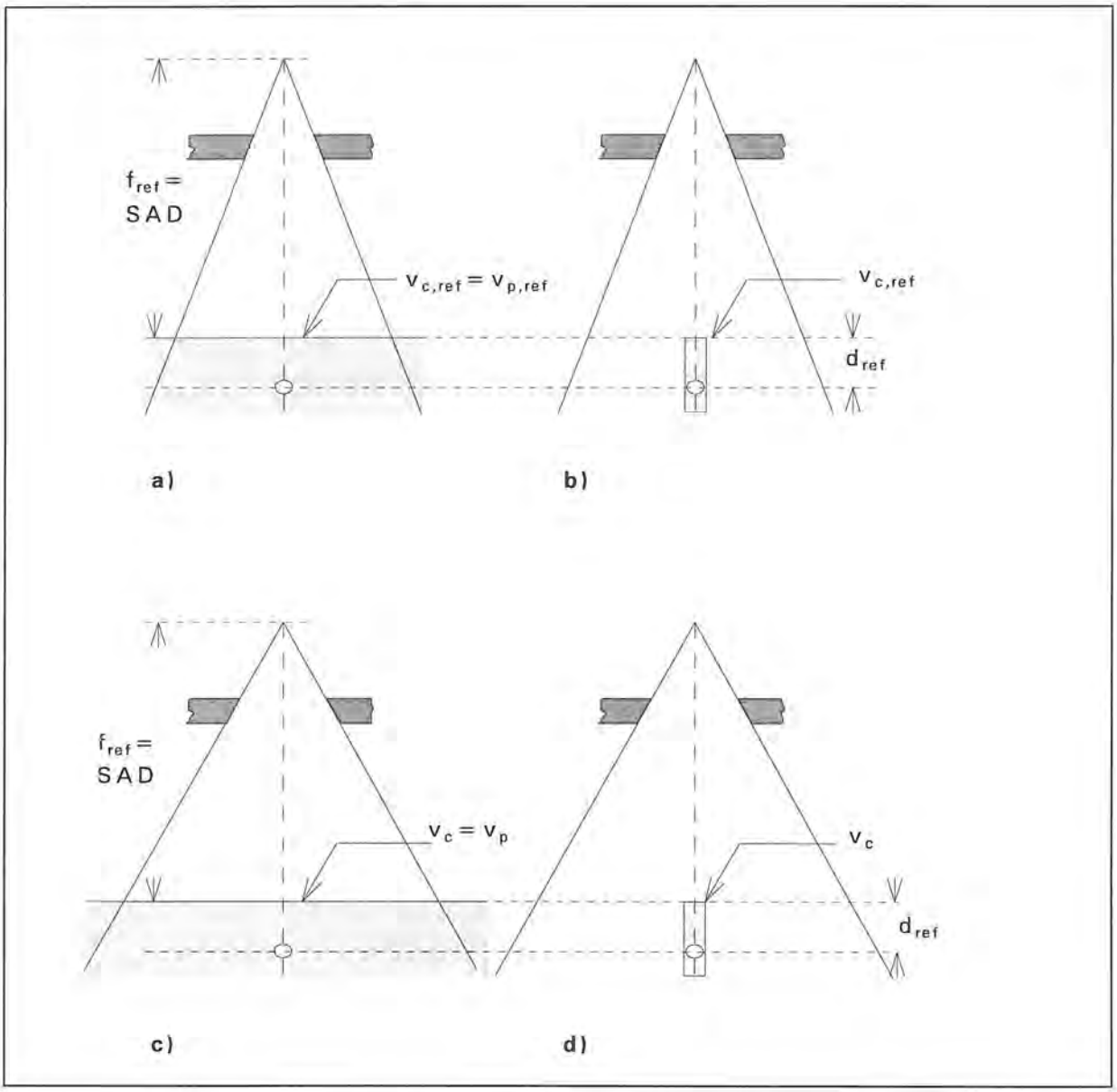

Figure 2.1 Measurement of the scatter correction factors S_{cp} (a, c) and S_c (b, d). S_{cp} and S_c data are derived directly from measurements relative to the reference irradiation set-up, using a full scatter water phantom and a mini-phantom, respectively. Phantom scatter data S_p are then obtained by dividing S_{cp} data by S_c data. SSD is taken equal to SAD ($=f_{ref}$, usually 100 cm); the depth of measurement d is taken equal to d_{ref} (= 10 cm).

2.2 Calibration and reference irradiation conditions

For calibration purposes, the treatment machine is set in such a way that $v_c = v_{c,ref}$ and $v_p = v_{p,ref}$ at source-surface distance f equal to SAD ($= f_{ref}$). Usually, the monitor chamber of the treatment unit is calibrated to deliver a dose D_{cal} per monitor unit (MU) of 1 cGy at the depth d_m of maximum absorbed dose on the central axis of the beam. This calibration setting is used throughout this report, although other calibration settings are possible.
We can then write (see figure 2.2):

$$D_{cal} = D(v_{c,ref}, v_{p,ref}, d_m, f_{ref}) = 1 \text{ cGy per monitor unit} \qquad (2.2.1)$$

Note: for ^{60}Co therapy machines the output is expressed in units of dose per unit of time, e.g., Gy.min^{-1} at the date of calibration. Consequently, the quantity D_{cal} should be expressed in corresponding units. For these types of therapy machines, this is implicitly assumed in the following sections.

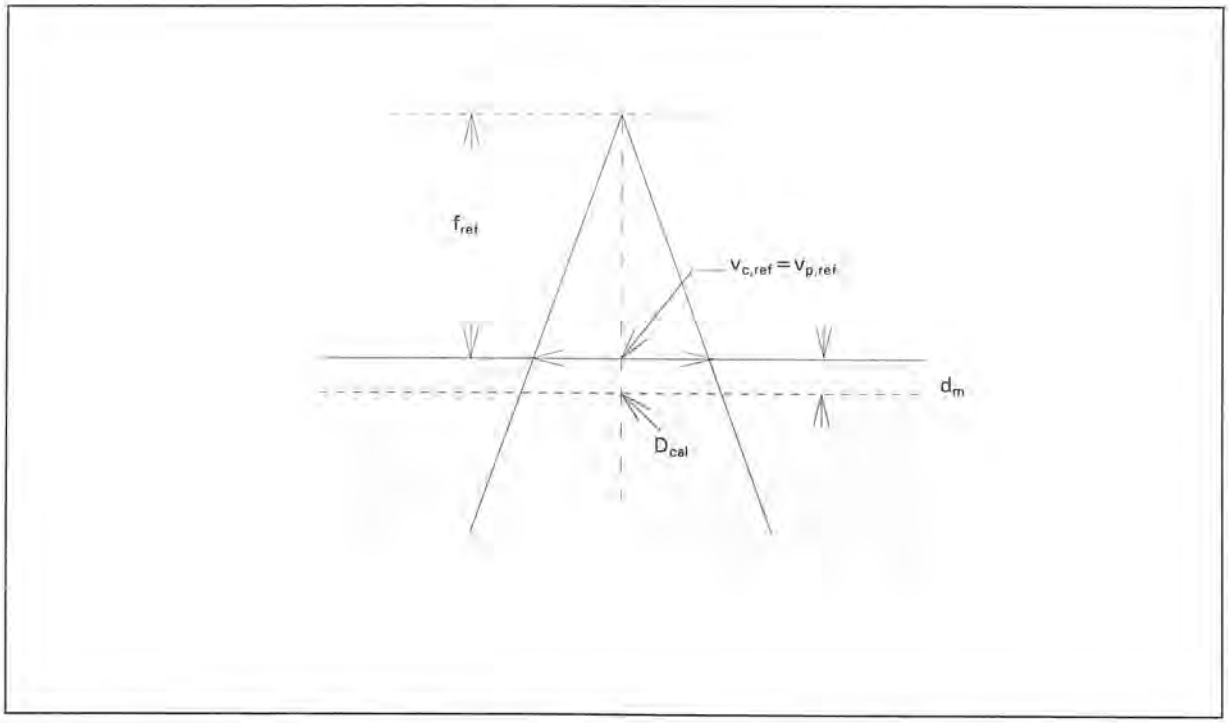

Figure 2.2 The monitor chamber of the treatment machine is calibrated to deliver a dose of 1 cGy per monitor unit at a depth of maximum absorbed dose, d_m, in the reference field: $D_{cal} = D(v_{c,ref}, v_{p,ref}, d_m, f_{ref})$, with $v_{c,ref} = v_{p,ref} = 10$ cm x 10 cm and $f_{ref} = 100$ cm.

Dosimetry protocols recommend determining the absorbed dose in a beam at a depth d_{ref} [28,47]. In order to relate the calibration dose at d_m to the dose at d_{ref},

use is made of the percentage depth dose of the calibration field, $PDD(v_{p,ref},d_{ref},f_{ref})$, see figure 2.3,

$$D_{ref} = D_{cal} \times PDD(v_{p,ref},d_{ref},f_{ref}) / 100 \quad (2.2.2)$$

which can be rewritten as:

$$D_{ref} = D_{cal} / RDD(v_{p,ref},d_m,f_{ref}) \quad (2.2.3)$$

This expression introduces the *relative depth dose*, RDD. For a given source-surface distance f and a given field v_p, RDD is defined as the absorbed dose at a certain depth d, normalized to unity at the reference depth d_{ref}. Its behaviour is analogous to that of the PDD of the beam at the same SSD, although its normalization is at d_{ref} instead of d_m. The RDD can be derived from PDD data using:

$$RDD(v_p,d,f) = PDD(v_p,d,f) / PDD(v_p,d_{ref},f) \quad (2.2.4)$$

From the definition it is clear that at depth $d = d_{ref}$ RDD is always equal to unity, irrespective of field size, v_p, or source-surface distance, f.

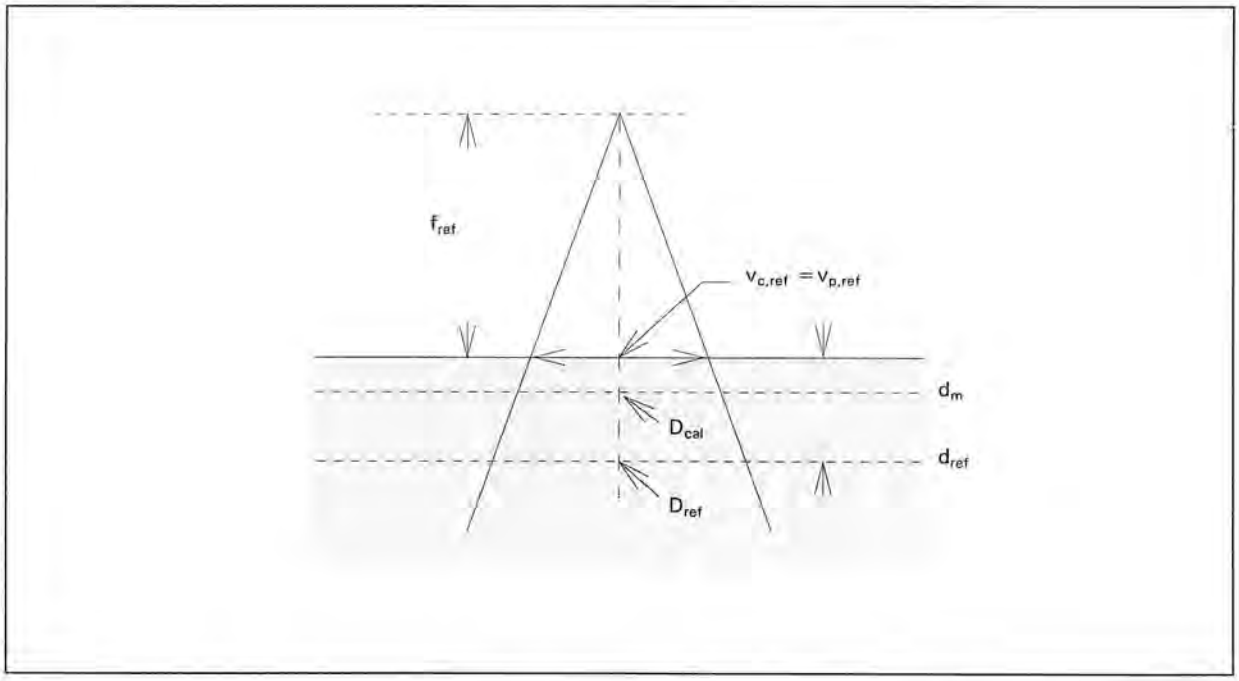

Figure 2.3 Dosimetry protocols recommend to calibrate a beam at the reference point in the reference field, i.e. at depth d_{ref} and field size $v_{c,ref} = v_{p,ref} = 10$ cm x 10 cm; $f_{ref} = 100$ cm.

2.3 Calculation of the dose under non-reference conditions

Beams with SSD = f_{ref}

The absorbed dose at a point at the reference depth d_{ref} in a beam with arbitrary field size (v_c,v_p) and a reference source-surface distance f_{ref}, is given by (see figure 2.4):

$$D(v_c,v_p,d_{ref},f_{ref}) = D_{ref} \times S_c(v_c) \times S_p(v_p) \qquad (2.3.1)$$

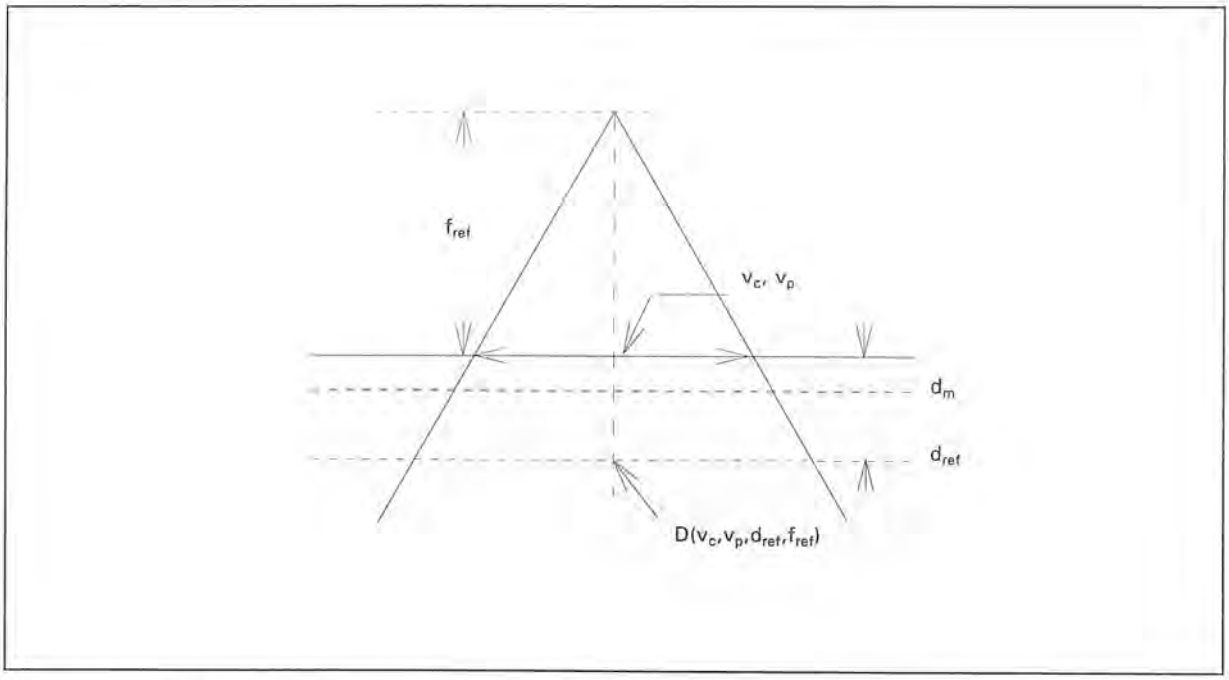

Figure 2.4 Dose in an arbitrary field at depth d_{ref} and SSD equal to SAD: $D(v_c,v_p,d_{ref},f_{ref})$. The quantities $S_c(v_c)$ and $S_p(v_p)$ are defined at depth d_{ref} and at source-surface distance f_{ref}.

From the definition of the relative depth dose, the absorbed dose at other depths d can be written as (see figure 2.5):

$$D(v_c,v_p,d,f_{ref}) = D(v_c,v_p,d_{ref},f_{ref}) \times RDD(v_p,d,f_{ref})$$

$$= D_{ref} \times S_c(v_c) \times S_p(v_p) \times RDD(v_p,d,f_{ref}) \qquad (2.3.2)$$

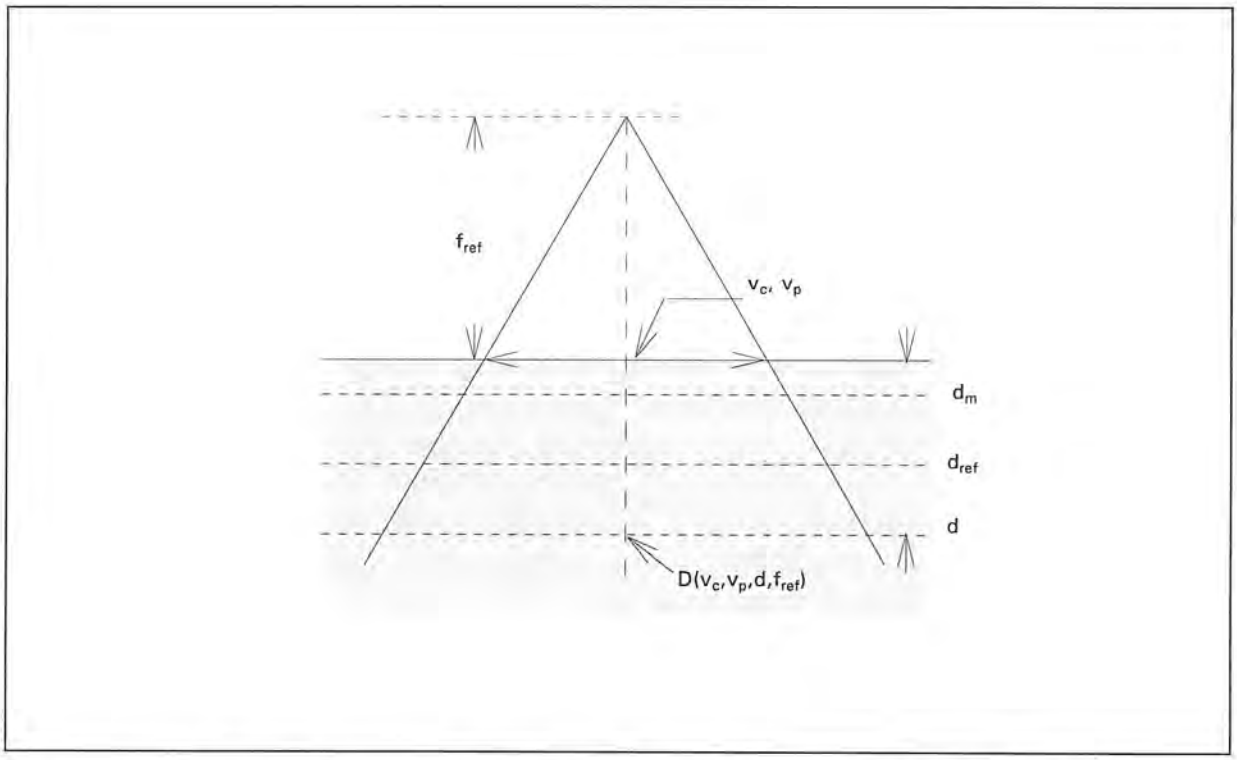

Figure 2.5 Dose in an arbitrary field at depth d and with SSD equal to SAD: $D(v_c,v_p,d,f_{ref})$.

Beams with SSD ≠ f_{ref}

In the general case, when the SSD of a beam deviates from the reference SSD, the numerical value of the field size $v_{p,f}$ is no longer numerically equal to that of the collimator defined field size v_c. This general situation is shown in figure 2.6. (Note that the term $v_{p,f}$ is used here for the field size defined at the phantom surface positioned at an arbitrary f; the term v_p is reserved for the case when f is equal to SAD. The term v(d) is used to indicate the field size at depth d, i.e. at a source-to-point distance f + d.)

According to the definitions in this report, $v_{p,f}$ and v_c can both be considered as those quantities describing the field size of the beam; see figure 2.6.a. Values of the collimator scatter correction factors can be derived directly from measurements of S_c, which will in general be tabulated as a function of v_c. However, values of the phantom scatter correction factor are determined at f_{ref}, and will in general be available in a format for this f_{ref}.

The phantom scatter contribution to the dose at depth d depends on the size of the field at that depth, v(d), rather than on the field size at the surface. This observation was first discussed by Johns et al. [32] and was taken into consideration in the relations between depth dose characteristics at different SSDs (see Burns, Appendix B in reference [8]). Phantom scatter correction factors can thus be used from measurements made at a reference source-surface distance (see figure 2.6.b) for a field size at f_{ref} that projects to the same field size v(d) at depth d as the field $v_{p,f}$.

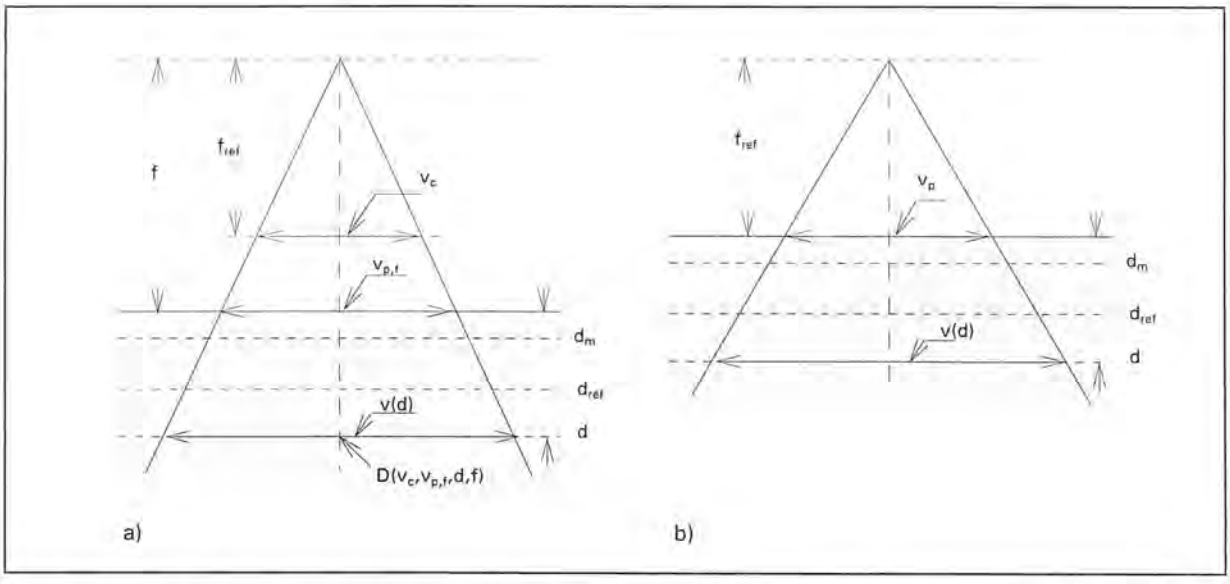

Figure 2.6 Dose in an arbitrary field at depth d and source-surface distance f, $D(v_c,v_{p,f},d,f)$. Here, the relations between field size at depth d, v(d), v_c, $v_{p,f}$ and v_p have to be taken into account (see text): $v_p = v_{p,f} / F$.

In order to obtain the correct phantom scatter correction factor at depth d_{ref}, a correction factor F is needed to relate the field size at depth to the field size at the surface, taking into account the different beam divergence for the different SSDs. The dose at a point can be calculated with the following expression, of which a more detailed derivation can be found elsewhere [71]. Here, only the resulting relation is shown between the dose at an arbitrary depth and an arbitrary SSD and the dose at reference conditions, D_{ref}:

$$D(v_c,v_{p,f},d,f) = D_{ref} \times S_c(v_c) \times S_p(v_{p,f}/F) \times \{(f_{ref}+d)/(f+d)\}^2 \times RDD(v_{p,f}/F,d,f_{ref}) \quad (2.3.3)$$

or rather, with equation (2.2.3) relative to the calibration dose, D_{cal}:

$$D(v_c,v_{p,f},d,f) = D_{cal} \times S_c(v_c) \times S_p(v_{p,f}/F) \times \{(f_{ref}+d)/(f+d)\}^2 \times RDD(v_{p,f}/F,d,f_{ref}) / RDD(v_{p,ref},d_m,f_{ref}) \quad (2.3.4)$$

In these equations, the factor F corrects the field size to be used in the phantom scatter correction factor and in the RDD, according to [8,9]:

$$F = \frac{f_{ref}+d}{f_{ref}} \times \frac{f}{f+d} \quad (2.3.5)$$

2.4 Calculation of treatment time and monitor units in the fixed SSD formalism

Beams with SSD = f_{ref}

For the situation where the source-surface distance equals SAD, the number of monitor units N, required to deliver a prescribed dose, D_{presc}, to the dose prescription point at any depth in an arbitrary field (i.e. with v_c, v_p, depth d, and f_{ref}), can now be calculated.

Substitution of D_{ref} from equation (2.2.3) into equation (2.3.2) yields a dose of

$D_{cal} \times S_c(v_c) \times S_p(v_p) \times RDD(v_p,d,f_{ref}) / RDD(v_{p,ref},d_m,f_{ref})\}$ per monitor unit.

In order to deliver the prescribed dose D_{presc} at the specification point, N monitor units are required according to:

$$N = D_{presc} / \{D_{cal} \times S_c(v_c) \times S_p(v_p) \times RDD(v_p,d,f_{ref}) / RDD(v_{p,ref},d_m,f_{ref})\} \quad (2.4.1)$$

Beams with SSD ≠ f_{ref}

For the more general case, where an arbitrary source-surface distance f is used, equation (2.4.1) can be rewritten using equation (2.3.5) to yield:

$$N = D_{presc} / \{D_{cal} \times S_c(v_c) \times S_p(v_{p,f}/F) \times \{(f_{ref}+d)/(f+d)\}^2 \times RDD(v_{p,f}/F,d,f_{ref}) / RDD(v_{p,ref},d_m,f_{ref})\} \quad (2.4.2)$$

2.5 Calculation of monitor units in the isocentric formalism

The isocentric set-up is widely used in external beam radiotherapy. In many institutions dose measurements are performed from which tissue-phantom ratios are derived as the basis for an isocentric calculation system. The reference irradiation conditions for these measurements are essentially different from those used in the fixed SSD formalism. In this paragraph, the basic definitions of the isocentric (or TPR) approach are given, together with the expression to calculate the number of monitor units for a certain prescribed dose; see also Appendix 8.3 [71].

Analogous to the fixed SSD situation, we consider the isocentric situations of figure 2.7.

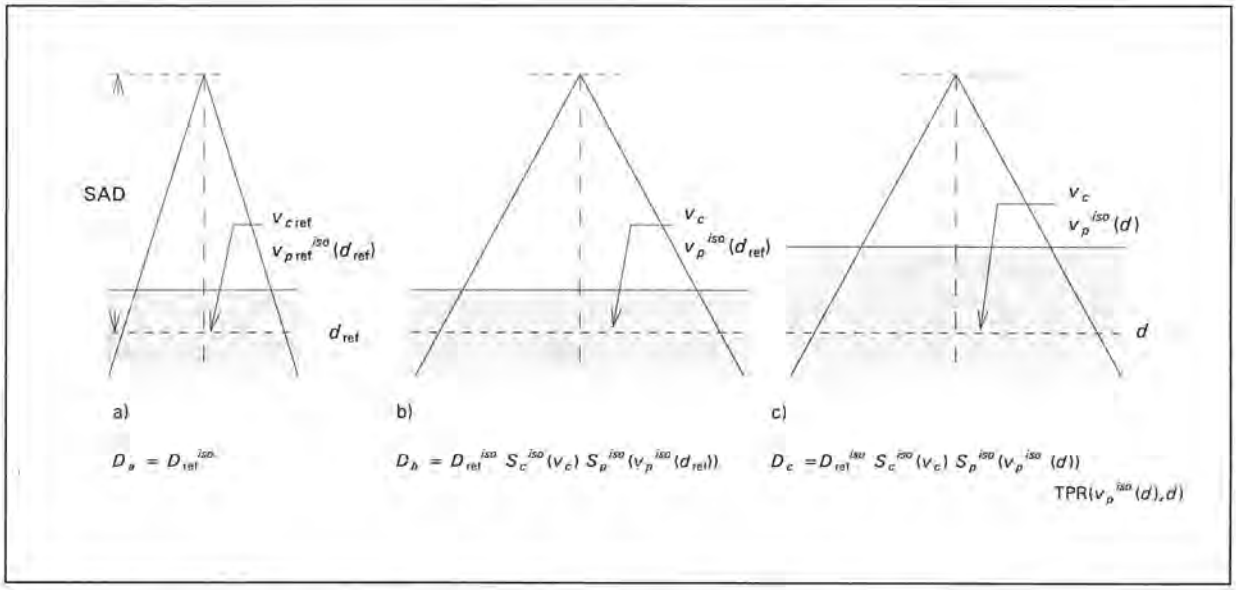

Figure 2.7 The use of the tissue-phantom ratio in dose calculations.

The reference dose per monitor unit in the isocentric approach, D_{ref}^{iso}, is usually specified at the isocentre, at a reference depth, d_{ref}, equal to 10 cm, in an open beam with a field size of 10 cm x 10 cm defined at the isocentre, which is in most cases at a distance from the focus (SAD) equal of 100 cm.

The collimator scatter correction factor for the isocentric approach, S_c^{iso}, is measured in the same manner as in the fixed SSD approach, i.e. using the mini-phantom with the detector at 10 cm depth, but now the detector is positioned at the SAD. As discussed in section 8.3, S_c^{iso} is equal to S_c. The phantom scatter correction factor for the isocentric approach, $S_p^{iso}(v(d_{ref}))$, is derived from the ratio $S_{cp}^{iso}(v_c,v(d_{ref}))$ / $S_c^{iso}(v_c)$, where $S_{cp}^{iso}(v_c,v(d_{ref}))$ is measured in a full

scatter phantom, again with the detector at the depth d_{ref}. $v(d_{ref})$ is the field size at depth d_{ref}, i.e. at the isocentre.

Beams with SSD = SAD-d

For a point at the isocentre at any depth d, the absorbed dose per monitor unit for a collimator defined field size v_c, field size v(d) at depth d and a source-surface distance equal to SAD-d, is given by:

$$D(v_c,v(d),d,SAD\text{-}d) = D_{ref}^{iso} \times S_c^{iso}(v_c) \times S_p^{iso}(v(d)) \times TPR(v(d),d) \quad (2.5.1)$$

The field size at the isocentre v(d) also takes into account possible blocking of the beam.

The number of monitor units N required to deliver the prescribed dose D_{presc} at the specification point is now given by:

$$N = D_{presc} / \{D_{ref}^{iso} \times S_c^{iso}(v_c) \times S_p^{iso}(v(d)) \times TPR(v(d),d)\} \quad (2.5.2)$$

Beams with SSD ≠ SAD - d

For the more general situation where the dose specification point is not at the isocentre (i.e. where the source-surface distance f ≠ SAD-d) the inverse square law with respect to the SAD has to be introduced and the dose is written as:

$$D(v_c,v(d),d,f) = D_{ref}^{iso} \times S_c^{iso}(v_c) \times S_p^{iso}(v(d)) \times \{SAD/(f+d)\}^2 \times TPR(v(d),d) \quad (2.5.3)$$

and equation (2.5.2) becomes:

$$N = D_{presc} / \{D_{ref}^{iso} \times S_c^{iso}(v_c) \times S_p^{iso}(v(d)) \times \{SAD/(f+d)\}^2 \times TPR(v(d),d)\} \quad (2.5.4)$$

Note that the quantities used in these equations are derived from the isocentric, i.e. the TPR approach, and these *should not be confused* with those from the fixed SSD approach. The relations between D_{ref}^{iso} and D_{ref}; S_c^{iso} and S_c; S_p^{iso} and S_p are given in Appendix 8.3 [71].

3. Scatter correction factors for non-square fields, fields with wedges, compensators and trays

3.1 Rectangular and irregularly shaped fields

The collimator scatter correction factor S_c in rectangular fields

It has been shown by several authors that for rectangular fields the collimator scatter correction factor S_c, and therefore the total scatter correction factor for a given collimator setting, will be different if the upper and lower collimator jaws are interchanged [24,57-59,62]. This effect is commonly described as *the collimator exchange effect*, CEE. The effect originates from different amounts of radiation scattered backwards from the upper and lower collimator jaws into the beam monitor chamber [14,18,24,41] and from differences in energy fluence of photons originating from the flattening filter reaching the point of interest [3]. The magnitude of the collimator exchange effect depends on the construction of the head of the treatment machine including such factors as the dimensions and material of the flattening filter, the presence of collimator satellites close to the monitor chamber, the distance between the upper collimator parts and the monitor chamber, and the presence of shielding material in the accelerator head.

Accurate calculation of the output of rectangular fields requires the determination of S_c values for the large range of irradiation geometries used routinely in the clinic. A two-dimensional table can be constructed, often obtained from measured and partly interpolated or fitted data. The use of a 2-D table is in principle simple and accurate. It can easily be incorporated in calculation systems using present-day computer technology. The beam data in this report have been presented in this way. However, the determination of the 2-D table of S_c values is time-consuming and, therefore, methods to minimize the number of measurements might be considered [24,31,57-59,62].

Analytical approximations

Most methods given in the literature for estimating S_c of a particular rectangular field are based on the determination of the equivalent square field yielding the same S_c value [4,55,57,62]. In general, equations are proposed for which parameters have to be determined from S_c measurements for a limited number of square and rectangular fields. Various methods, based on the equivalent square field method, have been analyzed by Jager et al. [31] for a large number of treatment machines and photon beam qualities with respect to the accuracy in estimating the S_c value of rectangular fields. The data-fitting method described in their paper is at the moment the most accurate one. Applying that methodology, S_c values can be estimated with deviations smaller than 0.8% between the estimated and actual S_c values for all collimator settings and for various types of treatment machines. However, the authors concluded that a model based on the physical characteristics of a treatment head might be helpful

for the accurate calculation of S_c values for all treatment machines in clinical use (Appendix 8.7).

Physical models

Other methods, based on a more fundamental consideration of the origin of the collimator scatter components, have been suggested. By using Monte Carlo calculations, the head of the treatment unit can be modelled, from which the relative importance of the different components of S_c can be deduced [2,3,11]. Using this method, the flattening filter and the primary collimator were clearly shown to be the most important contributors to S_c [3,11]. Ahnesjö et al. [3] developed a convolution method to describe the field size dependence of the output factors for use in a treatment planning system. Yu and Sloboda [74] applied an integration technique over the surface of the flattening filter as seen from the detector to predict S_c in a two-component x-ray source model. Some empirical methods based on the form of the flattening filter and its relative position in the treatment head were discussed by Lam et al. [40]. A simple equivalent square formula was proposed by Kim et al. [35], in which a field that is defined in the source plane is mapped back into the detector plane by an equivalent field relationship. All these approaches have in common that geometrical details of the treatment head, sometimes deduced from measurements, are used in the models. Some have been developed as treatment planning system algorithms [3], others can be used in hand calculations [35]. Another simple and accurate method of calculating S_c of a rectangular field was suggested by van Gasteren et al. [67]. In that paper, the amount of scatter is taken into account that arrives at the reference point from the beam flattening filter in the head of the treatment machine. When the scattering filter is viewed from this point, it is evident that for a square field (X,X) the lower set of collimator blocks defines a larger part of the flattening filter than the upper set. A scaling term can be used to find the effective field size that defines a square projection at the level of the flattening filter when viewed from the reference point. This approach is described in somewhat more detail in Appendix 8.7.2, including the iteration steps needed to obtain the scaling factor. See also reference [67] for open beams and reference [68] for wedged beams.

If any of these approaches to obtain S_c values for the full 2-D table of all rectangular field sizes used in the clinic is not possible, direct measurement is recommended instead.

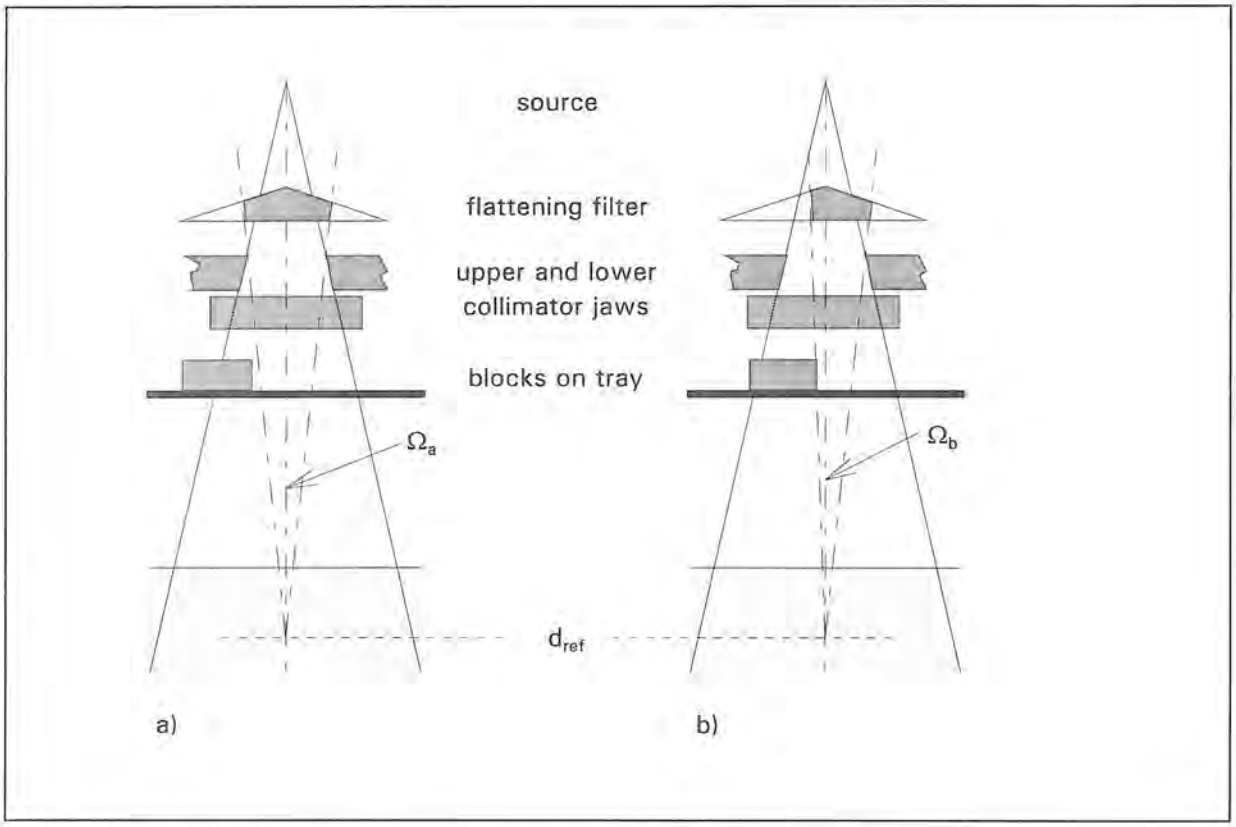

Figure 3.1 Two situations with blocks on the tray are shown: a) with an open 'view' of the flattening filter resulting in a solid angle Ω_a; b) with the 'view' of the flattening filter partly shielded by a block, resulting in a smaller solid angle Ω_b.

The effect of partial shielding of the flattening filter on S_c

It has been shown that the amount of photons scattered in the treatment head and directed to the point of dose measurement is almost completely determined by the scattering processes in the flattening filter and the primary collimator. Photon scattering at the adjustable secondary collimator jaws can be ignored or is of minor importance [2,11,44,60]. The variation of the collimator scatter correction factor with changing collimator setting can, therefore, be related directly to the volume of the flattening filter 'seen' from the point of interest. Positioning of customized blocks on a tray below the collimator jaws might influence S_c of the open beam due to the partial obscurance of the flattening filter as seen from the point of interest (see the solid angles Ω_a and Ω_b in figure 3.1). A general quantitative description of this effect on S_c is difficult, but a geometrical examination of the construction of the head of various treatment machines shows that *only* in the case of rather extreme blocking the effect of the additional customized blocks is more important than the shielding effect of the movable collimator jaws [41,45,60,63]. The point where customized blocks will start to influence the S_c value of the open field can be estimated (see Appendix 8.5) and depends on the construction details of the head of the treatment machine. These may differ considerably between the different types,

as shown in figure 3.2. A detailed description of the head is needed for a proper application of the method suggested in Appendix 8.5.

The value of the collimator scatter correction factor of the blocked irradiation field, $S_{c,block}$, can thus be taken equal to S_c of the unshielded beam, as long as the part of the flattening filter that can be seen from the point of measurement for the blocked field is determined by the collimator jaws only (figure 3.1.a). In other situations, $S_{c,block}$ must be determined by measurement and, consequently, must replace S_c in the equations of chapter 2 (figure 3.1.b).

The phantom scatter correction factor S_p

For rectangular fields, changes in the energy spectrum of the primary photon beam with varying field size can be neglected. S_p data for these fields can be obtained by applying Clarkson's method in a simple computer program using S_p data determined for square fields [13]. The equivalent square fields method [8,9,50] for the determination of the PDD and phantom scatter factors for non-square fields is widely used in clinical practice. Its accuracy is, however, somewhat inferior to that of the Clarkson method if the S_p values have to be determined for different beam qualities. The equivalent field sizes given in the BJR Supplements 17 and 25 [8,9] are *mean* values obtained by considering photon beams over a wide range of radiation qualities, and, furthermore, in the determination of the equivalent square fields, the head and phantom scatter dose contributions were not separated.

By carrying out this separation and applying Clarkson's method for each beam quality independently, improvements of the order of magnitude of 0.5 to 1.0% are possible in the determination of S_p especially for elongated fields. A new table of equivalent squares, to be used for S_p (as well as for PDD and TPR), has been proposed for this purpose by Venselaar et al. [70]. It is based on data gathered from a large number of beam qualities in the range of ^{60}Co to 25 MV and is included in this report (Appendix 8.6).

For irregular fields, neither the presence of shielding blocks nor the tray significantly influence the energy spectrum of the photon beam, and their phantom scatter correction factor $S_p(v_{p,block})$ can be calculated from S_p data for square fields, again applying Clarkson's method.

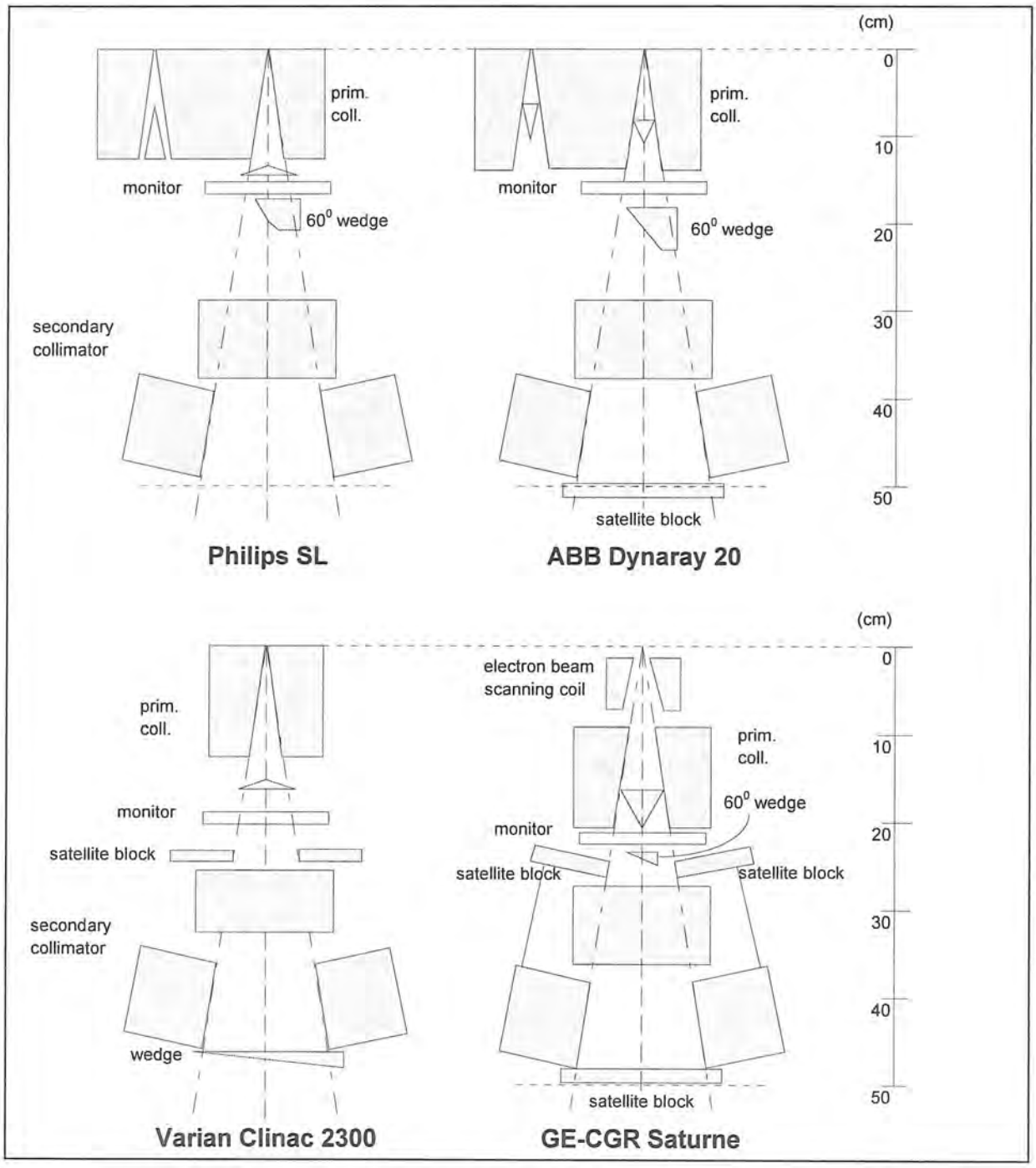

Figure 3.2 Construction drawings of the head of four different treatment machines. Note that the distance between the flattening filter and the upper collimator blocks differs considerably between the collimator designs. The geometry in which extreme blocking will influence S_c will be different for the four machines.

3.2 Wedges and compensators

Wedges and/or compensators are inserted in the beam to modify the dose distribution in the patient, e.g., to compensate for variations in body contour, for the presence of inhomogeneities or to generate intensity modulated beams that can be used to optimize the dose distribution. For these irradiation geometries S_c values deviate from the values of the open beam due to changes in the energy fluence at the point of interest as well as in the amount of radiation scattered backwards into the monitor chamber in the head of the treatment machine [22,26]. Wedges and compensators are generally made of high-Z materials. Depending on the construction of the treatment machine, wedges can be situated below the collimator jaws, or mounted in the head of the treatment machine between the monitor chamber and the collimator jaws. Compensators are, in general, placed below the collimator jaws. Both devices must be considered as an important additional extended source of scattered photons. These additional scattered photons in the beam can be taken into account by applying an *effective source-surface distance* in the inverse square law term in the dose calculation formalism instead of the geometrical distance as used for the open beam situation. Furthermore, the energy spectrum of the primary beam will be modified [20,22,26,52,61].

In principle, both the wedge and the compensator influence the energy fluence per monitor unit at the point of interest in a similar way. Therefore, only the effect of the wedge will be discussed here.

Definition of the reference wedge transmission factor, WF_{ref}

For the open beam situation of an arbitrarily defined field, equation (2.3.3) is written as:

$$D_{open}(v_c,v_{p,f},d,f) = D_{ref,open} \times S_{c,open}(v_c) \times S_{p,open}(v_{p,f}/F) \times \{(f_{ref}+d)/(f+d)\}^2 \times RDD_{open}(v_{p,f}/F,d,f_{ref}) \quad (3.2.1)$$

while for the same beam with a wedge the corresponding equation is:

$$D_w(v_c,v_{p,f},d,f) = D_{ref,w} \times S_{c,w}(v_c) \times S_{p,w}(v_{p,f}/F) \times \{(f_{ref,w}+d)/(f_w+d)\}^2 \times RDD_w(v_{p,f}/F,d,f_{ref}) \quad (3.2.2)$$

The subscripts of the quantities refer to the open and wedged beam situations, respectively. Note that in the wedged case the subscript w is added to the source-surface distance, f_w, in the inverse square law term to indicate that an effective source-surface distance is used.

The *wedge transmission factor* WF is defined as the ratio of the dose per monitor unit measured with and without the wedge in the beam. It is emphasized that, by convention, this definition is given here *only for the reference depth, d_{ref}*. This limitation is in agreement with the definitions of other quantities at the same depth (e.g. S_p, S_c, D_{ref}), and with the practical use of wedge transmission factors. At the same time, it is concluded from this definition that the possible depth dependence of the wedge transmission factor is taken into account via the different RDDs of the wedged and open beam. These should be made available as separate measurements for the open and wedged beams. Thus:

$$WF(v_c, v_p, d_{ref}, f) = D_w(v_c, v_p, d_{ref}, f) / D_{open}(v_c, v_p, d_{ref}, f) \qquad (3.2.3)$$

The wedge transmission factor WF is used as a measure of the wedge-induced change in the energy fluence per monitor unit measured at the point of interest (at the reference depth) in the beam [29]. Considering the arguments given above, the influence of the wedge varies with collimator setting v_c and with source-surface distance. We now define WF_{ref}, the *reference wedge transmission factor*, as the wedge transmission factor for the reference irradiation condition:

$$\begin{aligned} WF_{ref} &= WF(v_{cref}, v_{pref}, d_{ref}, f_{ref}) \\ &= D_w(v_{cref}, v_{pref}, d_{ref}, f_{ref,w}) / D_{open}(v_{cref}, v_{pref}, d_{ref}, f_{ref}) \\ &= D_{ref,w} / D_{ref,open} \end{aligned} \qquad (3.2.4)$$

Then, by combining (3.2.1) to (3.2.4) it is found that

$$\begin{aligned} WF(v_c, v_p, d_{ref}, f) = WF_{ref} &\times (S_{c,w}(v_c) / S_{c,open}(v_c)) \\ &\times (S_{p,w}(v_{p,f}/F) / S_{p,open}(v_{p,f}/F)) \\ &\times \{(f_{ref,w} + d_{ref})/(f_w + d_{ref})\}^2 / \{(f_{ref} + d_{ref})/(f + d_{ref})\}^2 \end{aligned} \qquad (3.2.5)$$

In order to simplify this expression, the factors are discussed separately.

WF_{ref}

Wedge induced changes in the energy spectrum of the scattered beam are larger for low energy than for high energy megavoltage photon beams. It was shown that for a 4 MV x-ray beam of an ABB linear accelerator this effect results in a 1.5% lower value of the wedge factor if measured in a full scatter phantom compared with values determined in a mini-phantom, independent of field size [22]. For this reason the general rule should be that the reference wedge transmission factor is determined in a full scatter phantom.

The ratio $S_{c,w}$ / $S_{c,open}$

Because the wedge behaves as an extended source of scattered photons, a stronger variation of the energy fluence per monitor unit at the point of interest with collimator setting will occur. For example, $S_{c,w}(v_c)$ varies with the collimator setting over a wider range than $S_{c,open}(v_c)$ for the open beams. Variations up to 8% have been reported [22,61,75]. If the wedge is situated at a fixed position in the treatment head the magnitude of this effect will be less pronounced if it is measured at larger wedge-to-point distances, i.e. at larger SSDs. This is explained by the fact that the contribution to the energy fluence per monitor unit at the point of interest of the photons coming from the wedge, relative to the contribution of the primary and scattered photons originating from the flattening filter, will decrease for larger SSDs because of the different relative positions of the wedge and the target with respect to the point of interest [22].

The ratio $S_{p,w}$ / $S_{p,open}$

For most photon beam qualities, no change in S_p has been observed if a wedge is inserted in a photon beam [22]. As the shift in the quality index of a wedged beam is relatively small compared with the open beam situation, this result is in agreement with the observed slow variation of S_p with beam quality (see also section 5.3.1) [56]. Consequently, the ratio of S_p values in wedged and open beams, as required in equation (3.2.5), is close to unity. For the purpose of calculation of monitor units, this means that S_p values of the open beam can also be applied for the wedged beam.

The ratio of inverse square law terms

The main source of photons in an open beam is a small focal spot on the target of the linear accelerator. If a wedge is inserted, a diffuse source of scattered photons is added to the beam. The angular distribution of the scattered photons from a wedge is relatively wide. If the wedge is positioned *high up* in the beam defining system of the machine, the extra photon contribution may still be assumed to obey the inverse square law at clinically used distances. The effective source-surface distance is then close to that of the open beam. Nevertheless, small deviations may occur and these should be taken into account in dose calculations. The magnitude of the deviations has to be determined for each beam separately, by performing measurements of wedge transmission factors at different source-surface distances. If a wedge is positioned *below* the collimator jaws (see figure 3.2 for an example), the effect is more pronounced because of the shorter distance between wedge and point of measurement.

Influence of a wedge on RDD (PDD)

The above mentioned wedge induced change in the energy spectrum of the primary photon beam can result in a different RDD (PDD) curve compared to the open beam. This variation is usually attributed to *beam hardening*, although *beam softening* might also occur, especially for high energy photon beams

[22,52]. In addition, wedge-induced changes in the electron contamination can drastically change the RDD (PDD) curve in the first few centimeters. Therefore, for treatment planning purposes, it is strongly recommended to measure and implement depth dose curves for wedged photon beams, RDD_w.

Definition of the relative wedge transmission factor, RWF

We can now define the *relative wedge transmission factor*, $RWF(v_c,f)$, as the ratio of the wedge transmission factor at depth d_{ref} in a particular irradiation condition $WF(v_c,v_p,d_{ref},f)$, and the reference wedge transmission factor WF_{ref}, $RWF(v_c,f) = WF(v_c,v_p,d_{ref},f) / WF_{ref}$. Using the assumption, as described above, that the ratio of phantom scatter correction factors is close to unity, RWF is then found from equation (3.2.5) as,

$$RWF(v_c,f) = S_{c,w}(v_c)/S_{c,open}(v_c) \times \{(f_{ref,w}+d_{ref})/(f_w+d_{ref})\}^2/\{(f_{ref}+d_{ref})/(f+d_{ref})\}^2 \qquad (3.2.6)$$

Combining the equations now yields the dose in a wedged beam, which can be calculated according to:

$$D_w(v_c,v_{p,f},d,f) = D_{open}(v_c,v_{p,f},d,f) \times WF_{ref} \times RWF(v_c,f) \times RDD_w(v_{p,f}/F,d,f_{ref}) / RDD_{open}(v_{p,f}/F,d,f_{ref}) \qquad (3.2.7)$$

It should be noted here that expression (3.2.6) is only meant to show which factors influence the value of RWF. It is not meant to derive RWF values from experimentally determined effective source-surface distances. The most straightforward approach is to assume f_w to be equal to f and to determine RWF by experiment as a function of the collimator setting v_c for a number of different SSDs. From these measurements, interpolation and extrapolation will yield a good result for most clinical situations. $RWF(v_c,f)$ can be determined in a full scatter phantom *or* in a mini-phantom. The measurement geometries are shown in figure 3.3.

In summary, the factor WF_{ref} takes into account the reduction of the energy fluence per monitor unit at the point of interest with respect to the open beam for the reference irradiation condition. The factor RWF takes into account the variation in this reduction for non-reference field sizes and non-reference SSDs.

Influence of field elongation

The measurement of wedge transmission factors is often limited to square fields in the range of field sizes used clinically. Several authors presented measurements of wedge factors in rectangular fields [52,61,68]. The best approach appears to apply an equivalent square field size method and then to

interpolate between measured values of square fields, as long as the elongation ratio of the fields is less than 3. For ratios larger than 3, it is recommended to determine the wedge transmission factors by measurement. In this way, an agreement between prediction and measurement in rectangular wedged fields within 1% can be achieved [52,58,62].

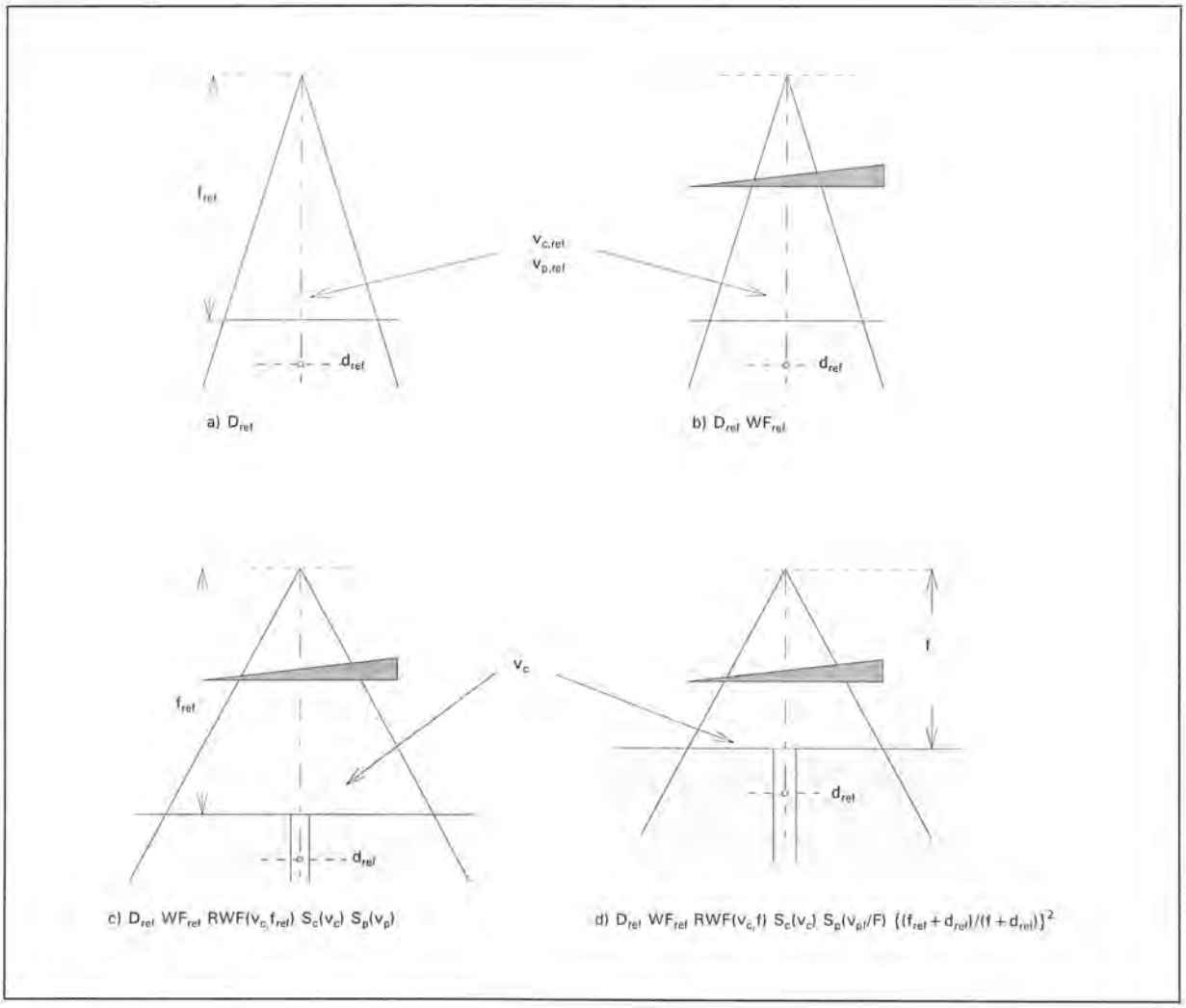

Figure 3.3 WF_{ref} is derived from measurements a) and b) in a full scatter phantom. For the reference source-surface distance f_{ref}, $RWF(v_c, f_{ref})$ is found as a function of v_c from the ionization chamber readings in the full scatter phantom or in a mini-phantom, resulting from measurements b) and c), with and without a wedge in the beam. To investigate the influence of the source-surface distance on the value of $RWF(v_c, f)$, measurements c) and d) at different SSDs, but with the same collimator setting, should be performed.

Compensators

A compensator can be considered as a more sophisticated type of wedge, influencing the dose distribution in any direction perpendicular to the beam axis, instead of the one-directional effect typical of a wedge. Compensators are generally customized for the individual patient and, therefore, published data are scarce. However, it can be expected that the influence of the compensator on the phantom scatter shows the same behaviour as that observed with a wedge. Only wedge induced effects are discussed here for this reason. In case compensators are used, the same recommendations apply, which should be verified for a few specific situations.

3.3 Fields with a tray

In clinical practice, irradiation fields are often partially shielded with customized blocks from high-Z material positioned on a tray which, in turn, is mounted below the collimator jaws of the treatment machine. The source-to-tray distance is approximately 2/3 of the SAD. For a clear understanding of the resulting changes in collimator scatter correction factors it is helpful to separate the origin of the changes of S_c into two parts: the influence of photon attenuation and scatter in the material of the block support, or tray, on the energy fluence at the point of interest, and the energy fluence reduction due to the partial shielding of the flattening filter by the additional customized blocks. This latter effect has already been discussed in section 3.1.

The effect of a tray on the dose

The tray on which the blocks are positioned attenuates the energy fluence of the primary photons in the beam. In addition, scattering of photons in the tray material takes place, contributing to the dose at the point of interest [30]. The relative importance of this effect depends on the beam quality, the thickness and material of the tray, the actual size of the irradiated tray surface, and the distance between the tray and the phantom or patient surface [21]. The presence of the tray in the photon beam will not result in an appreciable amount of backscattered photons into the monitor chamber, due to their large mutual distance. However, the effects on the dose distribution due to the presence of a tray in a beam are essentially the same as for wedges and compensators.

The effect of the tray on the dose value at a particular point is usually taken into account by applying a tray factor. This *tray transmission factor* TF is defined as the ratio of the dose measured at the reference depth, with and without the tray in the beam for the same number of monitor units:

$$TF(v_c,v_p,d_{ref},f) = D_{tray}(v_c,v_p,d_{ref},f) / D_{open}(v_c,v_p,d_{ref},f) \qquad (3.3.1)$$

Two comments with respect to the tray transmission factor can be made. Firstly, for a particular quality of the photon beam and tray design, the influence of the tray on the energy fluence varies with the actual field size projected on the tray, v_{tray}, taking the blocked area into account. The magnitude of this variation depends on the tray-phantom distance TPD and therefore on the source-surface distance, since the tray is mounted at a fixed position below the head of the treatment machine. In a similar way as for the wedge transmission factor, TF can be written as the product of the *reference tray transmission factor* TF_{ref} and a *relative tray factor* $RTF(v_{tray},TPD)$, which takes into account the field size and distance dependence. The reference tray transmission factor TF_{ref} is the transmission factor measured in the reference irradiation set-up:

$$TF_{ref} = TF(v_{cref}, v_{pref}, d_{ref}, f_{ref})$$

$$= D_{tray}(v_{cref}, v_{pref}, d_{ref}, f_{ref}) \,/\, D_{open}(v_{cref}, v_{pref}, d_{ref}, f_{ref}) \qquad (3.3.2)$$

The relative tray transmission factor $RTF(v_{tray}, TPD)$ can be found from the ratio of $TF(v_{tray}, TPD)$ and TF_{ref}, which is equivalent to the ratio of collimator scatter correction factors measured with and without a tray in the beam:

$$RTF(v_{tray}, TPD) = TF(v_{tray}, TPD) \,/\, TF_{ref} = S_{c,tray}(v_c) \,/\, S_{c,open}(v_c) \qquad (3.3.3)$$

As discussed previously for wedges, the presence of the tray has only a minor influence on the phantom scatter contribution and, therefore, on the percentage depth dose value at depth d_{ref} [22].

The second comment about the tray factor is that $RTF(v_{tray}, TPD)$ is close to unity when nearly water equivalent materials, e.g. PMMA, with thicknesses up to 10 mm are applied: RTF varies less than 2% for field sizes varying from 4 cm x 4 cm to 40 cm x 40 cm [69]. A more pronounced variation will be observed for larger thicknesses of the tray material and/or shorter TPDs. Because of the relatively small effects found experimentally for PMMA thicknesses $\leq$ 10 mm, one may in general replace v_{tray} by the collimator setting v_c, unless extreme blocking is applied: $RTF(v_{tray}, TPD) = RTF(v_c, TPD)$.

From these observations it can be concluded that the tray transmission factor can be measured with the mini-phantom as well as in a full scatter phantom, according to the measurement geometries of figure 3.4. The values of $RTF(v_{tray}, TPD)$ have to be obtained for a number of square field sizes covering the full range of clinically used fields and a number of tray-phantom distances (see figure 3.4). In a similar way as for wedges, it is recommended to repeat the measurements at two other source-surface distances, for example 80 and 120 cm. For rectangular fields, an equivalent square field method can be used to obtain a reliable interpolation.

Influence of a tray on RDD

It has to be noted that for short distances between the tray and phantom surface, electron contamination will substantially increase the surface dose. This effect will not influence the readings resulting from the choice of d_{ref} at a depth larger than the range of the contaminating electrons. The variation in the amount of contaminating electrons, however, will affect the RDD of the open beam in the first few centimeters. If clinically relevant, these deviations could be determined by measurements and incorporated in a RDD_{block}.

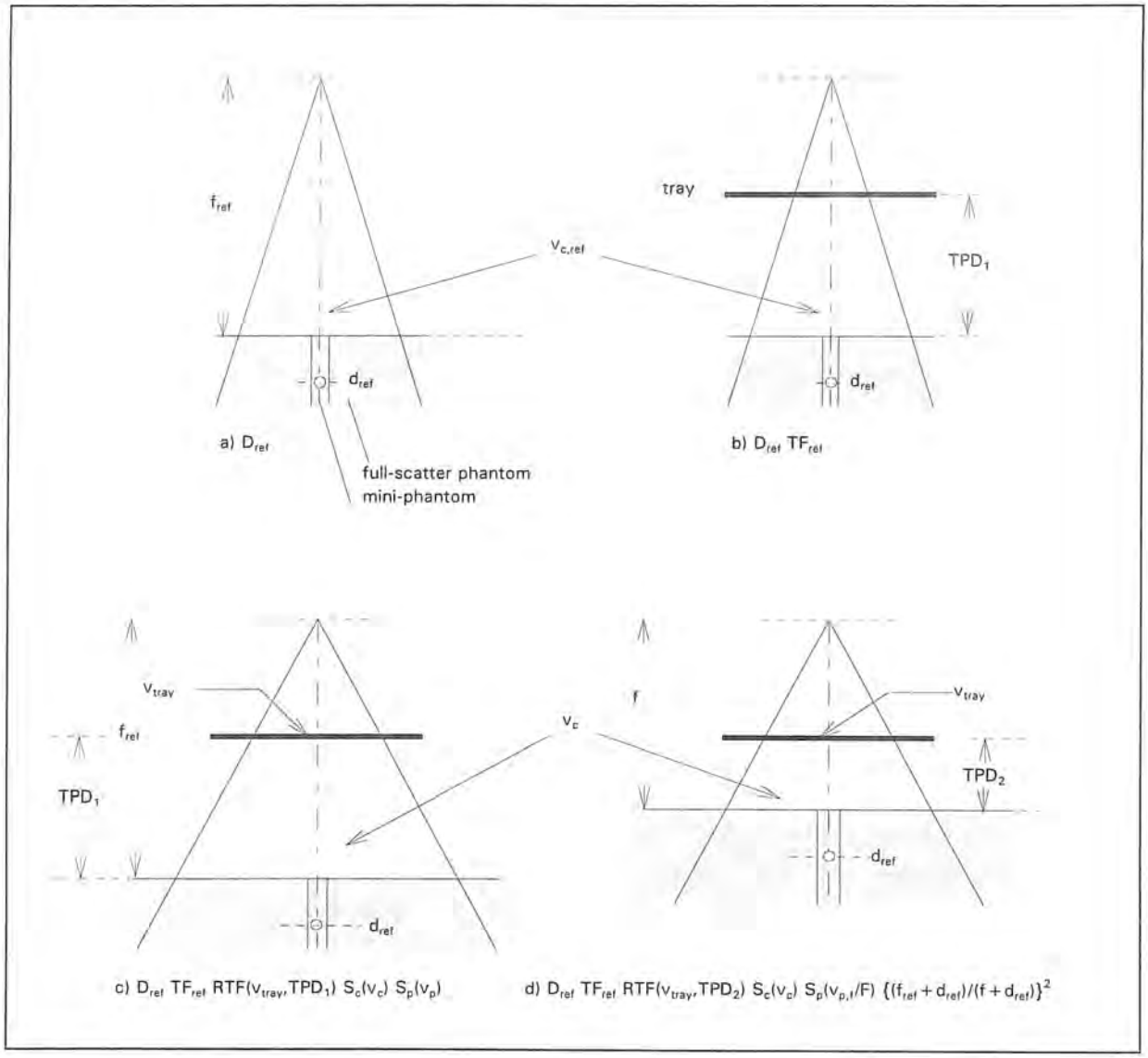

Figure 3.4 The reference tray transmission factor TF_{ref} is derived from measurements a) and b); then, for a specified tray-phantom distance TPD, the relative tray factor $RTF(v_{tray},TPD)$ can be derived from b) and c) as a function of v_{tray}. For a specified v_{tray}, $RTF(v_{tray},TPD)$ can be derived from measurements c) and d) at other SSDs. Measurements can be performed both in the mini-phantom and in the full scatter phantom. In most cases, v_{tray} can be replaced by v_c (see text).

3.4 Recommendations with respect to monitor unit calculations

Wedges and compensators

It is recommended to determine by measurement the wedge transmission factor WF_{ref} in the reference irradiation set-up. The relative wedge factor $RWF(v_c,f)$ has to be measured as a function of the collimator setting v_c, i.e. for the full range of square fields. This measurement of RWF has to be repeated for a number of source-surface distances f, covering the range of SSDs applied in clinical routine. Furthermore, the relative depth dose curves of the wedged photon beam, $RDD_w(v_p,d,f)$, have to be measured.

In the calculation of the number of monitor units N, equations (2.4.1) and (2.4.2) must be modified to take the presence of the wedge into account. The product of $S_c(v_c)$ x $RDD(v_p,d,f)$ of the open field is replaced by the product of $S_c(v_c)$ x WF_{ref} x $RWF(v_c,f)$ x $RDD_w(v_p,d,f)$, which leads for beams with a source-surface distance = f_{ref} to:

$$N = D_{presc} / \{D_{cal} \times WF_{ref} \times RWF(v_c,f) \times S_c(v_c) \times S_p(v_p) \times RDD_w(v_p,d,f_{ref}) / RDD_{open}(v_{p,ref},d_m,f_{ref})\} \quad (3.4.1)$$

and for beams with source-surface distance $\neq f_{ref}$ to:

$$N = D_{presc} / \{D_{cal} \times WF_{ref} \times RWF(v_c,f) \times S_c(v_c) \times S_p(v_{p,f}/F) \times \{(f_{ref}+d)/(f+d)\}^2 \times RDD_w(v_{p,f}/F,d,f_{ref}) / RDD_{open}(v_{p,ref},d_m,f_{ref})\} \quad (3.4.2)$$

Fields with tray and blocks

It is recommended to determine the tray transmission factor TF_{ref} in the reference irradiation set-up. Also, the relative tray factor $RTF(v_{tray},TPD)$ has to be determined by measurement of the full range of square field sizes defined at the level of the tray, v_{tray}, and for a few representative tray-phantom distances, TPD. Tray transmission factors may be measured with the mini-phantom as well as in a full scatter phantom. In addition, $S_{c,block}$ has to be determined by the measurement of irradiation geometries where extreme blocking is applied.

In the calculation of the number of monitor units, equations (2.4.1) and (2.4.2) must be modified to take into account the effect of the tray and of the shielding blocks. The factor $S_c(v_c)$ for the open fields is replaced by the product of TF_{ref} x $RTF(v_{tray},TPD)$ x $S_{c,block}(v_{tray})$, which leads for beams with source-surface distance f_{ref} to:

$$N = D_{presc} / \{D_{cal} \times TF_{ref} \times RTF(v_{tray}, TPD) \times S_{c,block}(v_{tray}) \times S_p(v_p) \times RDD_{block}(v_p, d, f_{ref}) / RDD(v_{p,ref}, d_m, f_{ref})\} \quad (3.4.3)$$

and for beams with source-surface distance $\neq f_{ref}$ to:

$$N = D_{presc} / \{D_{cal} \times TF_{ref} \times RTF(v_{tray}, TPD) \times S_{c,block}(v_{tray}) \times S_p(v_{p,f}/F) \times \{(f_{ref}+d)/(f+d)\}^2 \times RDD_{block}(v_{p,f}/F, d, f_{ref}) / RDD(v_{p,ref}, d_m, f_{ref})\} \quad (3.4.4)$$

Note 1: for compensators, the recommendation is similar to that for wedged fields.

Note 2: if combinations of wedges and blocked fields are used, *both* correction steps have to be introduced in the calculation procedures.

4. Experimental determination of scatter correction factors

4.1 Square and rectangular fields

$S_c(v_c)$ has to be measured for each available photon beam quality. The ionization chamber is placed in the mini-phantom on the central axis of the beam, with the surface of the phantom positioned at an SSD equal to the SAD (figure 2.1). The chamber axis may be parallel to the axis of the beam to allow measurements of small fields (see also Appendix 8.8). The ionization chamber readings have to be corrected for stem and/or cable effects, if present. The construction of the mini-phantom is such that the centre of the air cavity of the chamber, assumed to be the effective point of measurement, is positioned at a depth of 10 cm. Note that the actual position of the effective point of measurement is not critical. It is, however, essential that the measurements are restricted to field sizes larger than the size of the mini-phantom itself, to avoid any penumbra effect and/or field size dependent phantom scatter dose contribution in the measurement of S_c.

$S_c(v_c)$ has to be determined for square and rectangular collimator settings corresponding to those generally used in the clinic, from a minimum field size of 4 cm x 4 cm or smaller if possible, up to the maximum field size, e.g. 40 cm x 40 cm. In order to obtain S_c values for the rectangular fields, two approaches can be followed. In the first approach, S_c is simply measured for the full range of rectangular collimator settings, with the X- and Y-jaws set independently at, for example, 3, 4, 5, 6, 8, 10, 12, 15, 20, 25, 30, 35 and 40 cm. In the second approach, a limited set of square and rectangular fields could be measured, after which a data fitting method must be applied to complete the 2-D table of S_c values. For this purpose, a method based on a physical model of the beam is suggested by van Gasteren et al. [67], while analytical methods were discussed by Jager et al. [31]. The proposed approach of Jager et al. is based on a set of measurements of eight square and twelve rectangular fields. For both approaches and for references to other methods, more details are given in Appendix 8.7.2.

$S_{cp}(v_c,v_p)$ has to be measured for each available beam quality using the geometry shown in figure 2.1. An ionization chamber, with its effective point of measurement at depth d_{ref} = 10 cm on the beam axis, is placed in a full scatter water phantom. The phantom surface is set at an SSD equal to the SAD, usually 100 cm for linear accelerators and 80 cm for ^{60}Co units. The reading of the ionization chamber should be corrected for stem and/or cable effects if present.

It is recommended to measure S_{cp} data in the same square field size settings as used in the S_c measurements. For the purpose of checking the results, it is recommended to obtain S_{cp} values by direct measurement for a number of rectangular fields.

Phantom scatter correction factors $S_p(v_p)$ for square fields can be derived from the ratio of $S_{cp}(v_c,v_p)$ and $S_c(v_c)$ by using expression (2.1.3). These results should be compared with data published in this report; see section 5.3 and Appendix 8.7.1. Deviations in S_p values larger than 1% should be investigated.

The procedures used in the clinic to derive S_c and S_p values for rectangular fields, e.g. based on an equivalent squares method or on look-up tables, should be checked for consistency with the measurements. It is recommended to try and maintain the difference between the product of the S_c and S_p data, obtained in this way, and the S_{cp} values from direct measurement within 1%.

4.2 Wedges and compensators

For wedged fields the reference wedge transmission factor WF_{ref} should be determined in a full scatter phantom, while the relative wedge transmission factor for other field sizes and source-surface distances, $RWF(v_c,f)$, may be determined in the full scatter phantom or in the mini-phantom (see figure 3.3). The use of higher density build-up caps, e.g. brass, instead of a mini-phantom for the measurement of RWF is not recommended [23,73]. WF_{ref} is the ratio of the dose per monitor unit in the reference irradiation set-up with a wedge in the beam to the dose per monitor unit in the same field without the wedge: $WF_{ref} = D_w(v_{c,ref},v_{p,ref},f_{ref}) / D_{open}(v_{c,ref},v_{p,ref},f_{ref})$. RWF is found from the ratio of the wedge transmission factors determined for a specified field size and SSD, normalized to unity for the reference geometry: $RWF(v_c,f) = WF / WF_{ref}$.

The number of relative wedge transmission factor measurements can be limited to square fields in the range of field sizes used clinically. It has been shown that for rectangular wedged fields, the relative wedge transmission factor can be determined in a first approximation by applying the equivalent square field size method and interpolating between measured S_c values of square fields [52,58,61]. This should be checked by direct measurements of a few elongated fields. As for the open beams, relative depth dose curves for wedged beams $RDD_w(v_p,d,f_{ref})$ have to be determined for square field sizes.

Systematic determination of the influence of a compensator on S_c, S_p and RDD is not easy to perform due to the variability in the 3-D geometrical characteristics of the compensator. Therefore, it is recommended to directly measure the effect of a number of compensators typically used in the clinic on the dose at the specification point.

4.3 Blocked fields

For the determination of the reference tray transmission factor TF_{ref} measurements must be performed in the reference irradiation set-up (with and without the tray in the beam) for the same number of monitor units. The field size dependence, accounted for in the relative tray transmission factor RTF, should be determined for a number of square field sizes covering the range of 4 cm x 4 cm to 40 cm x 40 cm. The dependence of TF on the tray-phantom distance TPD is found by repeating this measurement at other source-surface distances, for example, at SSD equal to 80 cm and 120 cm. RTF is found from the ratio of the tray transmission factors determined for a specified field size and tray-phantom distance, normalized to unity for the reference field: $RTF(v_c) = TF/TF_{ref}$. TF and RTF can be determined using either a mini-phantom or a full scatter water phantom. The measurement set-up is similar to that used for the determination of S_c and S_{cp} and is illustrated in figure 3.4.

If extreme blocking of fields is used, $S_{c,block}$ has to be determined by measurements using a mini-phantom. The measurements are only needed for situations where the flattening filter, as seen from the point of interest, is partially or totally shielded by the additional blocks. The most practical way to perform this measurement is to leave the tray in the beam in both situations and to remove the field size dependence of the tray by dividing the readings for the blocked fields by the relative tray factor RTF. The result of the division is $S_{c,block}$, which replaces S_c of open fields in the mathematical expressions. For blocked fields it is not necessary to determine S_p from direct measurements of S_{cp}. It is sufficient to use the phantom scatter correction factor of a field v_p equivalent to that of the blocked field size.

As a final check, it is recommended to check by direct measurement the calculated product $TF_{ref} \times RTF(v_{tray}, TPD) \times S_{c,block}(v_{tray}) \times S_p(v_p)$ for several blocked fields. Correspondence should be within 1%.

4.4 Summary

Table 4.1 Summary of measurements to obtain the data needed for dose calculation procedures.

quantity	*field description*	*square fields*[1]	*rectangular fields*	*SSD*	*phantom*[2]
RDD	open	+	+[3]	100	fsp
	wedged	+	+[3]	100	fsp
S_{cp}	open	+	+[3]	100	fsp
	wedged	+	+[3]	100	fsp
S_c	open	+	+[4]	100	mp
	wedged	+	+[3]	100	mp
	tray	+	-	100	mp
WF_{ref}	wedged/open	10 cm x 10 cm	-	100	fsp
TF_{ref}	tray/open	10 cm x 10 cm	-	100	mp or fsp
RWF	wedged	+	+[3]	80, 100, 120	mp or fsp
RTF	tray	+	-	80, 100, 120	mp or fsp

1. For these measurements the side of the square fields can, for example, be set to 3, 4, 5, 6, 8, 10, 12, 15, 20, 25, 30, 35 and 40 cm.
2. fsp = full scatter phantom; mp = mini-phantom
3. For these sets of measurements a limited number of elongated fields has to be chosen for the purpose of checking the data against published data (e.g. S_p) and/or confirmation of the outcome of calculations; for example, the application of the equivalent square field method.
4. Full sets of rectangular fields are needed, with independent setting of the X- and Y-collimator jaw at, for example, 3, 4, 5, 6, 8, 10, 12, 15, 20, 25, 30, 35 and 40 cm. Fitting procedures may be applied to limit the number of measurements of rectangular fields.

5. Experimental data

S_{cp}, S_c and S_p data have been collected for a wide range of photon beam qualities (from ^{60}Co to 25 MV photon beams) and a variety of treatment machines, using the methods described in the previous sections. In table 5.1, some characteristics of these beams and machine types are listed. Nominal beam energies and quality indices have been tabulated. The last columns show whether data of square and rectangular fields or only square fields were available. The most typical observations will be briefly discussed in the following sections.

5.1 Total scatter correction factors, S_{cp}

5.1.1 S_{cp} for square fields

S_{cp} values determined in a number of photon beams are shown in figures 5.1.c to 5.8.c as a function of the side of a square field. The data given in these figures indicate that beams with the same nominal energy, but generated by different machines, give different S_{cp} values. Note that the S_{cp} curves from the GE-CGR accelerator beams are much steeper than those from other machines with the same nominal beam energy. This effect was observed earlier by several other groups [33,45,57] and is explained by the construction details of the treatment head (see figure 3.2). The flattening filter of GE-CGR machines is much wider, and is positioned at a more downstream position compared with other machines.

5.2 Collimator scatter correction factors, S_c

5.2.1 S_c for square fields

S_c values of the same beams are shown in figures 5.1.a to 5.8.a as a function of the side of a square field. For reasons of comparison, S_c was measured with a mini-phantom, also with a water-equivalent build-up cap in two ^{60}Co beams and in a 4 MV x-ray beam. Within the experimental uncertainty of approximately 0.5%, both methods yielded the same results. For higher nominal beam energies, larger differences were observed [73].

It can be noted that similar to the S_{cp} curves the S_c curves from the GE-CGR accelerator beams are much steeper than those of other machines. An overall variation of the S_c values of the order of 15% is observed for the GE-CGR accelerators compared with 8% for the other accelerators when varying the field sizes from 4 cm x 4 cm up to 40 cm x 40 cm.

Table 5.1 Some characteristics of the beams of which data are available. Indicated are: nominal accelerator potential (E), quality index (QI) and whether S_c and S_p data for square and rectangular fields (r), or only for square fields (s) are available.

#	*Manufacturer*[1]	*Type*	*E (MV)*	*QI*	*square (s) or rectangular (r) fields measured*	
					S_c	S_p
1	AECL	Theratron 780	^{60}Co	0.572	s	s[2]
2	Philips		^{60}Co	0.572	s	s[2]
3	Philips		^{60}Co	0.572	s	s[2]
4	Varian	Clinac-4	4	0.616	s	s
5	ABB	Dynaray-4	4	0.614	s	s
6	Philips	SL75-10	6	0.650	s	s
7	Siemens	MV	6	0.675	s	s
8	Philips	SL25	6	0.678	s	s
9	Varian	Clinac-6	6	0.650	s	s
10	GE-CGR	Saturne-41	6	0.670	r	r
11	Philips	SL15	6	0.680	r	r
12	Philips	SL20	6	0.679	r	r
13	ABB	Dynary-20	6	0.687	r	r
14	Philips	SL75-20	8	0.714	s	s
15	Philips	SL75-14	8	0.714	s	s
16	GE-CGR	Saturne-41	10	0.729	r	r
17	Siemens	Mevatron74	10	0.734	s	s
18	Philips	SL15	10	0.737	r	r
19	Philips	SL75-20	16	0.763	s	s
20	ABB	Dynaray-20	16	0.772	r	r
21	Philips	SL20	18	0.774	r	r
22	GE-CGR	Saturne	18	0.758	s	s
23	GE-CGR	Saturne	23	0.783	s	s
24	Philips	SL25	25	0.783	r	r
25	GE-CGR	Sagittaire	25	0.783	s	s

[1] AECL/Theratronics, Kanata, Canada; GE-CGR, Buc, France; ABB, Baden, Switzerland; Varian, Palo Alto, USA; Philips, Crawley, UK; Siemens, Erlangen, Germany.

[2] S_p data for the ^{60}Co beams were taken from reference [8] and recalculated to d_{ref}.

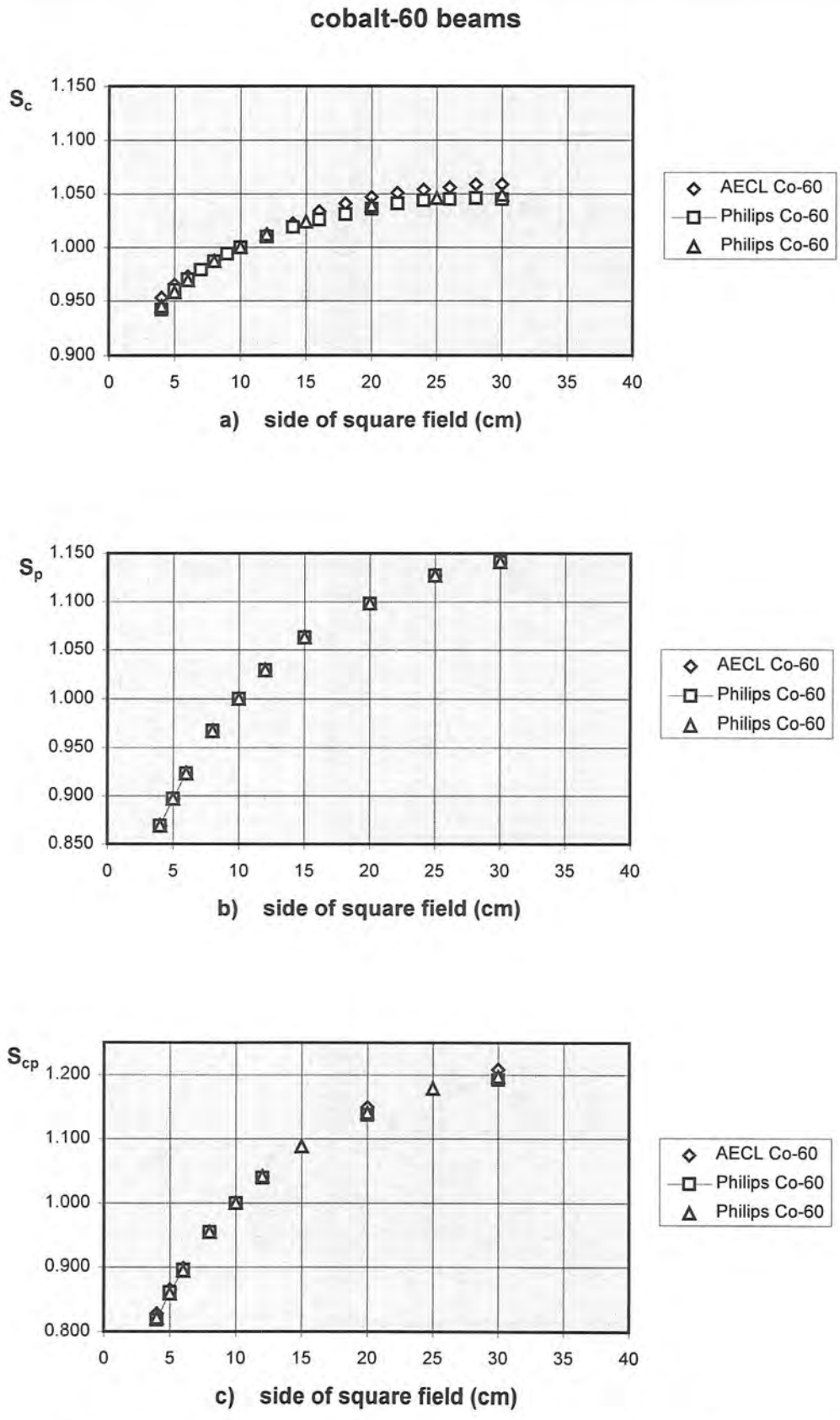

Figure 5.1 S_c, S_p and S_{cp} data as a function of the side of a square field of ^{60}Co beams (beams 1-3). Data are normalized at depth d_{ref}.

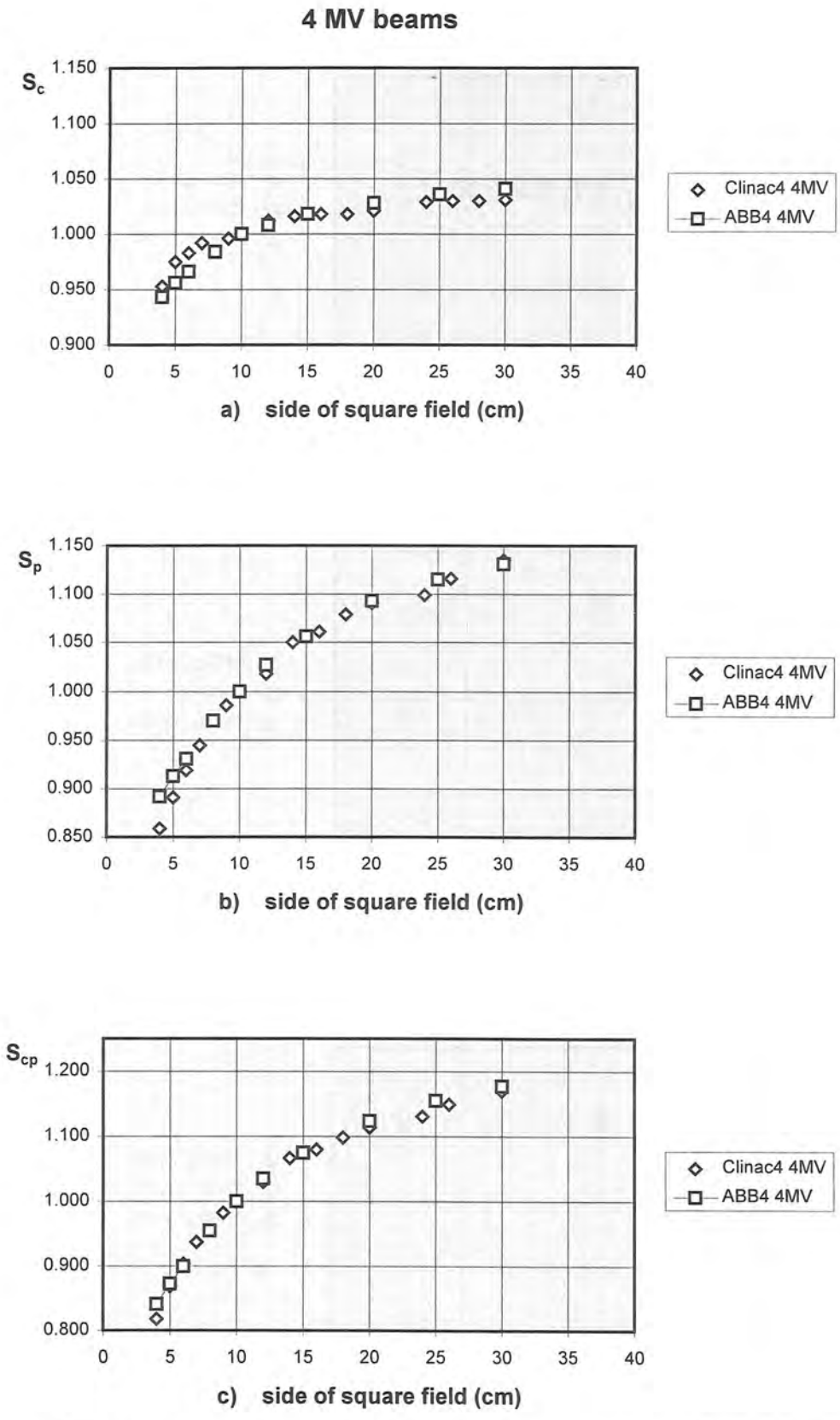

Figure 5.2 S_c, S_p and S_{cp} data as a function of the side of a square field of 4 MV beams (beams 4-5). Data are normalized at depth d_{ref}.

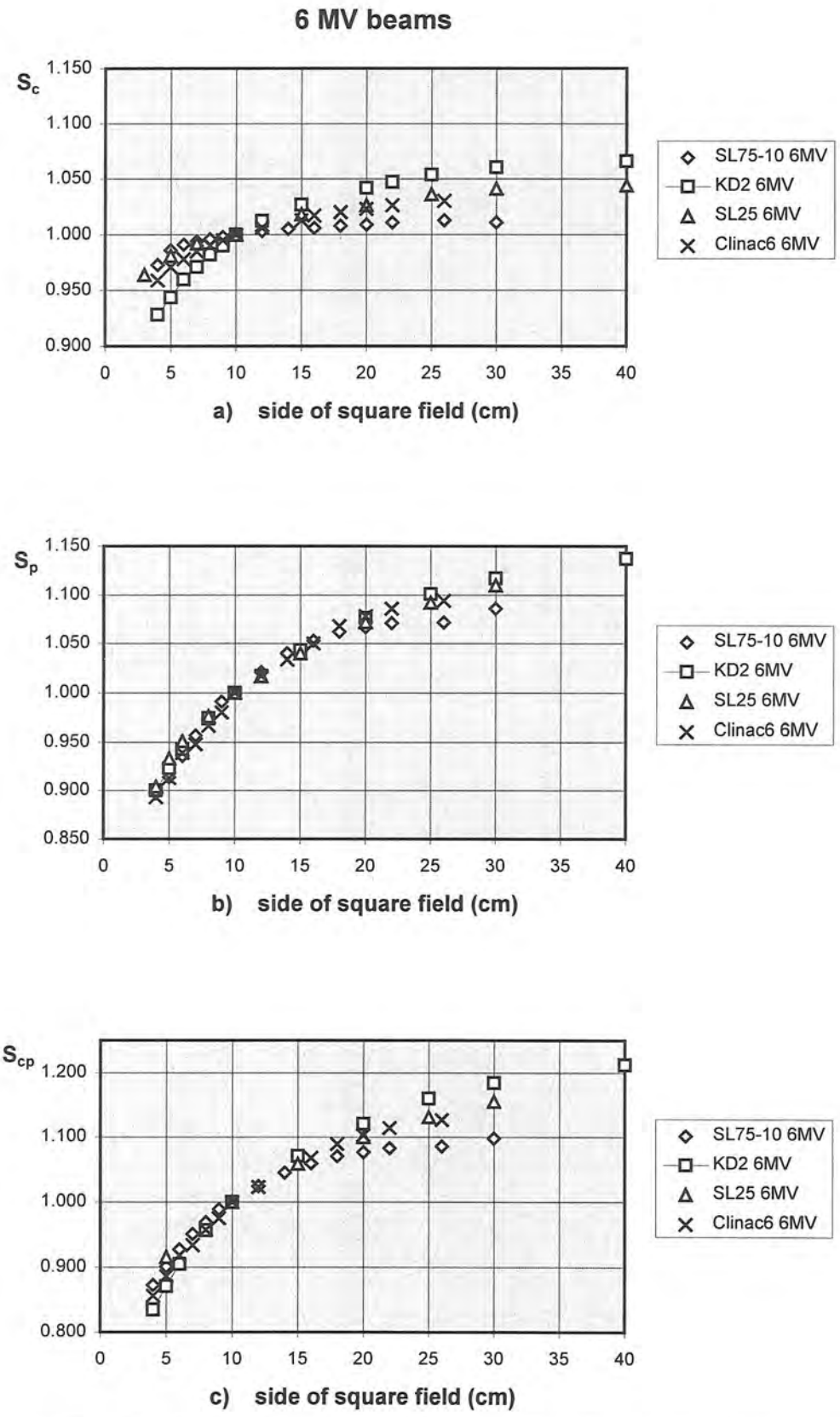

Figure 5.3 S_c, S_p and S_{cp} data as a function of the side of a square field of the first four 6 MV beams of table 5.1 (beams 6-9). Data are normalized at depth d_{ref}.

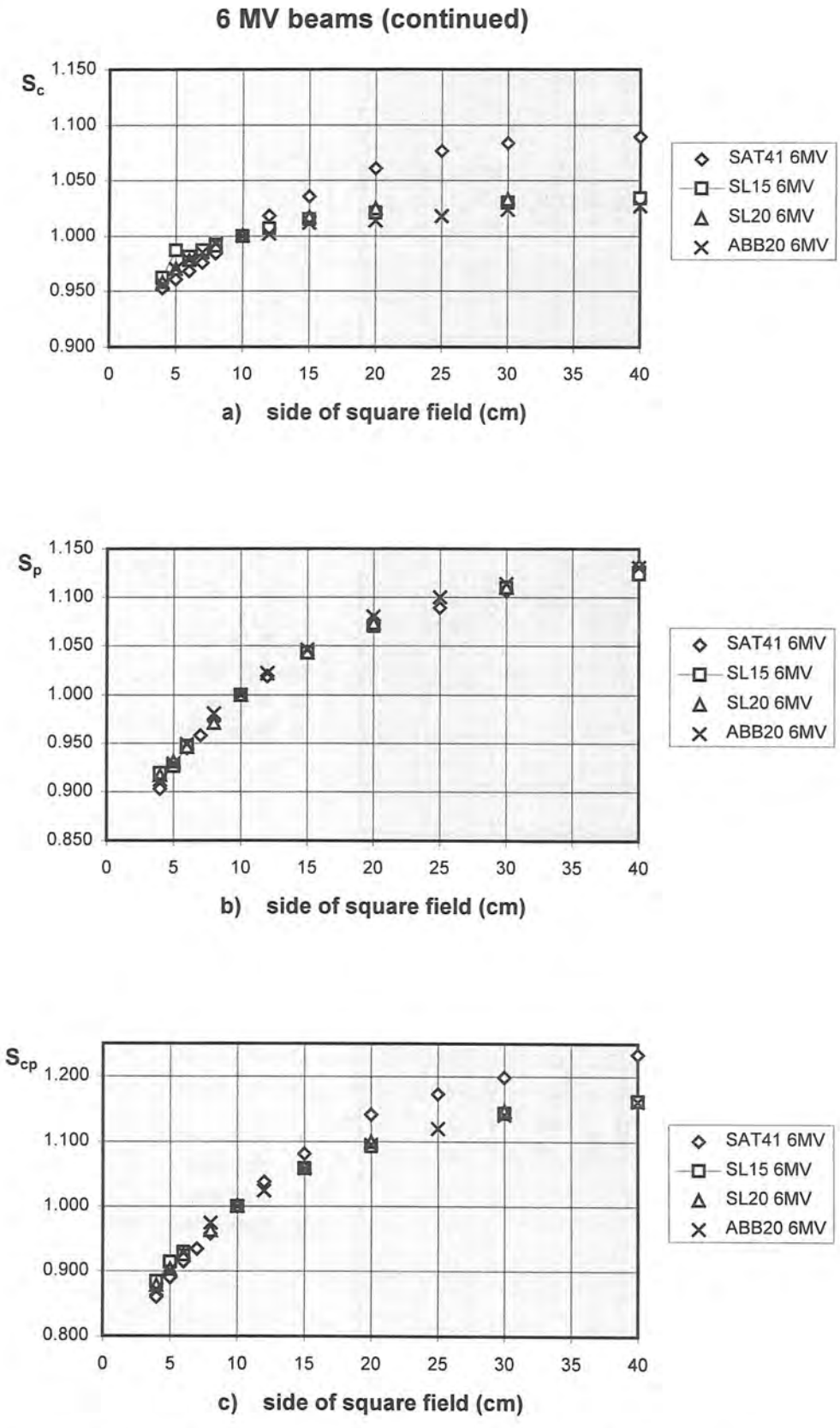

Figure 5.4 S_c, S_p and S_{cp} data as a function of the side of a square field of 6 MV beams (continued with beams 10-13). Data are normalized at depth d_{ref}.

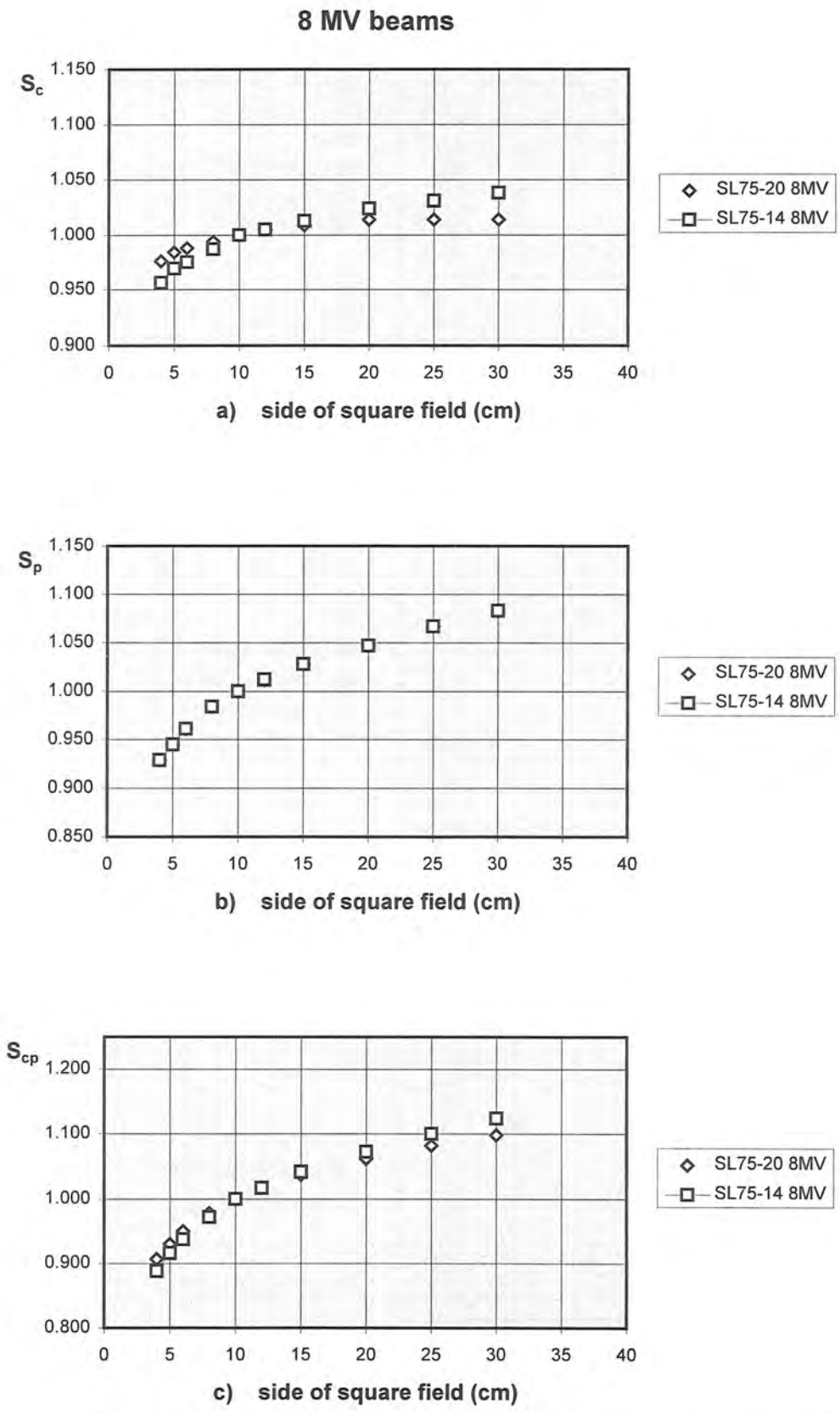

Figure 5.5 S_c, S_p and S_{cp} data as a function of the side of a square field of 8 MV beams (beams 14-15). Data are normalized at depth d_{ref}.

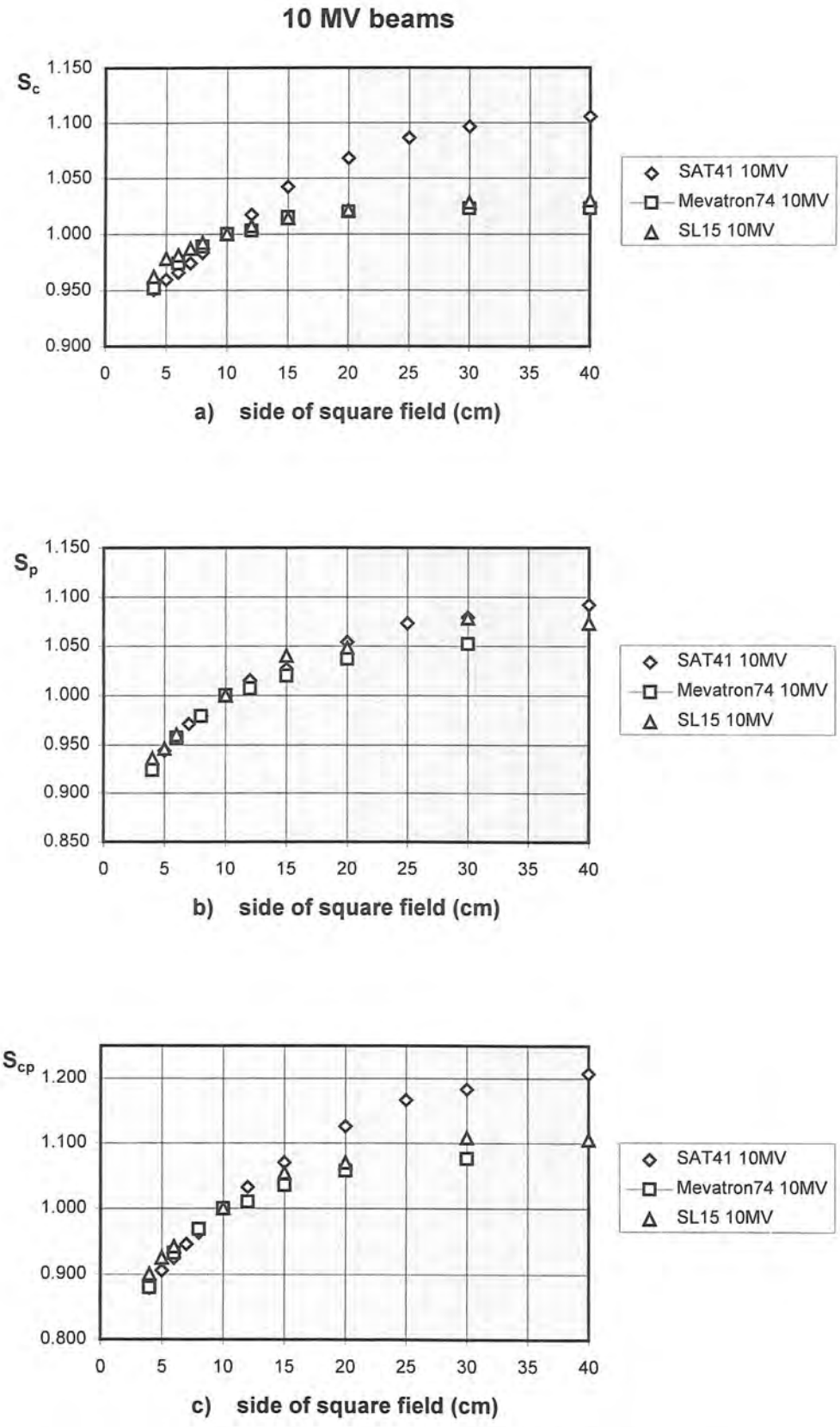

Figure 5.6 S_c, S_p and S_{cp} data as a function of the side of a square field of 10 MV beams (beams 16-18). Data are normalized at depth d_{ref}.

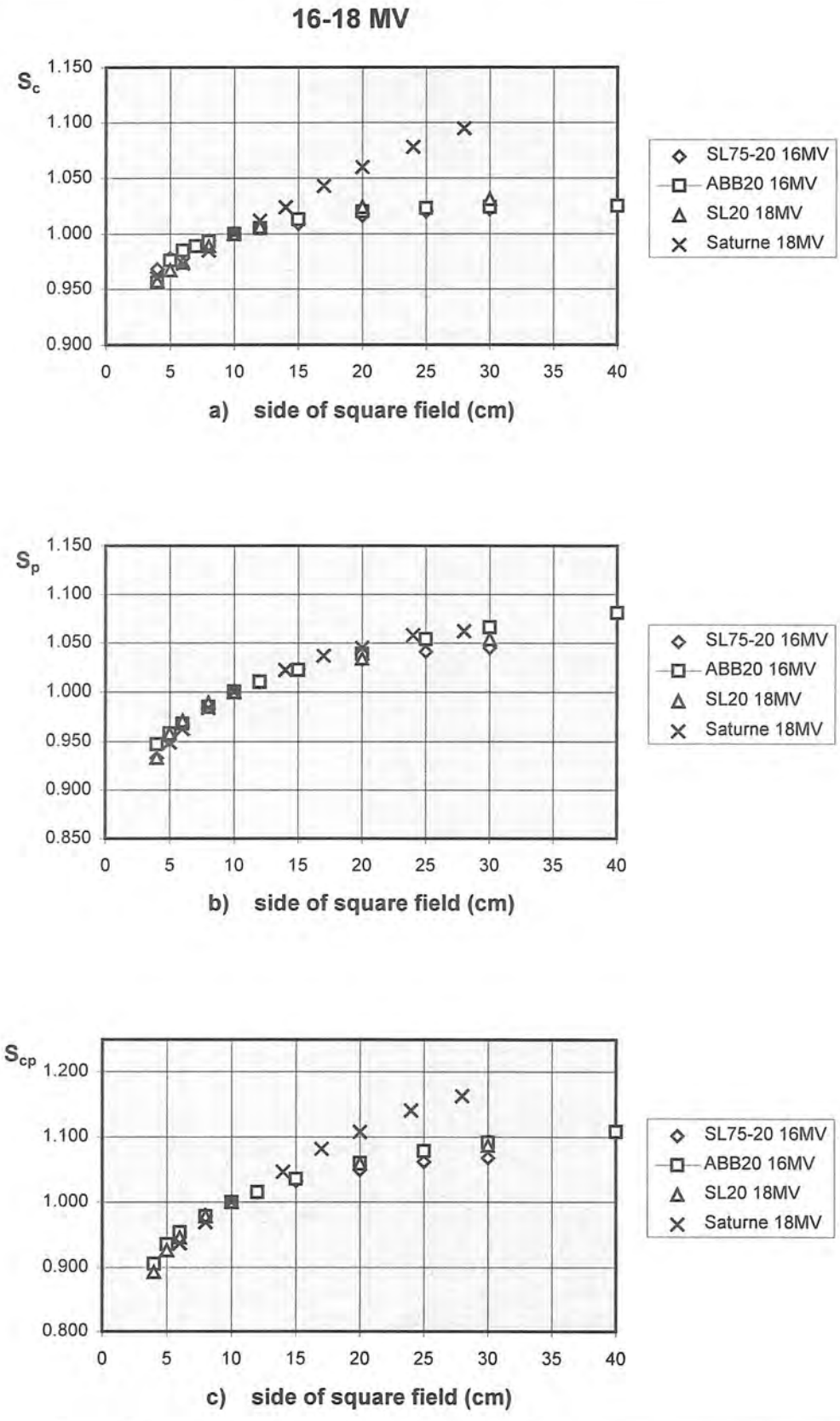

Figure 5.7 S_c, S_p and S_{cp} data as a function of the side of a square field of 16-18 MV beams (beams 19-22). Data are normalized at depth d_{ref}.

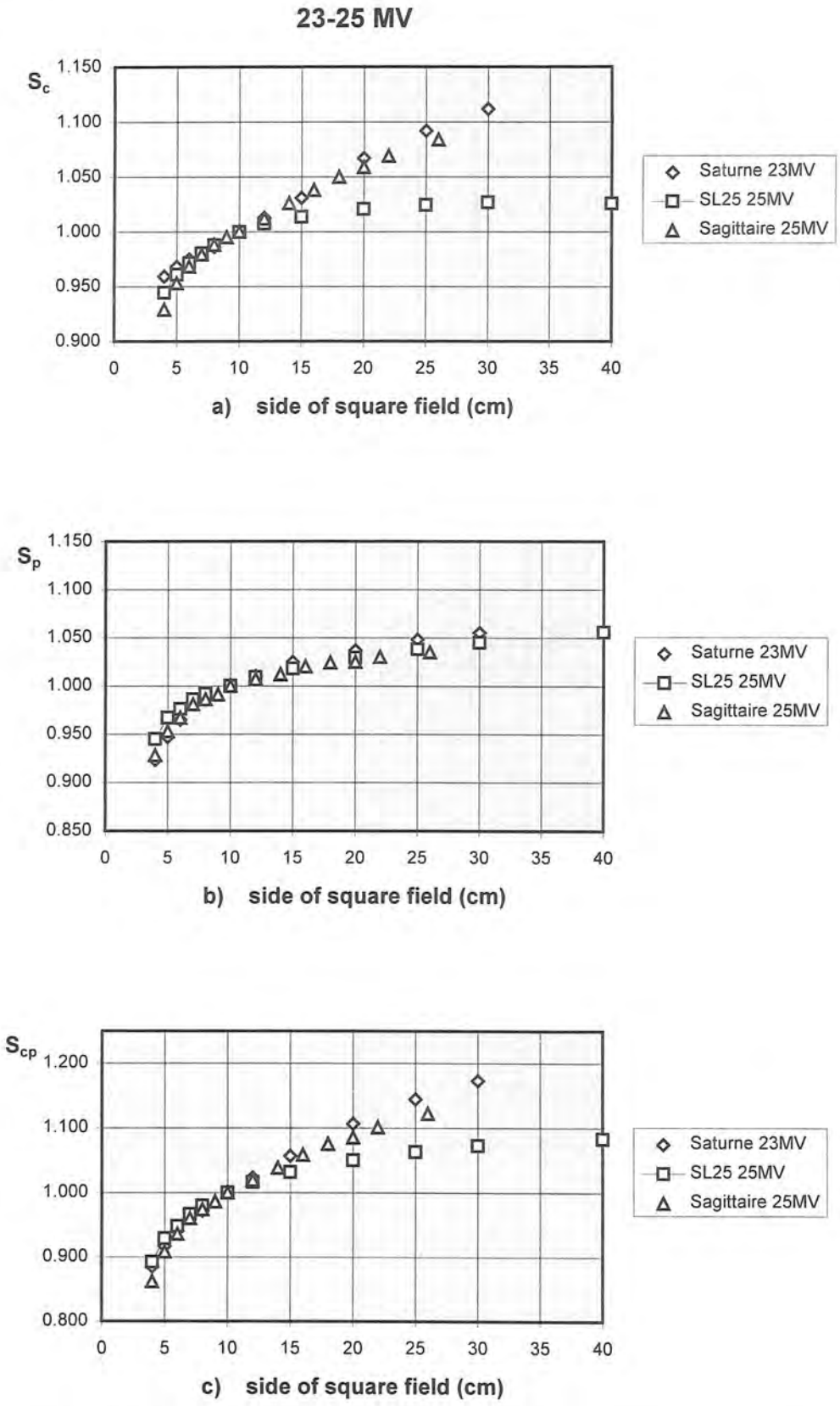

Figure 5.8 S_c, S_p and S_{cp} data as a function of the side of a square field of 23-25 MV beams (beams 23-25). Data are normalized at depth d_{ref}.

5.2.2 S_c for rectangular fields

For several beams, S_c data have been determined for rectangular fields as a function of the independent setting of the X and Y collimators (see table 5.1). These experimental data showed that S_c is an asymmetrical function of the X and Y collimator settings, as observed by various other groups [24,33,57,58]. The order of magnitude of this effect (the collimator exchange effect, CEE) is about 2% for the linear accelerators investigated in this report. Figures 5.9.a and 5.9.b illustrate this effect for two different machines.

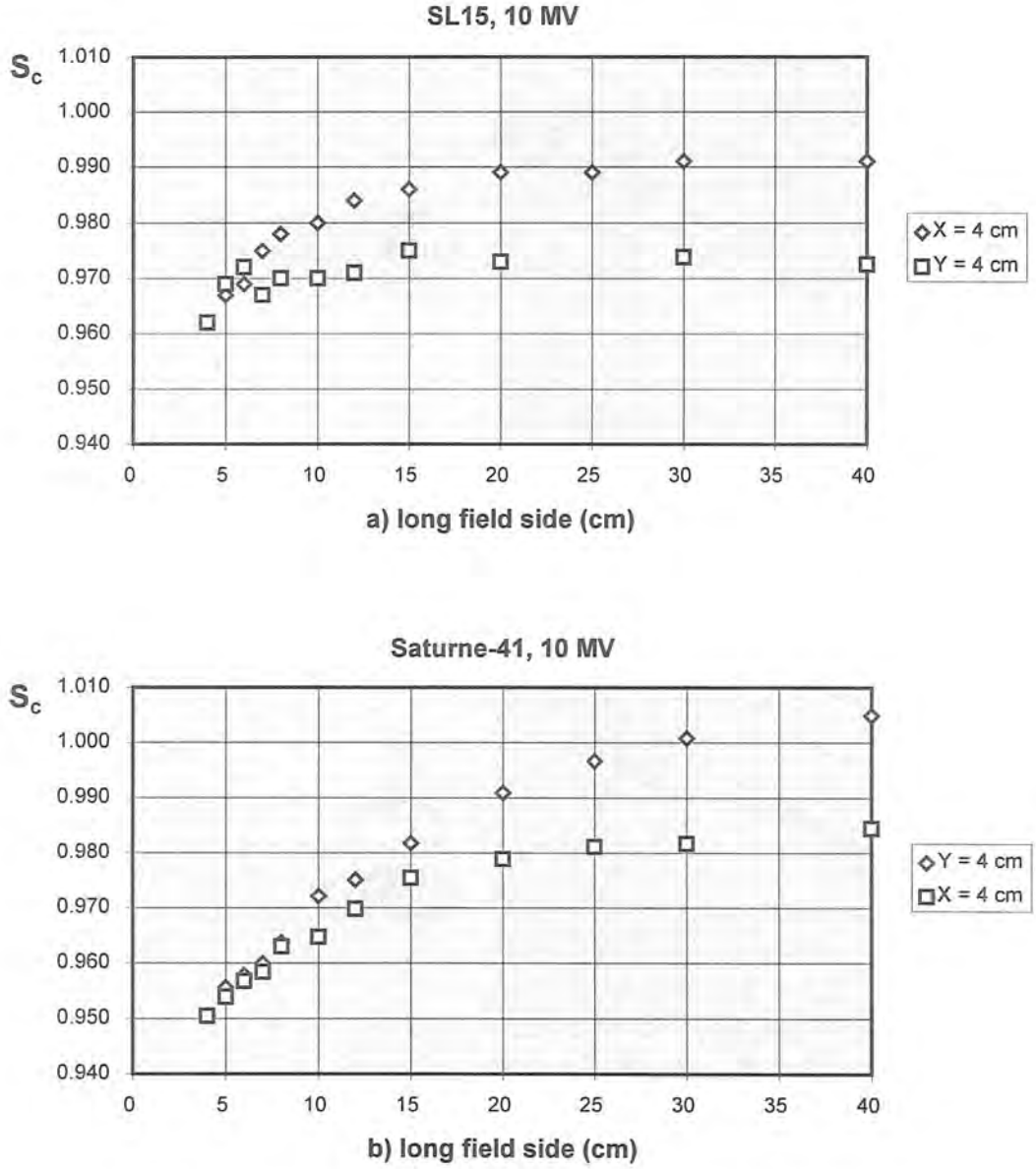

Figure 5.9 The collimator exchange effect measured in a Philips SL15 10 MV x-ray beam (a) and in a GE-CGR Saturne-41 10 MV x-ray beam (b). S_c is shown as a function of the long field side, set-up with either the X or Y collimator fixed to 4 cm.

5.2.3 Influence of SSD and d_{ref} on S_c

The influence of the choice of SSD and d_{ref} on the value of S_c was measured in a high and a low quality photon beam. Data were obtained from a 25 MV x-ray beam for SSD = 90 cm and d_{ref} = 20 cm, for SSD = 100 cm and d_{ref} = 10 cm, and for SSD = 150 cm and d_{ref} = 10 cm. These data are presented as a function of the the side of a square field at SAD in figure 5.10.a. A similar experiment was performed in a 4 MV beam, where the following combinations of SSD and d_{ref} were used (in cm): 80 / 10; 105 / 10; 65 / 10 and 80 / 15. The results are shown in figure 5.10.b.

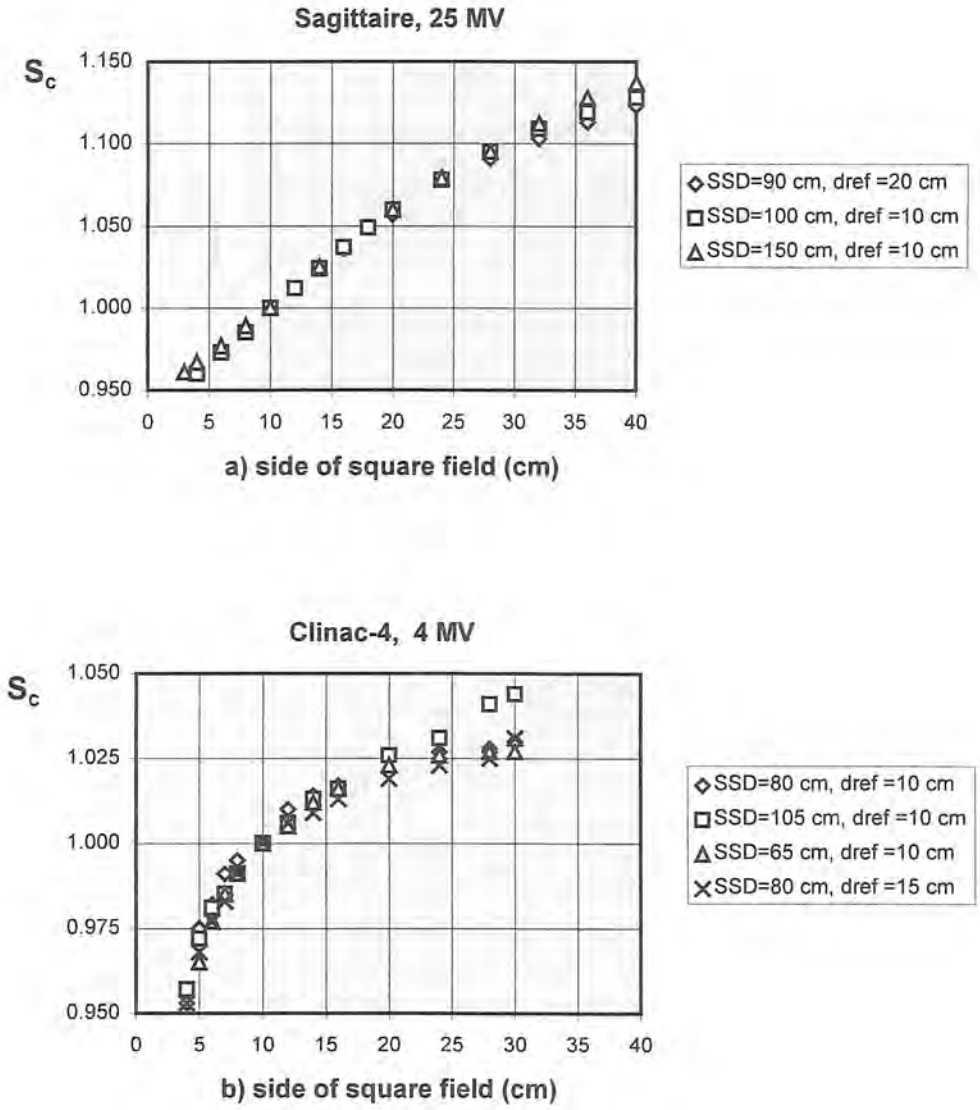

Figure 5.10 The influence of the source-surface distance on S_c measured in two different beams, 25 MV (a) and 4 MV (b); see text for further details.

From these results it can be concluded that:

- S_c is independent of the choice of SSD within the range of clinically applied distances;
- S_c does not depend on the choice of the depth d_{ref}, provided d_{ref} is beyond the range of the contaminating electrons.

5.2.4 Influence of a wedge on S_c

The influence of the presence of a wedge on the value of S_c has been the subject of several studies [22,61,75]. As an example, S_c data of the 6, 10 and 25 MV photon beams of a Saturne-43 linear accelerator (GE-CGR, Buc, France) are shown here. These data are presented in figure 5.11 as a function of the side of the square field, obtained with a mini-phantom at SSD = 100 cm and a measurement depth of 10 cm. The 10 cm x 10 cm field is used as the reference field. Open symbols are used in this graph for the open beams, closed symbols for the wedged beams. For a specified field size, the relative wedge transmission factor, RWF, can be deduced from the ratio of $S_{c,w}$ and $S_{c,open}$. For this machine, typical values of the RWF are found of approximately 2.5% for the largest square field size. For other machines, however, the values of RWF are more or less pronounced, depending on the construction and material of the wedge and its position in the head of the treatment machine. Values for RWF up to 8% have been reported [22,61,75].

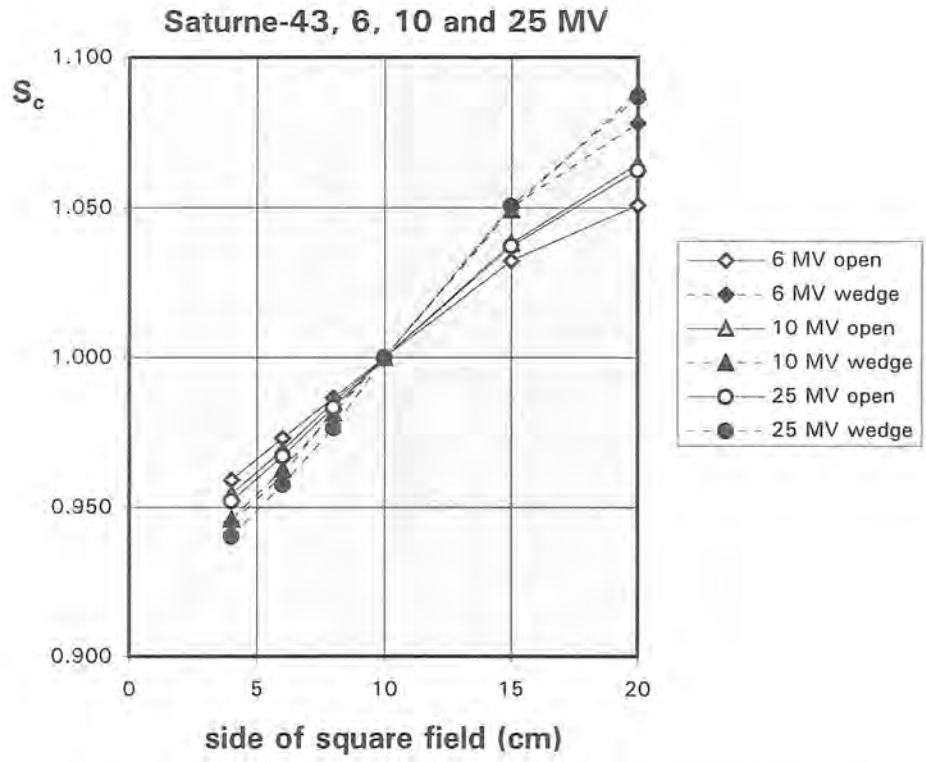

Figure 5.11 S_c data with and without a 60° wedge in the beam as a function of the side of a square field for three different nominal photon beam energies of a Saturne-43 linear accelerator.

5.3 Phantom scatter correction factors, S_p

5.3.1 S_p for square fields

S_p data have been derived from the S_{cp} and S_c data for each photon beam quality under investigation and for each field size according to expression (2.1.3). The results are presented as a function of the side of a square field in figures 5.1.b to 5.8.b. Within the experimental uncertainty, which is less than approximately 1%, the S_p curves of different machines with the same QI coincide. The overall variation in S_p with field size depends strongly on the beam quality. For S_p defined at the reference depth of 10 cm, this variation is 0.87 to 1.15 for a ^{60}Co beam, and 0.93 to 1.06 for a 25 MV x-ray beam for the range of field sizes of 4 cm x 4 cm up to 40 cm x 40 cm.

The S_p data for several square field sizes are shown as a function of the quality index in figure 5.12. From this plot it can be concluded that S_p is a smooth function of the beam quality.

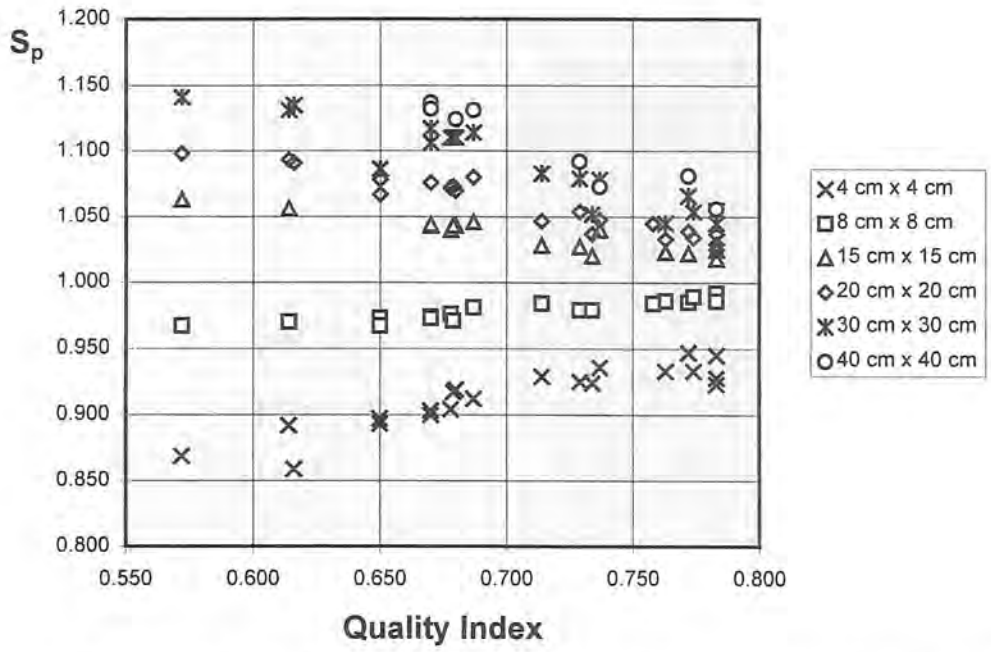

Figure 5.12 S_p data for a number of square field sizes, presented as a function of the quality index.

Based on the same experimental data, a complete set of phantom scatter factors was constructed by Storchi and van Gasteren [56] as a function of the field size and the quality index (table 5.2). The authors state that the error, made by applying the phantom scatter factor values from the table rather than measuring them separately, is less than 1%.

Table 5.2 The phantom scatter factor S_p, defined at the reference depth of 10 cm. This table has been computed from S_p values measured at 27 different beam qualities for square fields of various sizes. (From [56]).

field size	*Quality index*										
(cm)	*.600*	*.620*	*.640*	*.660*	*.680*	*.700*	*.720*	*.740*	*.760*	*.780*	*.800*
4.0	0.858	0.875	0.889	0.901	0.911	0.919	0.925	0.930	0.932	0.934	0.934
5.0	0.890	0.902	0.912	0.921	0.929	0.936	0.942	0.947	0.951	0.954	0.957
6.0	0.917	0.926	0.934	0.941	0.948	0.953	0.958	0.962	0.965	0.968	0.970
7.0	0.942	0.948	0.953	0.958	0.962	0.966	0.970	0.973	0.976	0.979	0.981
8.0	0.965	0.968	0.971	0.973	0.976	0.978	0.980	0.983	0.985	0.987	0.989
9.0	0.984	0.985	0.986	0.987	0.989	0.990	0.991	0.992	0.993	0.994	0.994
10.0	1.000	1.000	1.000	1.000	1.000	1.000	1.000	1.000	1.000	1.000	1.000
12.0	1.030	1.027	1.024	1.021	1.019	1.016	1.014	1.013	1.011	1.010	1.009
14.0	1.052	1.047	1.042	1.038	1.034	1.030	1.026	1.023	1.020	1.018	1.016
16.0	1.067	1.061	1.056	1.051	1.047	1.042	1.037	1.033	1.029	1.025	1.021
18.0	1.079	1.074	1.069	1.063	1.058	1.053	1.047	1.042	1.036	1.030	1.024
20.0	1.099	1.091	1.083	1.076	1.068	1.061	1.054	1.048	1.041	1.035	1.028
22.0	1.108	1.100	1.093	1.085	1.077	1.070	1.062	1.055	1.047	1.039	1.032
24.0	1.115	1.108	1.101	1.093	1.085	1.077	1.069	1.061	1.052	1.044	1.035
26.0	1.121	1.115	1.107	1.100	1.092	1.084	1.075	1.066	1.057	1.047	1.037
28.0	1.128	1.121	1.114	1.106	1.098	1.089	1.080	1.070	1.060	1.050	1.040
30.0	1.134	1.127	1.120	1.112	1.103	1.094	1.084	1.074	1.064	1.053	1.042
32.0	1.141	1.134	1.125	1.117	1.108	1.098	1.088	1.078	1.067	1.056	1.044
34.0	1.148	1.140	1.131	1.122	1.112	1.102	1.091	1.081	1.070	1.058	1.047
36.0	1.156	1.146	1.137	1.126	1.116	1.105	1.094	1.083	1.072	1.061	1.049
38.0	1.164	1.153	1.142	1.131	1.120	1.108	1.097	1.086	1.074	1.063	1.051
40.0	1.172	1.160	1.147	1.135	1.123	1.111	1.099	1.088	1.076	1.065	1.054

These data have been used to calculate phantom scatter correction factors for use in the isocentric formalism, S_p^{iso}. Results are presented in table 5.3. The relations between the quantities in the fixed SSD and in the isocentric formalism are given in Appendix 8.3 of this report. For the conversion of S_p data in S_p^{iso} data, expression (8.3.7) was used. Differences between the tables amount up to 0.9%, especially for the low energy beams and the larger field sizes [71].

Table 5.3 The phantom scatter factor S_p^{iso}, defined at the reference depth of 10 cm for the isocentric treatment set-up. This table has been derived from the data of table 5.2.

field size	*Quality index*										
(cm)	*.600*	*.620*	*.640*	*.660*	*.680*	*.700*	*.720*	*.740*	*.760*	*.780*	*.800*
4.0	0.859	0.877	0.892	0.904	0.914	0.921	0.926	0.931	0.931	0.932	0.931
5.0	0.888	0.902	0.913	0.923	0.930	0.937	0.942	0.946	0.948	0.950	0.952
6.0	0.916	0.926	0.934	0.941	0.947	0.952	0.957	0.961	0.963	0.966	0.968
7.0	0.940	0.947	0.953	0.959	0.963	0.967	0.970	0.973	0.975	0.977	0.979
8.0	0.962	0.967	0.970	0.974	0.976	0.978	0.981	0.983	0.985	0.987	0.989
9.0	0.983	0.985	0.986	0.987	0.988	0.989	0.990	0.992	0.993	0.994	0.995
10.0	1.000	1.000	1.000	1.000	1.000	1.000	1.000	1.000	1.000	1.000	1.000
12.0	1.029	1.026	1.024	1.022	1.019	1.017	1.015	1.013	1.011	1.010	1.010
14.0	1.053	1.049	1.044	1.039	1.035	1.030	1.027	1.024	1.021	1.018	1.017
16.0	1.072	1.065	1.059	1.054	1.048	1.043	1.037	1.033	1.029	1.026	1.023
18.0	1.085	1.078	1.072	1.066	1.060	1.054	1.047	1.042	1.037	1.032	1.027
20.0	1.097	1.090	1.084	1.077	1.070	1.063	1.056	1.050	1.043	1.036	1.030
22.0	1.115	1.106	1.097	1.089	1.079	1.071	1.063	1.056	1.048	1.041	1.034
24.0	1.124	1.114	1.106	1.097	1.087	1.079	1.070	1.062	1.053	1.044	1.037
26.0	1.130	1.122	1.114	1.105	1.094	1.086	1.077	1.068	1.058	1.049	1.040
28.0	1.136	1.128	1.120	1.111	1.101	1.092	1.082	1.072	1.062	1.052	1.042
30.0	1.142	1.134	1.126	1.117	1.107	1.097	1.087	1.076	1.066	1.055	1.045
32.0	1.148	1.140	1.132	1.123	1.112	1.102	1.091	1.080	1.069	1.057	1.047
34.0	1.154	1.146	1.137	1.128	1.116	1.106	1.095	1.084	1.072	1.060	1.049
36.0	1.160	1.152	1.142	1.132	1.121	1.110	1.098	1.087	1.075	1.063	1.051
38.0	1.167	1.157	1.147	1.137	1.124	1.113	1.101	1.089	1.077	1.065	1.053
40.0	1.175	1.163	1.153	1.140	1.128	1.116	1.104	1.091	1.079	1.067	1.055

5.3.2 S_p for rectangular fields

Because S_p represents the dose due to radiation scattered from the phantom volume to the measuring point at the central axis, S_p should be a symmetrical function of the field dimensions (section 3). Consequently, $S_p(X=a,Y=b)$ should be equal to $S_p(X=b,Y=a)$. For the beams of table 5.1, where S_{cp} and S_c were measured at independent settings of the X and Y collimator, this has been confirmed within the experimental uncertainty.

5.3.3 Comparison of measured and calculated S_p values for rectangular fields

The method to calculate S_p values for rectangular and arbitrarily shaped fields, as described in Appendix 8.4, using S_p data measured in square fields, has been applied for a number of beam qualities: S_p data were calculated for ^{60}Co and 6, 10 and 25 MV photon beams for rectangular field sizes with dimensions of X and Y between 4 and 40 cm. The overall agreement between calculation and measurement was better than 0.5% [56,70].

The use of tables of equivalent square fields for the derivation of the phantom scatter correction factor and phantom scatter related quantities, such as PDD and TPR, of rectangular fields is further discussed in Appendix 8.6 of this report.

5.

6. Recommendations

It is recommended to separate the total scatter correction factor S_{cp} in two parts: the collimator scatter correction factor S_c and the phantom scatter correction factor S_p. The use of S_c and S_p is recommended for calculations of treatment time and monitor units in clinical situations, as described in sections 2 and 3.

S_{cp} and S_c are ratios of measured values, defined for each field size and normalized to unity for the reference field of 10 cm x 10 cm, the reference depth of 10 cm and the reference SSD (equal to SAD). This reference irradiation set-up should be the same, irrespective of the photon beam energy.

S_c data have to be determined with a narrow cylindrical beam-coaxial phantom (mini-phantom) according to the method described in section 4. A description of the mini-phantom is given in Appendix 8.8. S_c factors have to be obtained for square and rectangular field sizes, with field sizes in the range used in clinical practice, i.e. from a minimum field size of 4 cm x 4 cm or smaller, up to 40 cm x 40 cm. Data for rectangular fields can be obtained by direct measurement and/or by interpolation or data fitting methods. In this way, a full two-dimensional table of S_c values has to be obtained.

S_{cp} data have to be determined by using a full scatter water phantom, according to the method described in section 4. S_{cp} values have to be measured for square fields. For consistency checks, the same measurements should be performed for a number of rectangular fields.

S_p factors are derived with expression (2.1.3) from measured S_{cp} and S_c data for square field sizes. Results should be compared with published data; see section 5.3.1. Results of rectangular or arbitrarily shaped fields should be compared with interpolated values from the table, or with S_p data taken for the equivalent square field ([8,9], see Appendices 8.4 and 8.6).

Methods to reduce the number of measurements of S_{cp} and S_c in rectangular fields can be applied. Several references to methods for accurate data fitting are given in this report, see section 3.1.1 and Appendix 8.7. It is recommended, in these cases, to check and verify the product of S_c x S_p data for a number of elongated fields against direct measurement of S_{cp}. Differences between measured and calculated data should be within 1%.

Reference wedge and tray transmission factors have to be determined for the reference irradiation set-up. Field size and SSD dependence of the wedge and tray factors have to be measured and accounted for in the relative wedge transmission factor and the relative tray transmission factor. The procedures are

described in section 3. Equations for calculation of monitor units given in section 2 should be replaced by those given in section 3 if beam modifiers are applied.

A summary of the measurements needed to obtain the data for the calculations is given in table 4.1.

It is strongly recommended to compare the data found in the clinic with the data presented in this report. Note that especially S_c data depend on the beam defining system and may vary considerably from one treatment machine to the other. S_c data provided in the figures have to be considered as a first estimate. S_p data are machine independent, but are uniquely related to the quality index of the beam. If the measured S_p data differ from those presented in this report, further investigation of the dosimetry procedures is recommended.

7. Acknowledgements

The data presented in this report have been measured by physicists in a large number of radiotherapy departments in The Netherlands. Those who have contributed to this work are gratefully acknowledged by the members of the task group for their efforts, their helpful discussions and comments on the draft of this report and for making the measurement data available.

7.

8. Appendices

8.1 Definition of scatter correction factors

In this report, the total scatter correction factor S_{cp} is defined as the absorbed dose per monitor unit, measured at the reference depth and the reference SSD for a specified collimator setting and a specified field size at the phantom surface, normalized to unity for the reference irradiation set-up:

$$S_{cp}(v_c,v_p,d_{ref},f_{ref}) = D(v_c,v_p,d_{ref},f_{ref}) / D_{ref} \qquad (8.1.1)$$

Here, v_c and v_p express the field size at the SAD, defined by the collimator jaws, and the field size at the phantom surface, respectively. The reference irradiation set-up is defined as: a collimator setting yielding a 10 cm x 10 cm field at the isocentre $v_{c,ref}$; a phantom depth equal to d_{ref} (= 10 cm); and an SSD equal to the SAD; the field size $v_{p,ref}$ at the phantom surface is then numerically equal to $v_{c,ref}$. From this definition it follows that d_{ref} and f_{ref} are fixed values and, therefore, S_{cp} depends only on the variables v_c and v_p: $S_{cp}(v_c,v_p)$.

A less strict definition is given by several other authors, and was also applied previously in reference [64], where S_{cp} was deduced *without defining* f_{ref},

$$S_{cp}(v_c,v_p,d_{ref}) = D(v_c,v_p,d_{ref}) / D(v_{c,ref},v_{p,ref},d_{ref}) \qquad (8.1.2)$$

S_{cp} is then written in those papers as:

$$S_{cp}(v_c,v_p,d_{ref}) = S_c(v_c,v_p,d_{ref}) \times S_p(v_c,v_p,d_{ref}) \qquad (8.1.3)$$

In the definitions of S_{cp} given by equations (8.1.2) and (8.1.3) d_{ref} is a variable and f_{ref} is not specified. Both d_{ref} and f_{ref} can be chosen freely by the user, e.g., at d_{max}, 5 or 10 cm for d_{ref} [34,64]. Consistency in definition requires that S_c data, measured for different but well-described phantom depths or SSD, should convert unambiguously into each other. This conversion is not a problem, as long as the phantom depth has been chosen beyond the range of the electron contamination [64]. However, difficulties arise when S_c values are determined within the range of the electron contamination, i.e. when S_c values are measured at shallow depths, see Appendix 8.2.

A second problem arises in the conversion, if S_{cp} has been defined for SSD values not equal to the SAD. In that situation the requirements with respect to $v_{c,ref}$ and $v_{p,ref}$ can not be fulfilled simultaneously. A choice between both reference field sizes has to be made and redefinition is then needed.

In conclusion, the mutual relation between S_c data, determined for different but well-described phantom depths and SSDs, is essentially a part of the S_{cp}

definition according to equation (8.1.2), to maintain the consistency of that definition. The S_{cp} definition according to equation (8.1.1) is inherently consistent due to the requirement that $D(v_c,v_p,d_{ref},f_{ref})$ and D_{ref} have to be determined under the same conditions, i.e. S_{cp} is defined for only a single phantom depth and SSD. Conversion problems of S_{cp} values, defined according to equation (8.1.2), to dose values at other phantom depths or SSDs remain, therefore, part of the dose calculation algorithms. The more restrictive S_{cp} definition in equation (8.1.1) is preferred over the one in equation (8.1.2).

8.2 Scatter correction factors at other reference depths

Within the context of this report S_c, S_p, and S_{cp} values have been strictly defined for a reference irradiation set-up (Appendix 8.1). However, the reference values are a particular choice and these conventions may differ in principle from one radiotherapy department to another. Different definitions of the scatter correction factors found in the literature or required for a treatment planning system, can be reasons to deviate from what is adopted here. A comparison of scatter correction factors measured in different radiotherapy departments might be helpful in quality control programs. A conversion is then required. The reference field size is generally taken equal to 10 cm x 10 cm and the reference SSD equal to SAD. Conversion methods for other reference field sizes are therefore considered to be irrelevant; for other SSDs an example is given in Appendix 8.3. Differences in the choice of the reference depth are most likely to occur.

Two practical situations can now be distinguished: the reference depth, which should be taken equal for field sizes v and v_{ref} (see figure 8.1), is defined:

a) beyond the range of electron contamination, but different from the reference depth of 10 cm given in this report;

b) within the range of electron contamination.

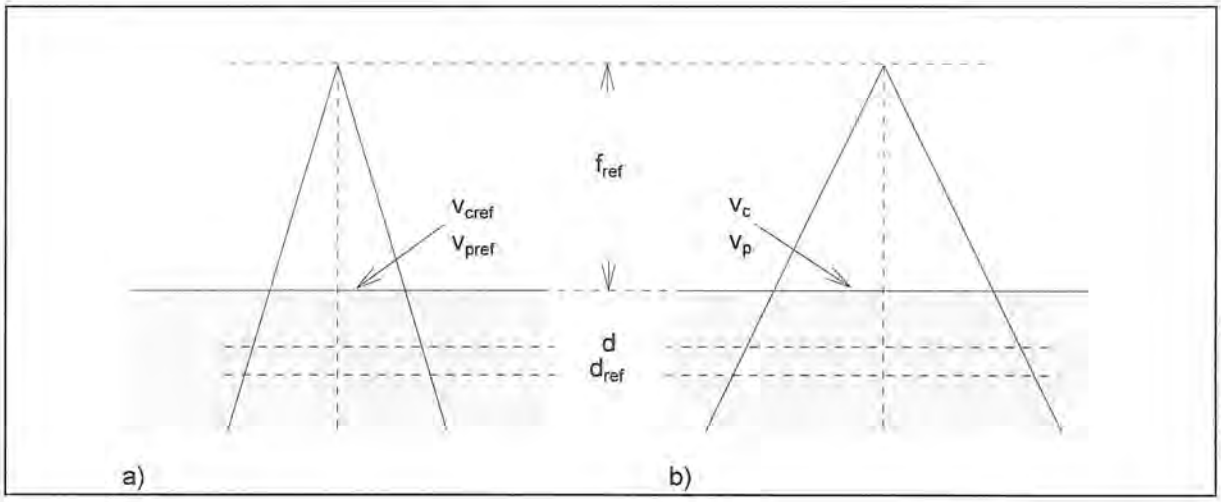

Figure 8.1 Two dose points, one at the reference depth, d_{ref}, and one at the new depth, d. a) in the reference field, v_{ref}; b) in an arbitrary field, v; both with a source-surface distance equal to f_{ref}.

Situation a: beyond the range of the electron contamination

For this situation, the S_c definition is basically identical to the one recommended in this report, as long as the SSD is equal to SAD. The conversion can be obtained using equation (2.3.1):

$$S_c(v_c,d) \times S_p(v_p,d) = D(v_c,v_p,d,f_{ref}) / D(v_{c,ref},v_{p,ref},d,f_{ref}) \quad (8.2.1)$$

in which the phantom depth, d, is now introduced as a variable. The value of d can be defined by the user, e.g. 10 cm, as is done in this report. As discussed in section 2 and shown by van Gasteren et al. [64], in this case the magnitude of S_c does not depend on the phantom depth, i.e.:

$$S_c(v_c,d) = S_c(v_c,d_{ref}) \quad (8.2.2)$$

Both dose values in equation (8.2.1) can be rewritten to dose values at other phantom depths by:

$$D(v_c,v_p,d,f_{ref}) = D(v_c,v_p,d_{ref},f_{ref}) \times RDD(v_c,v_p,d,f_{ref}) \quad (8.2.3)$$

By combining equations (8.2.1) to (8.2.3), S_p can be written as [65]:

$$S_p(v_p,d) = S_p(v_p,d_{ref}) \times RDD(v_c,v_p,d,f_{ref}) / RDD(v_{c,ref},v_{p,ref},d,f_{ref}) \quad (8.2.4)$$

Equations (8.2.2) and (8.2.4) can be applied without any limitation, as long as the phantom depths have been chosen beyond the range of electron contamination.

Situation b: within the range of the electron contamination

If measurements of S_c are performed in a radiotherapy department at shallow depths d, the resulting values, $S_c(v_c,d)$, will include the dose contribution of the electron contamination. In that case, equation (8.2.2) is no longer valid. As discussed in Appendix 8.1, a conversion from $S_c(v_c,d)$ to $S_c(v_c,d_{ref})$ or vice versa, would require an exact knowledge of the dose contribution of the electron contamination as a function of field size and depth. Algorithms calculating that conversion are not readily available (e.g., [5,6,71]) and conversion has, therefore, to be done based on measurements. It is easy to show that the ratio of measured $S_c(v_c,d)$ and $S_c(v_c,d_{ref})$ values just yields that conversion factor, $S_{c,el}(v_c,d)$, for that field size and depth [72]. $S_{c,el}(v_c,d)$ can thus be considered as a factor which describes the contribution of the electron contamination to the collimator scatter correction factor if measured at shallow depths.

In summary, the conversion of collimator scatter correction factors measured at phantom depths beyond the range of contamination, to a value at shallow depth is not easy to perform. Therefore, it is strongly recommended to determine and use the collimator scatter correction factor S_c *only with its definition at the reference depth of 10 cm.*

8.3 Relations between the quantities in the fixed SSD and the isocentric formalism

S_{cp} is defined in this report as a function of the field size at the phantom surface for a specifically described geometry: the fixed SSD system. Another possibility would have been to define and measure S_{cp} in such a way that the distance between source and measuring point, f + d, equals SAD: the isocentric approach. There are no physical arguments supporting the choice for either one of these methods. The choice of the task group for the fixed SSD approach as a starting point in this report, is lead by the fact that measurements are generally performed within such a geometry with the surface of the full scatter water phantom and the mini-phantom placed at a distance equal to SAD. In this approach there is no need to change water levels. Measurements are performed very straightforward, and results can be used directly in the fixed SSD calculation system. In many radiotherapy departments measurements are performed in such a way and, if necessary, TPR data for use in isocentric calculations are derived by using conversion rules. For example, the conversion rules given by Burns [8] transform PDD and peak scatter factor data into TPR data, and vice versa. It is sometimes usefull to measure directly in an isocentric set-up [18], but then also conversion rules are necessary to enable fixed SSD calculations.

This appendix discusses the geometries and definitions of both the fixed SSD approach *and* the isocentric approach and shows what the relation is between the corresponding quantities in these two approaches [71].

The fixed SSD formalism

In this situation, the quantities percentage depth dose PDD and phantom scatter correction factor S_p are defined as a function of field size at the phantom surface, while S_c is defined by the collimator setting at SAD. In the reference situation, in which the basic data are measured, the source-surface distance is set at f_{ref}. PDDs, S_c and S_p are measured as a function of field size at f_{ref}. The ionization chamber is placed at $f_{ref} + d_{ref}$ ($= 100 + 10$ cm).

The isocentric formalism

In this situation, the quantities tissue-phantom ratio TPR, collimator scatter correction factor S_c^{iso} and phantom scatter correction factor S_p^{iso} are given as a function of field size at SAD. Note that the notation S_c^{iso}, S_p^{iso}, S_{cp}^{iso} and D_{ref}^{iso} is used consistently for the quantities in the isocentric formalism. In the reference situation, in which the basic data are measured, the source-to-point distance is now fixed, while the source-surface distance is variable and depends on the depth of the measuring point in the phantom. S_c^{iso} and S_p^{iso} are measured as a function of field size at SAD, while the depth is equal to d_{ref}.

Consequently, definitions and measurement geometries are essentially different for the fixed SSD and the isocentric formalism. Data obtained in one irradiation set-up *should therefore not be confused with those obtained in the other.* A summary of the definitions is given in table 8.1.

Table 8.1 Summary of the definitions of the reference irradiation set-up as used in the fixed SSD and the isocentric formalism. It is important to note that in both formalisms the same d_{ref} is used.

Quantity	*Fixed SSD formalism*	*Isocentric formalism*
reference depth:	d_{ref} = 10 cm	d_{ref} = 10 cm
source-surface distance (for linacs):	f = f_{ref} = 100 cm	f = f_{ref}-d_{ref} = 90 cm
field size related to collimator scatter:	v_c, defined at f_{ref}	v_c, defined at f_{ref}
field size related to phantom scatter:	v_p, defined at surface at f	$v_{ref}(d_{ref})$, defined at depth d_{ref}
field size at reference depth:	(110/100) x v_p	v(d)
field size at phantom surface:	v_p	(90/100) x v(d)
dose per MU at the reference point:	$D_{ref} = D(v_{c,ref}, v_{p,ref}, d_{ref}, f_{ref})$	$D_{ref}^{iso} = D^{iso}(v_{c,ref}, v_{ref}(d_{ref}), d_{ref}, f_{ref}-d_{ref})$

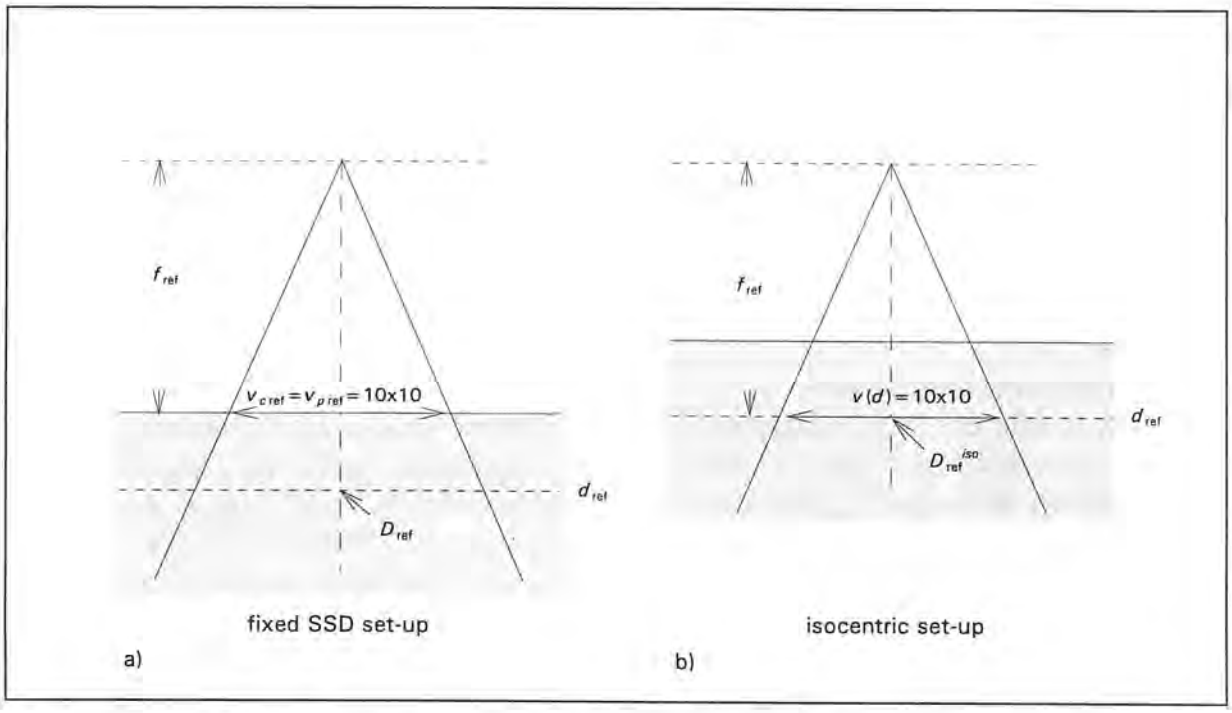

Figure 8.2 Reference conditions for both the fixed SSD (a) and the isocentric (b) formalism.

The relation between D_{ref} and D_{ref}^{iso}

Using the numerical data of table 8.1 for treatment units with $f_{ref} = 100$ cm, the situation in the isocentric set-up of figure 8.2.b can be described with the parameters from the fixed SSD formalism. The reference dose D_{ref}^{iso} is then given by:

$$D_{ref}^{iso} = D_{ref} \times \{(f_{ref} + d_{ref})/f_{ref}\}^2 \times S_p\{(f_{ref}/(f_{ref} + d_{ref}))v_{p,ref}\} \quad (8.3.1)$$

or, more specifically, by using the reference values:

$$D_{ref}^{iso} = D_{ref} \times 1.21 \times S_p(9.1) \quad (8.3.2)$$

where $S_p(9.1)$ is the phantom scatter correction factor, in the fixed SSD formalism, of a square 9.1 cm x 9.1 cm field.

In the same way, the situation in the fixed SSD set-up of figure 8.2.a can be described using the parameters from the isocentric formalism, where the reference dose D_{ref} is given by:

$$D_{ref} = D_{ref}^{iso} \times \{f_{ref}/(f_{ref} + d_{ref})\}^2 \times S_p^{iso}\{((f_{ref} + d_{ref})/f_{ref})v_{ref}(d_{ref})\} \quad (8.3.3)$$

and, with the reference values:

$$D_{ref} = D_{ref}^{iso} \times 0.826 \times S_p^{iso}(11) \quad (8.3.4)$$

Calculation of S_c^{iso} from S_c data, and vice versa

Comparison of the isocentric situations described above with those of the fixed SSD formalism, shows that the collimator scatter correction factor is identical, provided the same normalization is applied, i.e.:

$$S_c(v_c) = S_c^{iso}(v_c) \quad (8.3.5)$$

with $v_{c,ref}$ = 10 cm x 10 cm at f_{ref} = SAD.

Calculation of S_p^{iso} from S_p data

It is assumed that in the isocentric approach field sizes are taken at SAD = 100 cm, at a phantom depth of 10 cm, $v(d_{ref})$. According to Johns et al. [32], the relative phantom scatter contribution in a 10 cm x 10 cm (TPR) field is identical to that found in the (PDD) field with the size 9.1 cm x 9.1 cm at the phantom surface at SSD = 100 cm. It has to be taken into account that values of S_p^{iso} are normalized to unity for the field 10 cm x 10 cm at SAD. In this case one finds S_p^{iso} values from S_p values with (see tables 5.2 and 5.3):

$$S_p^{iso}(v(d_{ref})) = S_p\{(f_{ref}/(f_{ref} + d_{ref}))v(d_{ref})\} \,/\, S_p\{(f_{ref}/(f_{ref} + d_{ref}))v_{ref}(d_{ref})\} \quad (8.3.6)$$

or, by using the reference values:

$$S_p^{iso}(v(d_{ref})) = S_p(0.91v(d_{ref})) / S_p(9.1) \quad (8.3.7)$$

Calculation of S_p from S_p^{iso} data

In the same way we need to consider the fixed SSD situation from the point of view of the isocentric situation, with a reference (PDD-) field of 10 cm x 10 cm at the phantom surface corresponding to a 11 cm x 11 cm (TPR-) field. Again, the normalization at d_{ref} = 10 cm has to be taken into account. So, using the present definitions, S_p data are calculated from S_p^{iso} data with:

$$S_p(v_p) = S_p^{iso}\{((f_{ref}+d_{ref})/f_{ref})v_p\} / S_p^{iso}\{((f_{ref}+d_{ref})/f_{ref})v_{p,ref}\} \quad (8.3.8)$$

Or, by using the reference values:

$$S_p(v_p) = S_p^{iso}(1.1v_p) / S_p^{iso}(11) \quad (8.3.9)$$

Relation between TPR, S_p and RDD

It can be derived that the following expression relates TPR, written as a function of v(d), i.e. the field size defined at the depth d, to S_p and RDD [71]:

$$TPR(v(d),d) = \frac{S_p\{(f_{ref}/(f_{ref}+d))v(d)\}}{S_p\{(f_{ref}/(f_{ref}+d_{ref}))v(d)\}} \times \{(f_{ref}+d)/(f_{ref}+d_{ref})\}^2$$

$$\times RDD\{(f_{ref}/(f_{ref}+d))v(d),d,f_{ref}\} \quad (8.3.10)$$

In this way TPRs can be calculated using existing RDD (or PDD) and S_p data.

The relation between RDD, S_p^{iso} and TPR

We can now use equations (8.3.8) and (8.3.10) to find the relation of the relative depth dose RDD with the phantom scatter correction factor S_p^{iso} and TPR. When the appropriate field size relationships are taken into account, it can be found that:

$$RDD(v_p,d,f_{ref}) = \frac{S_p^{iso}\{((f_{ref}+d)/f_{ref})v_p\}}{S_p^{iso}\{((f_{ref}+d_{ref})/f_{ref})v_p\}} \times \{(f_{ref}+d_{ref})/(f_{ref}+d)\}^2$$

$$\times TPR\{((f_{ref}+d)/f_{ref})v_p,d\} \quad (8.3.11)$$

In this way, RDDs (and PDDs) can be calculated using existing TPR and S_p^{iso} data.

8.4 S_p and PDD (and RDD) for arbitrarily shaped fields

According to equation (2.3.2), the dose D in a phantom at depth d at the beam axis with collimator field size v_c, phantom surface field size v_p, and a source-surface distance equal to SAD, is written as:

$$D(v_c,v_p,d,f_{ref}) = D_{ref} \times S_c(v_c) \times S_p(v_p) \times RDD(v_p,d,f_{ref}) \qquad (8.4.1)^1$$

In the situation that rectangular or blocked fields are used, S_c and S_p have to be determined for that specific geometry. S_c can to be determined by measurement; see section 2.1 and Appendix 8.5. However, S_p can also be derived from S_p values tabulated for square field sizes. S_p values of square fields should then be transformed into S_p values of equivalent circular fields, e.g. by using the method described by Day and Aird [8,9], see also Appendix 8.7. Then, when we subdivide the arbitrarily shaped field v_p into small sectors with angle ϕ, which each contribute to the scatter dose, we may integrate over these sectors [13]:

$$\begin{aligned} D(v_c,v_p,d) &= (1/2\pi) \int_0^{2\pi} D(v_c,v_p(\phi),d) \cdot d\phi \\ &= (1/2\pi) \times D_{ref} \times S_c(v_c) \times \int_0^{2\pi} S_p(v_p(\phi))\ RDD(v_p(\phi),d) \cdot d\phi \end{aligned} \qquad (8.4.2)$$

This means that the total scatter contribution $S_p(v_p)$ is the result of a summation of the scatter contribution of the small sectors. So:

$$S_p(v_p) \times RDD(v_p,d) = (1/2\pi) \times \int_0^{2\pi} S_p(v_p(\phi))\ RDD(v_p(\phi),d) \cdot d\phi \qquad (8.4.3)$$

i.e. not $RDD(v_p,d)$ itself, but the product $S_p(v_p) \times RDD(v_p,d)$ is the quantity of interest. In the calculation of RDD of an arbitrarily shaped field at an arbitrary depth, S_p must be used as a weighting function.

Both equation (8.4.2) and equation (8.4.3) can be simplified if d has been taken equal to d_{ref}. In that case, RDD is equal to unity and (8.4.3) is reduced to:

$$S_p(v_p) = (1/2\pi) \times \int_0^{2\pi} S_p(v_p(\phi)) \cdot d\phi \qquad (8.4.4)$$

This relationship may be used to calculate S_p data of arbitrarily shaped fields, i.e. for rectangular and blocked fields, using a suitable set of S_p data for equivalent circular fields.

[1] Because f_{ref} is not relevant in the expressions of this paragraph, it has been omitted.

8.5 S_c for partially blocked fields

In clinical routine the S_c value of a partially blocked irradiation field, $S_{c,block}$, can be taken equal to the S_c value of the field size set by the collimator jaws $S_c(v_c)$ as long as the amount of photons scattered from the primary collimator and the flattening filter, as observed from the point of interest, is limited by the collimator jaws and not by the additional blocks on the tray [41,45,60,63]. For these situations, $S_{c,block}$ values can be found from S_c data which are already available for rectangular fields. In other situations, $S_{c,block}$ has to be determined experimentally. The decision whether or not the $S_{c,block}$ value has to be determined by measurement, depends on the construction of the head of the treatment machine and the distance between the focus and the point of interest (see figures 3.1 and 8.3.a). Based on the specific geometry, a decision criterion can be developed.

In figure 8.3.b, the rectangular field size, set-up by the collimator jaws at SAD, has been divided into four quadrants by the two cross-wires. For each quadrant it has to be determined whether the additional block or the collimator hides the flattening filter from the point of view at depth d. In the situation that the additional block is the limiting factor in one of these quadrants, S_c has to be determined by measurement. Using figure 8.3.b, the next criterion whether the block or the collimator jaw hides the filter has been derived for the X-collimator jaws:

$b_x \; |\cos(\theta))| \; C_x / (X/2) \quad < 1$: $S_{c,block}$ has to be determined, in principle, by measurement;

$b_x \; |\cos(\theta))| \; C_x / (X/2) \quad \geq 1$: $S_{c,block}$ can be taken equal to $S_c(v_c)$.

In this criterion (see figure 8.3.a):

- b_x is equal to the minimum distance between the block edge and the central photon beam axis, determined at the isocentre, i.e. at SAD;
- θ is equal to the angle between b_x and the X-axis;
- $$C_x = \frac{(f + d - U_x)\ T}{(f + d - T)\ U_x} \qquad (8.5.1)$$

  where d is the depth in the phantom, T is the distance from the focus to the additional shielding blocks and $U_x$is the distance from the focus to the X-collimator jaw.

- X/2 is equal to the position of the X-collimator jaw at the isocentre; i.e. half the side of a symmetrical field with setting X.

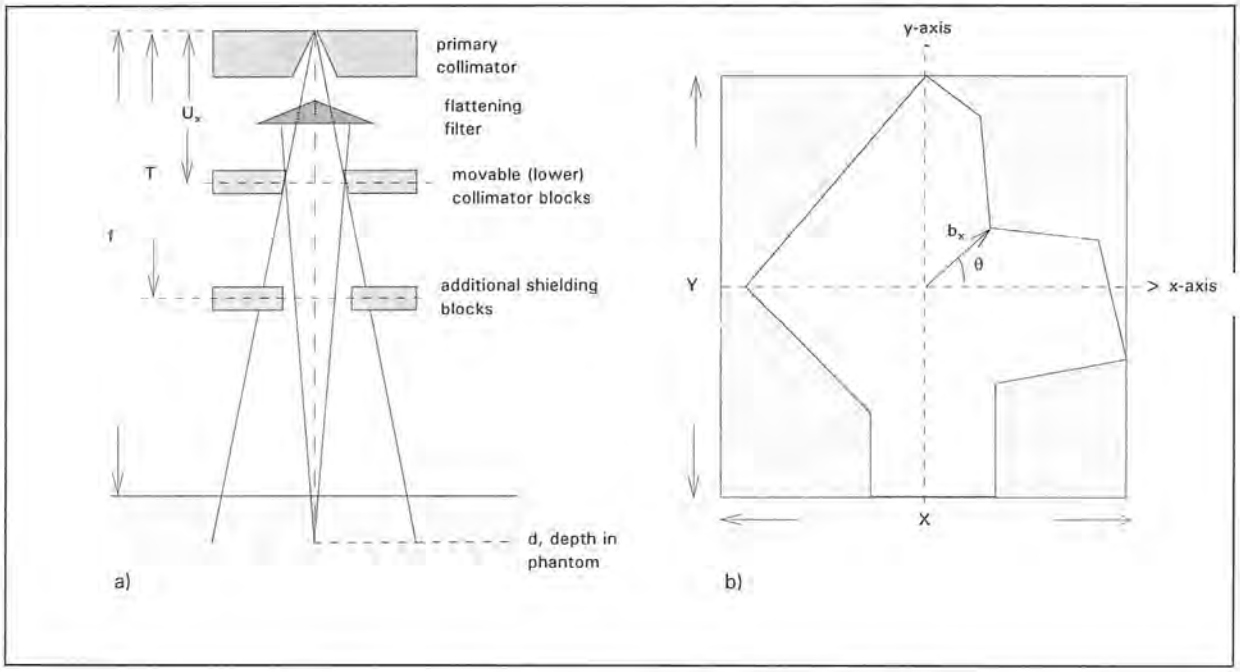

Figure 8.3 Definition of quantities used in the decision rule whether or not $S_{c,block}$ can be taken equal to S_c. a) Side view of the beam; b) top view of blocked field at SAD.

In clinical situations several methods can be used to deduce b_x either with a simple computer program or estimated by eye.

For the Y-collimator jaws a similar expression can be used, replacing the indices x by y, $|\cos(\theta)|$ by $|\sin(\theta)|$, and the variable X by Y. The U_x , U_y and T values can be found from the details of the treatment machine from the manufacturer.

As an example, these values have been presented for one type of treatment machine in table 8.2, with f equal to SAD and the phantom depth d equal to d_{ref}. Finally, two numerical examples are given.

Table 8.2 C values, required for the decision criterion whether or not to measure S_c values.

Manufacturer	*Type*	U_x *(cm)*	U_y *(cm)*	*T (cm)*	*SAD (cm)*	C_x	C_y
Philips	SL25	44	34	67	100	2.34	3.48

Examples

For the Philips SL25 treatment unit, the following data are derived, using the values of table 8.2:

A field size of 20 cm x 20 cm is defined at the isocentre; reduced by blocks on the tray to a field of 10 cm x 10 cm. Then: $b_x\ C_x\ /\ (X/2) = 1.17$ (resp. 1.74 for the Y collimator setting). *Conclusion*: $S_{c,block} = S_c(20)$.

A field size of 20 cm x 20 cm is defined at the isocentre; reduced by blocks on the tray to a field of 5 cm x 5 cm. Then: $b_x\ C_x\ /\ (X/2) = 0.585$ (resp. 0.87 for the Y collimator setting). *Conclusion*: $S_{c,block} \neq S_c(20)$, and needs to be measured.

8.6 The concept of equivalent fields

The use of BJR Supp. 17 tables [8] of equivalent square fields for dose calculations is widespread. The revised version, BJR Supp. 25 [9], contains a more thorough discussion on this topic, but without changes in the contents of the tables. The *equivalent square field* is defined in BJR Supp. 25 as "that standard square field which has the same central axis depth dose characteristics as the non-standard field". This method was developed at a time when beam data were measured and applied in calculations, based on PDD, BSF, PSF and d_m. The current philosophy in calculation methods, however, is based on data defined and measured at a reference depth d_{ref} = 10 cm, on a separation of phantom and collimator scatter and on the use of the relative depth dose, RDD. In this concept, problems related to the influence of contaminating electrons in the beam at shallow depths are eliminated. If the reference conditions are changed, it is not a priori evident that the tools for calculating the dose, such as a table of equivalent square fields, remain unchanged. In principle, separate equivalent square fields may be necessary for the derivation of the phantom scatter factor and for the phantom scatter related quantities such as PDD, TAR and TPR of a rectangular or irregular field on the one hand, and for the collimator scatter factor on the other hand.

Phantom scatter

The equivalent square field, to be used for the determination of the phantom scatter factor and phantom scatter related quantities, is defined here as the square field which has the same phantom scatter contribution at the reference point in the beam: at 10 cm depth on the central axis, as the arbitrarily shaped field under consideration.

The use of the BJR Supp. 25 tables of equivalent square fields in relation to phantom scatter was recently discussed by Venselaar et al. [70]. In their analysis, energy-specific tables of equivalent squares for phantom scatter were derived for 4 beam qualities, based on S_p data included in this report and covering the range of QI of 0.573 to 0.783 (^{60}Co to 25 MV). It was shown that the use of the energy-specific tables could eventually lead to a difference of 0.5 - 1.0% in the value of S_p, compared to the use of the BJR-table, in which the use of the BJR-table systematically leads to a lower value of S_p. The relatively small differences between the 4 energy-specific tables mutually allowed the construction of a new *average* table of equivalent square fields. When this average table is applied instead of the BJR-table, improvements were obtained, especially in the median beam qualities, for example the 6 and 10 MV beams. For the highest energy, 25 MV, the benefit is less, while for ^{60}Co no improvements were found.
Because of the relatively small deviations in the S_p values and because of the widespread use of the BJR-table, its continued use is considered justified for clinical routine. However, it was concluded that a higher accuracy in dose

calculation can indeed be obtained by the application of energy-specific tables of equivalent square fields for phantom scatter, or by using the average table discussed above. In cases where optimal accuracy is needed, it is necessary to pay attention to all aspects of the dose calculation procedures. Then, the use of the most accurate table of equivalent square fields is recommended. The new average table 8.3 can fulfil this recommendation and is therefore presented in this report.

Table 8.3 Table of equivalent square fields for the derivation of phantom scatter factors and phantom scatter related quantities for rectangular fields with field sides s1xs2. The new table was constructed by averaging 4 energy-specific tables for ^{60}Co, 6, 10 and 25 MV photon beams. Dimensions are in cm. See [70] for more details.

s1 \ s2	*2.0*	*4.0*	*6.0*	*8.0*	*10.0*	*12.0*	*14.0*	*16.0*	*18.0*	*20.0*	*22.0*	*24.0*	*26.0*	*28.0*	*30.0*	*32.0*	*34.0*	*36.0*	*38.0*	*40.0*
2.0	2.0																			
4.0	2.8	4.0																		
6.0	3.3	4.9	6.0																	
8.0	3.6	5.4	6.9	8.0																
10.0	3.7	5.7	7.4	8.8	10.0															
12.0	3.8	5.9	7.7	9.4	10.9	12.0														
14.0	3.9	6.0	7.9	9.9	11.6	12.9	14.0													
16.0	4.0	6.1	8.1	10.3	12.2	13.8	15.0	16.0												
18.0	4.0	6.2	8.3	10.6	12.7	14.5	15.9	17.1	18.0											
20.0	4.0	6.2	8.5	10.9	13.2	15.1	16.6	18.0	19.1	20.0										
22.0	4.0	6.3	8.6	11.2	13.7	15.7	17.3	18.7	20.0	21.1	22.0									
24.0	4.1	6.4	8.7	11.5	14.1	16.1	17.9	19.4	20.7	22.0	23.1	24.0								
26.0	4.1	6.4	8.8	11.7	14.4	16.6	18.4	19.9	21.4	22.7	24.0	25.1	26.0							
28.0	4.1	6.4	8.9	11.9	14.7	16.9	18.8	20.4	22.0	23.4	24.7	26.0	27.1	28.0						
30.0	4.1	6.5	9.0	12.0	14.9	17.2	19.1	20.9	22.5	24.0	25.4	26.7	28.0	29.1	30.0					
32.0	4.1	6.5	9.1	12.2	15.1	17.5	19.4	21.2	22.8	24.4	25.9	27.3	28.7	29.9	31.0	32.0				
34.0	4.1	6.5	9.1	12.3	15.3	17.7	19.7	21.5	23.2	24.8	26.4	27.9	29.3	30.6	31.9	33.0	34.0			
36.0	4.1	6.5	9.1	12.4	15.4	17.8	19.9	21.7	23.4	25.1	26.7	28.3	29.8	31.2	32.6	33.8	35.0	36.0		
38.0	4.1	6.5	9.2	12.5	15.5	17.9	20.0	21.9	23.7	25.3	27.0	28.7	30.2	31.7	33.2	34.6	35.8	36.9	38.0	
40.0	4.1	6.5	9.2	12.5	15.6	18.1	20.1	22.0	23.8	25.6	27.3	28.9	30.5	32.1	33.6	35.1	36.5	37.8	39.0	40.0

Collimator scatter

In exactly the same way, the equivalent square field to be used for the determination of the collimator scatter factor, is defined here as the square field that has the same collimator scatter contribution to the reference point in the beam at 10 cm depth at the central axis, as the arbitrarily shaped field under consideration.

The same approach as describe above for phantom scatter, can be applied to determine a full table of equivalent square fields from the measured collimator scatter data of a specific photon beam. This should be done with caution, because the resulting table will be typically machine dependent and should incorporate the collimator exchange effect (CEE). Some papers report differences in collimator

scatter with X-Y vs. Y-X setting of up to 6% [44,57], although others report smaller differences (2%, see for example section 5.2.2 of this report). It is therefore, in all cases, recommended to measure the collimator scatter factors for each individual treatment machine and photon beam quality.

The use of a 2-D table of S_c values is considered to be relatively simple in practice with present-day computer technology. Parametrization methods, which take the CEE into account, might be considered [12,31,57,62,67] for use in monitor unit calculation programs, as well as for a reduction of the number of measurements needed to determine S_c under all circumstances. In these parametrization methods, the equivalent squares are used as an auxilliary step in the calculation of S_c of rectangular fields, see Appendix 8.7.2.

8.7 Parametrization of scatter correction factors

8.7.1 Parametrization of phantom scatter correction factors

S_p data can be parametrized using the assumption that the phantom scatter at a specified depth for circular fields can be described as the sum of pencil beam contributions [66]. Each pencil is assumed to consist of three gaussian components, $a_i.\exp(-b_i.r^2)$ with i = 1, 2 and 3. It was shown by van Gasteren et al. [66] that the following expression describes S_p with sufficient accuracy as a function of the field radius r_d (in cm, taken at the depth of consideration, for example at d_{ref}):

$$S_p(r_d) = b_1 + a_1\{ (a_2/b_2) (1-\exp(-b_2.r_d^2)) + (a_3/b_3) (1-\exp(-b_3.r_d^2)) \} \quad (8.7.1)$$

Parameters a_1 to a_3 and b_1 to b_3 (see table 8.4) were found with a least square method. For quality indices in between, values of a_1 to b_3 can be interpolated in first approximation, while the S_p data of table 5.2 can be used for comparison.

Table 8.4 Quality index, QI, and parameters used in expression (8.7.1) for the calculation of $S_p(r_d)$ of circular fields with radius r_d of four nominal photon beam energies [66].

parameter	*^{60}Co*	*6 MV*	*10 MV*	*25 MV*
QI	0.572	0.670	0.729	0.783
a_1	0.5380	0.5519	0.5694	0.6991
b_1	0.8092	0.8614	0.8792	0.8819
a_2	0.0180	0.0150	0.0140	0.0180
b_2	0.0600	0.0650	0.0700	0.1200
a_3	0.0026	0.0013	0.0009	0.0006
b_3	0.0070	0.0050	0.0045	0.0060

The next step is to transform the phantom scatter data for circular fields to those for square fields. This can be done with a Clarkson integration, or by using the conversion method, which was previously described by Day and Aird [8] and discussed, in more detail, by Bjärngard and Siddon [4]:

$$s/2r_{eq} = 0.891 + 0.00092\, r_{eq}$$

and

$$2r_{eq}/s = 1.123 - 0.00067\, s \quad (8.7.2)$$

where r_{eq} is the radius of the (equivalent) circular, and s the side of the (equivalent) square field, both in cm and defined at the surface, i.e. at SSD. For a proper application of equation (8.7.1), r_{eq} has to be transformed to the radius

at depth d_{ref}, r_d, according to the divergence of the beam using a multiplication with $(SSD + d_{ref})/SSD$. The correspondence between the calculated and measured values of S_p is better than 0.5% [66,70].

8.7.2 Parametrization of collimator scatter correction factors

The collimator exchange effect (CEE) necessitates that S_c should be determined for a large number of fields [15,33,58]. For example, if the X- and Y- blocks are set to 3, 4, 5, 6, 8, 10, 12, 15, 20, 25, 30, 35 and 40 cm, as is recommended in section 4, S_c has to be measured for 169 fields. Then, for each type of beam modifier, this number of measurements should be repeated, see section 3.1. A parametrization method for S_c could considerably decrease the number of measurements. Two approaches have been used in the literature. One is based on analytical models, using suitable functions through the data [4,55,57,62]. The second approach makes use of more sophisticated, physical models [2,3,15,35,40,58,67,74]. The latter approach requires knowledge of properties of the accelerator, like the energy spectrum of the beam and/or the exact construction of the head of the treatment machine, that may not be available. However, analytical models are most valuable if these would be universally applicable. For any method the required accuracy is: 1% as the maximum difference between a measured and a calculated value of S_c; 0.5% as the root of the mean of the squares of differences (RMS) between calculated and measured S_c values in a table. In a study of Jager et al. [31] several published methods were compared, using measured S_c data from the treatment machines listed in table 5.1 of this report.

An analytical model for S_c of square fields

Jager et al. [31] compared several published methods to fit S_c data of square fields for a number of different linear accelerators. They found that S_c could be described accurately by:

$$S_c(X,X) = a_1 + a_2 \ln(X/10) + a_3 \ln^2(X/10) + a_4 \ln^3(X/10) \qquad (8.7.3)$$

In this expression a_1, a_2, a_3 and a_4 are constants, of which the numerical values can be obtained with a least squares method on the difference between measured and fitted data. It was shown that by applying this polynomial, the RMS of the differences between measured and fitted S_c values for square fields was less than 0.25% and the maximum deviation less than 0.5% for all treatment machines in the study.

To determine the parameters of equation (8.7.3) with the optimal accuracy, a minimum set of measured S_c data of square fields must include the field sides 4, 5, 6, 10, 12, 25, 30 and 40 cm [31].

The equivalent square field size of rectangular fields and parametrisation of S_c

In a further step, the equivalent field size for collimator scatter v_c^{eq} was used, defined as that equivalent square field that has the same S_c value as the given rectangular field. A well-known concept to find v_{eq} of a rectangular field is the *area-perimeter* relation of Sterling et al. [55]: $v_{eq} = 2XY/(X+Y)$. Since this relation is symmetrical in X and Y, it cannot include the CEE. A modification of this formulation has been presented by Vadash and Bjärngard [62]. Jager et al. [31] introduced the relation:

$$v_{c,eq}(X,Y) = \{(a_1/X) + (a_2/X^2) + (b_1/Y) + (b_2/Y^2)\}^{-1} \qquad (8.7.4)$$

Sterling's relation [55] is found for the parameter values $a_1 = b_1 = 0.5$ and $a_2 = b_2 = 0$. Applying equation (8.7.4), the resulting equivalent square field size can now be used in the polynomial of (8.7.3) to obtain $S_c(v_{c,eq})$. Parameter values of a_1, ... b_2 can be found from the least squares method.

For rectangular fields, the RMS of the differences between measured and fitted data for equation (8.7.4) was shown to be below 0.35% for a number of measured S_c tables. The maximum deviations were less than 0.80% for all accelerators tested [31]. It was recommended to measure S_c of the before mentioned set of square fields, and of twelve non-square fields: 4 x 8, 4 x 30, 4 x 40, 5 x 40, 8 x 4, 8 x 40, 30 x 4, 30 x 40, 40 x 4, 4 x 5, 40 x 8 and 40 x 30 (all dimensions in cm), and to apply equation (8.7.4) to fit the data.

The parameters that were found for the fitting methods described here are typically dependent on the construction of the head of the treatment machine. A correlation between the parameters and the quality index was not found [31].

A physical model for the parametrization of S_c of rectangular fields

The influence of the CEE can be taken into account by using a correction factor on the X- or Y-collimator field size (C_{fx} of C_{fy}, respectively). This correction factor C_f converts the two-dimensional, asymmetrical data set of S_c values vs. the independent X- and Y- settings into a symmetrical data set (i.e. with C_{fx} x X and C_{fy} x Y). Values of C_f can be found by using construction data of the treatment machine: from the ratio of distances from focus to upper, or lower collimator pairs, respectively. Another method is to use the measured 2-D data set of S_c values and to apply C_f iteratively as a multiplicative factor to the X- or Y- field side dimension, until a symmetrical table is obtained. Whether $C_{fx} = 1$ and $C_{fy} \neq 1$ or vice versa, depends on the construction details of the machine, i.e. whether the X or Y setting is determined by the upper or lower pair of jaws.

The curves of S_c data versus field size show, in its form, the same behaviour as the previously discussed S_p curves. It is, then, not surprising to find that collimator scatter data can be described as a sum of pencil beam contributions in practically the same way as this was done for the phantom scatter data in the

previous paragraph. This idea was developed by van Gasteren et al. [66]. The collimator scatter factor as a function of the radius, r, of a circular field can be found from:

$$S_c(r) = b_1 + a_1\{ (a_2/b_2) (1-\exp(-b_2.r^2)) + (a_3/b_3) (1-\exp(-b_3.r^2))\} \quad (8.7.5)$$

where parameters a_1 to a_3 and b_1 to b_3 again can be found with a least square method by comparing measured and fitted data.

Having obtained a symmetrical set of data, a conventional table of equivalent field sizes can then be used to convert the rectangular field size C_{fx} x X, C_{fy} x Y, into an equivalent square, or rather an equivalent circular field [8,9]. The equivalent radius r_{eq} can be used in the expression (8.7.5) to derive S_c. Thus, the set of measured square field sizes (X,X) are converted to effective field sizes (C_{fx}X, C_{fy}Y), which are equivalent to the effective circular fields with radii r_{eq}. The set of $S_c(r_{eq})$ can be applied to calculate S_c(X,Y) with the Clarkson integration method using the set $S_c(r_{eq})$ for the r_{eq} of each Clarkson sector.

The method was tested using beam data of several treatment machines, including Philips SL15 and SL20, ABB Dynaray20 and GE Saturne-43 linear accelerators, for photon beam qualities of 6 to 25 MV. Average deviations between measured and calculated data were in general below 0.5%. The method was also tested for a number of beam data from asymmetrical collimator machines [67] and (a)symmetrical wedged fields [68].

In summary, if this method is applied, the following steps have to be taken:

1. Measure the S_c(X,X) values from 4 cm x 4 cm to 40 cm x 40 cm; measure also the S_c(X,Y) of a number of extremely elongated fields: for example (4,40), (5,40),.., and (40,4), (40,5).
2. Replace the measured square field sizes $(X,X)_{meas}$ and the rectangular field sizes $(X,Y)_{meas}$ by (X,C_{fy}X) and (X,C_{fy}Y), respectively.
3. Determine for all fields (X,C_{fy}X) the equivalent radius by geometric Clarkson integration, i.e. take for every degree the length of the radius to the contour (X,C_{fy}X) and determine the average value of r_{eq} of these radii. This results in a set of $S_c(r_{eq})$ values. Thus, $S_c(r_{eq}) = S_c(X,C_{fy}X) = S_c(X,X)_{meas}$.
4. Calculate for all measured rectangular fields $(X,Y)_{meas}$ the corresponding S_c(X,C_{fy}Y) by Clarkson integration of the field (X,C_{fy}Y), using $S_c(r_{eq})$. The Clarkson integration now determines for every degree the length of the radius r to the field contour and interpolates the corresponding $S_c(r)$, using the set of $S_c(r_{eq})$ values.
5. If the fit between measured and calculated S_c values for the rectangular fields is not optimal, adjust the Y-collimator factor C_{fy} and repeat the procedure, starting at step 2.
6. Note: depending on the machine type, it may be necessary to change (X,C_{fy}Y) into (C_{fx}X,Y), etc. in these procedures.

8.8 The narrow cylindrical beam-coaxial phantom (mini-phantom)

In this report, the use of the mini-phantom is recommended for the measurement of the collimator scatter correction factor of the megavoltage photon beam. The results of the measurements should reflect as accurately as possible the change in the energy fluence due to primary photons coming from the treatment head at the reference depth with variation of the collimator setting. The collimator scatter correction factor is defined as the ratio of two measurements: one in an arbitrary field and one in the reference field. In each measurement, the resulting ionization is caused by the direct radiation from the head of the treatment machine and a small contribution of radiation scattered within the mini-phantom. Due to the material above the ionization chamber, a certain fraction of the direct radiation is absorbed. Because the amount of absorption in the material and the scattered radiation created within the phantom are directly proportional to the amount of direct radiation from the treatment head, both effects on the ionization in the detector cancel when we take the ratio of the two readings. The resulting collimator scatter correction factor is therefore almost independent of the construction details of the mini-phantom.

Two conditions must be met. First, the measurements have to be performed using the same mini-phantom, in which the depth of measurement is chosen large enough to eliminate the contaminating electrons in the beam. Second, the minimum field size in which measurements are performed, must be large enough to cover the phantom surface completely.

The depth of measurement is set to 10 cm, according to the definitions and recommendations of this report. Experiments performed by the Task Group members and others have shown only minor deviations in the resulting S_c values when the construction details were changed. The mini-phantom may be constructed with diverging side walls and square or circular cross sections. As construction materials solid PMMA or other water-equivalent materials may be used. A hollow PMMA phantom, to be filled with water, has also been used. The bottom side of the phantom may be provided with more backscattering material (i.e. the "length" of the mini-phantom).

The diameter of the mini-phantom also appears to be of minor importance. Several experiments have been performed with mini-phantoms of different sizes: 4 cm diameter down to 2 cm. No significant differences have been observed, which is in agreement with the results of Li et al. [42]. However, care has to be taken in case of high energy beams in combination with a relatively small mini-phantom. For these qualities, it is possible that the thin side walls can be penetrated by higher energy contaminating electrons from the treatment head, which influences the determination of S_c [42]. For photon beams with a nominal beam quality exceeding 16 MV, it is recommended to have a minimum diameter of 3 cm. Beams are supposed to have a relatively flat beam profile in air at the

position of the surface of the mini-phantom. For large fields this is always the case. However, in some situations, for example in small ^{60}Co fields, this may not be true, which may lead to small deviations. Therefore, a 3 cm diameter seems to be a good compromise between the different requirements.

The need for measurement of the collimator scatter correction factor for very small fields is another topic, e.g. encountered in the field of stereotactic radiosurgery techniques. For these situations, high Z build-up caps of different materials and different sizes are sometimes recommended. This is, however, not the subject of this report. More details can be found in the relevant literature (e.g., [53,73]).

Two drawings of the mini-phantom are shown in figures 8.4 and 8.5. The upright position of the ionization chamber in figure 8.4 is preferred because the chamber is now symmetrically placed with respect to the beam axis. The influence of the stem effect on the readings has to be checked, but is in this situation of less importance than in the situation of figure 8.5, where the chamber is placed horizontally in the beam. The effective point of measurement is determined by the dimensions and the construction of the ionization chamber and is dependent on the way in which it is irradiated, but it will be independent of the field size. Therefore, the depth is not a critical parameter in the determination of the collimator scatter correction factors and knowledge of the exact position of the effective point of measurement is not essential.

In case S_{cp} measurements are performed in a large water-phantom, usually the same depth is chosen as applied for the calibration of the beam. Then, for absolute dose measurements, knowledge of the position of the effective point of measurement is necessary and a horizontal position of the ionization chamber is preferred.

When these considerations are taken into account, all ionization chambers available in the clinic may be used. No preference for a certain type of instrument exists.

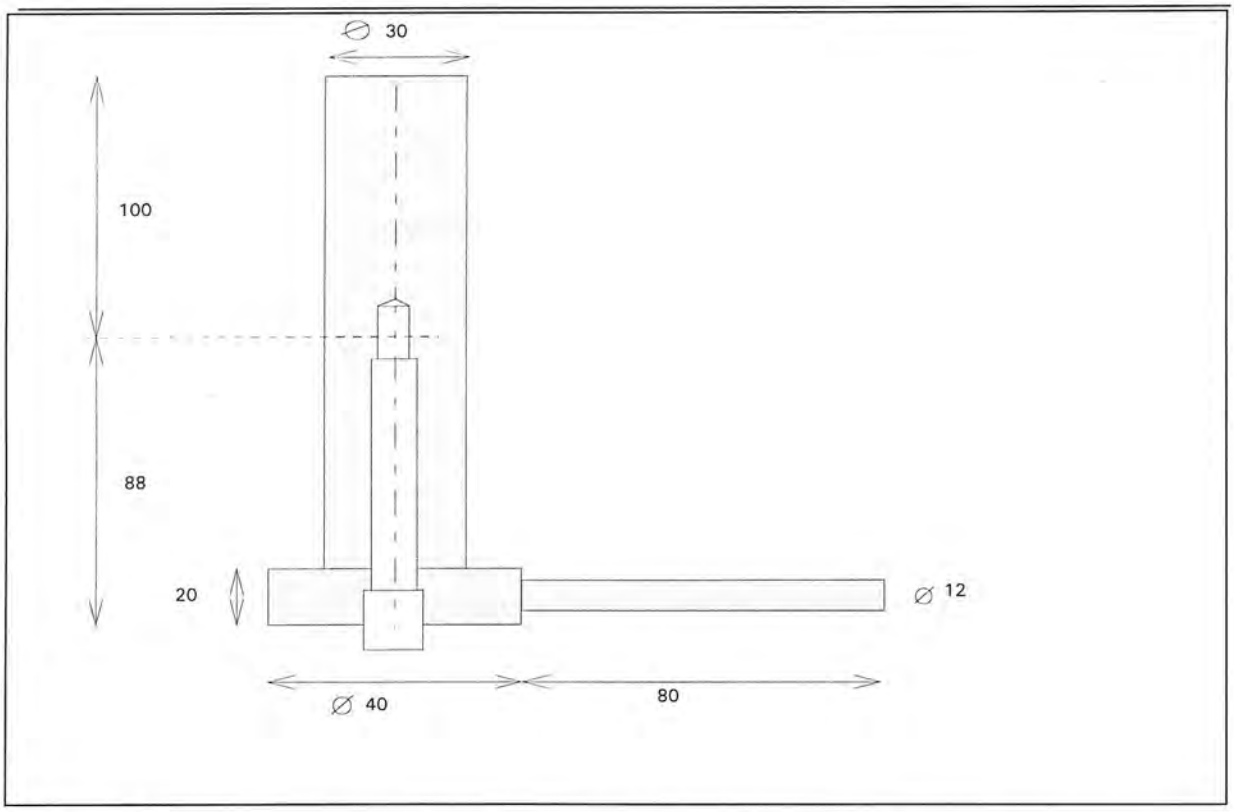

Figure 8.4 Construction drawing of the narrow cylindrical beam-coaxial (mini) phantom, in upright position. All dimensions in mm.

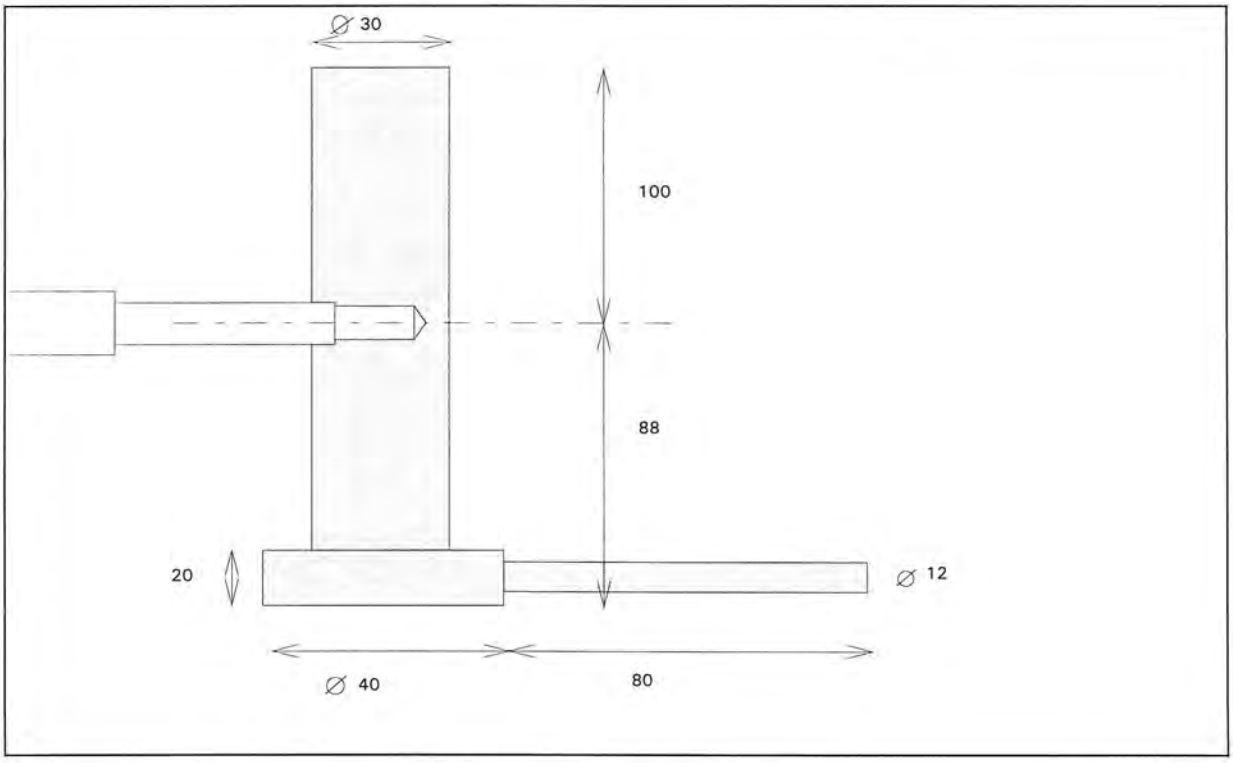

Figure 8.5 Construction drawing of the narrow cylindrical beam-coaxial (mini) phantom, in horizontal position.

9. References

[1] Aget, H. Calcul de la dose sur l'axe dans des conditions autres que celles de référence, pour des faisceaux de photons. In: De la mesure à la dose absorbée en radiothérapie. pp 212-235, Clinique d'Oncologie et Radiothérapie, Hôpital Bretonneau C.H.U. Tours, France.

[2] Ahnesjö, A. Collimator scatter in photon therapy beams. Med. Phys. 22: 267-278, 1995.

[3] Ahnesjö, A., Knöös, T. and Montelius, A. Application of the convolution method for calculation of output factors for therapy photon beams. Med. Phys.19: 295-301, 1992.

[4] Bjärngard, B.E. and Siddon, R.L. A note on equivalent circles, squares and rectangles. Med. Phys. 9: 258-260, 1982.

[5] Bjärngard, B.E. and Vadash, P. Analysis of central-axis dose for high-energy x rays. Med. Phys. 22: 1191-1195, 1995.

[6] Bjärngard, B.E., Zhu, T.C. and Ceberg, C. Tissue-phantom ratios from percentage depth doses. Med. Phys. 23: 629-634, 1996.

[7] Brahme, A., Chavaudra, J., Landberg, T., McCullough, E., Nüsslin, F., Rawlinson, A., Svensson, G. and Svensson, H. Accuracy requirements and quality assurance of external beam therapy with photons and electrons. Supplementum 1 to Acta Oncologica, 1988.

[8] Central Axis Depth Dose Data for Use in Radiotherapy. Brit. J. Radiol. Suppl. 17. Editors: D.K. Bewley, A.L. Bradshaw, D. Greene, J.L. Haybittle and L.F. Secretan. The British Institute of Radiology, 1983.

[9] Central Axis Depth Dose Data for Use in Radiotherapy: 1996. Brit. J. Radiol. Suppl. 25. Editors: E.G.A. Aird, J.E. Burns, M.J. Day, S. Duane, T.J. Jordan, A. Kacperek, S.C. Klevenhagen, R.M. Harrison, S.C. Lillicrap, A.L. McKenzie, W.G. Pitchford, J.E. Shaw and C.W. Smith. The British Institute of Radiology, 1996.

[10] CFMRI (Comité Français Mesure des Rayonnements Ionisants). Recommendations pour la mesure de la dose absorbée en radiothérapie dans faisceaux de photons et d'électrons d'énergie comprise entre 1 MeV et 50 MeV. Rapport 2, CFMRI

[11] Chaney, E.L., Cullip, T.J. and Gabriel, T.A. A Monte Carlo study of accelerator head scatter. Med. Phys. 21: 1383-1390, 1994.

[12] Chen, F.S. Applying a polynomial formula to photon beam output and equivalent square field. Med. Phys. 6: 464-469, 1990.

[13] Clarkson, J.R. A note on depth doses in fields of irregular shape. Brit. J. Radiol. 14: 265-268, 1941.

[14] Drouard, J., Rosenwald, J.C. and Simonian, M. Generation of primary and scatter tables for computer computations in high energy photon beams. Proc. 5th ESTRO meeting, Baden-Baden, 1986 (Abstract).

[15] Dunscombe, P.B. and Nieminen, J.M. On the field-size dependence of relative output from a linear accelerator. Med. Phys. 19: 1441-1444, 1992.

[16] Dutreix, A. When and how can we improve precision in radiotherapy? Radiother. Oncol. 2: 275-292, 1984.

[17] Dutreix, A. The French dosimetry protocol. Radiother. Oncol. 4: 301-304, 1985.

[18] Dutreix, A., Bjärngard, B.E., Bridier, A., Mijnheer, B., Shaw, J.E. and Svensson, H. Monitor unit Calculation for high energy photon beams. ESTRO Booklet 3, Garant ed., Leuven, 1997.

[19] Goitein, M. Nonstandard deviations. Med. Phys. 10: 709-711, 1983.

[20] Heukelom, S., Lanson, J.H. and Mijnheer, B.J. Wedge factor constituents of high energy photon beams: field size and depth dependence. Radiother. Oncol. 30: 66-73, 1994.

[21] Heukelom, S., Lanson, J.H. and Mijnheer, B.J. Quality assurance of the simultaneous boost technique for prostatic cancer: dosimetric aspects. Radiother. Oncol. 30: 74-82, 1994.

[22] Heukelom, S., Lanson, J.H. and Mijnheer, B.J. Wedge factor constituents of high energy photon beams: head and phantom scatter dose components. Radiother. Oncol. 32: 73-83, 1994.

[23] Heukelom, S., Lanson, J.H. and Mijnheer, B.J. Differences in wedge factor determination in air using a PMMA mini-phantom or a brass build-up cap. Med. Phys. 24: 1986-1991, 1997.

[24] Higgins, P.D., Sohn, W.H., Sibata, C.H. and McCarthy, W.A. Scatter factor corrections for elongated fields. Med. Phys. 16: 800-802, 1989.

[25] Holt, J.G., Laughlin, J.S. and Moroney, J.P. The extension of the concept of tissue-air-ratios (TAR) to high energy X-ray beams. Radiol. 96: 437-446, 1970.

[26] Huang, P., Chin, L.M. and Bjärngard, B.E. Scattered photons produced by beam-modifying filters. Med. Phys. 13: 57-63, 1986.

[27] Huang, P., Chu, J. and Bjärngard, B.E. The effect of collimator backscatter on photon output of linear accelerators. Med. Phys. 14: 268-269, 1987.

[28] IAEA (International Atomic Energy Agency). Absorbed dose determination in photon and electron beams. Technical Report 277, IAEA, Vienna, 1987.

[29] ICRU (International Commission on Radiation Units and Measurements). Determination of absorbed dose in a patient irradiated by beams of X or gamma rays in radiotherapy procedures. Report 24. ICRU Publications, Washington, D,C.,1976.

[30] Islam, M.K. and Van Dyk, J. Effects of scatter generated by beam-modifying absorbers in megavoltage photon beams. Med. Phys.22: 2075-2081, 1995.

[31] Jager, H.N., Heukelom, S., van Kleffens, H.J., van Gasteren, J.J.M., van der Laarse, R., Mijnheer, B.J., Venselaar, J.L.M. and Westermann, C.F. Comparison of parametrization methods of the collimator scatter correction factor for open rectangular fields of 6-25 MV photon beams. Radiother. Oncol. 45: 235-243, 1997.

[32] Johns, H.E., Bruce, W.R. and Reid, W.D. The dependence of depth dose on focal skin distance. Brit. J. Radiol. 31: 254-260, 1958.

[33] Kase, K.R. and Svensson, G.K. Head scatter data for several linear accelerators (4-18 MV). Med. Phys. 13: 530-532, 1986.

[34] Khan, F.M., Sewchand, W., Lee, J. and Williamson, J.F. Revision of tissue-maximum ratio and scatter maximum ratio concepts for cobalt-60 and higher energy X-ray beams. Med. Phys. 7: 230-237, 1980.

[35] Kim, S., Zhu, T.C. and Palta, J.R. An equivalent square field formula for determining head scatter factors of rectangular fields. Med. Phys. 24: 1770-1774, 1997.

[36] Krithivas, G. and Rao, S.N. A study of the characteristics of radiation contaminants within a clinically useful photon beam. Med. Phys. 12: 764-768, 1985.

[37] Krithivas, G. and Rao, S.N. Dosimetry of 24 MV x-rays from a linear accelerator. Med. Phys. 14: 274-281, 1987.

[38] Kubo, H. Telescopic measurements of backscattered radiation from secondary collimator jaws to a beam monitor chamber using a pair of slits. Med. Phys. 16: 295-298, 1989.

[39] Kubo, H. and Lo, K.K. Measurement of backscattered radiation from Therac-20 collimator and trimmer jaws into the beam monitor chamber. Med. Phys. 16: 292-294, 1989.

[40] Lam, K.L., Muthuswamy, M.S. and Ten Haken, R.K. Flattening-filter-based empirical methods to parametrize the head scatter factor. Med. Phys. 23: 343-352, 1997.

[41] Lam, K.L. and Ten Haken, R.K. In phantom determination of collimator scatter factor, Med. Phys. 23: 1207-1212, 1996.

[42] Li, X.A., Soubra, M., Szanto, J. and Gerig, L.H. Lateral electron equilibrium and electron contamination in measurements of head-scatter factors using miniphantoms and brass caps. Med.Phys. 22: 1167-1170, 1995.

[43] Ling, C.C., Schell, M.C. and Rustgi, S.N. Magnetic analysis of the radiation components of a 10 MV Photon beam. Med. Phys. 9: 20-26, 1982.

[44] Luxton, G. and Astrahan, M.A. Characteristics of the high-energy photon beam of a 25 MV accelerator. Med. Phys. 15: 82-87, 1988.

[45] Luxton, G. and Astrahan, M.A. Output factor constituents of a high-energy photon beam. Med. Phys. 15: 88-91, 1988.

[46] Meli, J.A. Output factors and dose calculations for blocked x-ray fields. Med. Phys. 13: 405-408, 1986.

[47] Mijnheer, B.J., Aalbers, A.H.L., Visser, A.G. and Wittkämper, F.W. Consistency and simplicity in the determination of absorbed dose to water in high-energy photon beams: A new code of practice. Radiother. Oncol. 7: 371-384, 1986.

[48] Mijnheer, B.J., Battermann, J.J. and Wambersie, A. What degree of accuracy is required and can be achieved in photon and neutron therapy? Radiother. Oncol. 8: 237-252, 1987.

[49] Mijnheer, B.J., Wittkämper, F.W., Aalbers, A.H. and van Dijk, E. Experimental verification of the air kerma to absorbed dose conversion factor $C_{w,u}$. Radiother. Oncol. 8: 49-56, 1987.

[50] Patomäki, L.K. The equivalent field principle and its use in beam therapy dose calculations. Brit. J. Radiol. 41: 381-383, 1968.

[51] Patterson, M.S. and Shragge, P.C. Characteristics of an 18 MV photon beam from a Therac-20 medical linear accelerator. Med. Phys. 10: 312-318, 1981.

[52] Podgorsak, M.B., Kubsad, S.S. and Paliwal, B.R. Dosimetry of large wedged high-energy photon beams. Med. Phys. 20: 369-373, 1993.

[53] Rice, R.K., Hansen, J.L., Svensson, G.K. and Siddon, R.L. Measurements of dose distributions in small beams of 6 MV X-rays. Phys. Med. Biol. 32: 1087-1099, 1987.

[54] Spicka, J., Herron, D. and Orton, C. Separating output factor in collimator and phantom scatter factor for megavoltage photon calculations. Med. Dos. 13: 23-24, 1988.

[55] Sterling, T.D., Perry, H. and Katz, L. Automation of radiation treatment planning. Brit. J. Radiol. 37: 544-550, 1964.

[56] Storchi, P. and van Gasteren, J.J.M. A table of phantom scatter factors of photon beams as a function of the quality index and field size. Phys. Med. Biol. 41: 563-571, 1996.

[57] Szymczyk, W., Goraczko, A. and Lesiak, J. Prediction of Saturne II+ 10 MV and 23 MV photon beam output factors. Int. J. Radiat. Oncol. Biol. Phys. 21: 789-793, 1991.

[58] Tatcher, M. and Bjärngard, B.E. Head-scatter factors in rectangular photon fields. Med. Phys. 20: 205-206, 1993.

[59] Tatcher, M. and Bjärngard, B.E. Equivalent squares of irregular photon fields. Med Phys. 20: 1229-1232, 1993.

[60] Tatcher, M. and Bjärngard, B.E. Head-scatter factors in blocked photon fields. Radiother. Oncol. 33: 64-67, 1994.

[61] Thomas, S.J. The variation of wedge factors with field size on a linear accelerator. Brit. J. Radiol. 63: 355-356, 1990.

[62] Vadash, P. and Bjärngard, B.E. An equivalent-square formula for head-scatter factors. Med Phys. 20: 733-734, 1993.

[63] van Dam, J., Bridier, A., Lasselin, C., Blanckaert, N. and Dutreix, A. Influence of shielding blocks on the output of photon beams as a function of energy and type of treatment unit. Radiother. Oncol. 24:55-59, 1992.

[64] van Gasteren, J.J.M., Heukelom, S., van Kleffens, H.J., van der Laarse, R., Venselaar, J.L.M. and Westermann, C.F. The determination of phantom and collimator scatter components of the output of megavoltage photon beams: measurement of the collimator scatter part with a beam-coaxial narrow cylindrical phantom. Radiother. Oncol. 20: 250-257, 1991.

[65] van Gasteren, J.J.M., Heukelom, S., van Kleffens, H.J., van der Laarse, R., van der Linden, P.M., Venselaar, J.L.M. and Westermann, C.F. The phantom scatter correction factor Sp of the photon beam output factor Scp as a function of the beam energy in the range from 2 to 25 MV. Proc. XIth ICCR (Intern. Conf. on the Use of Computers in Radiation Therapy), 1994, Manchester, U.K. 284-285.

[66] van Gasteren, J.J.M., Heukelom, S., Jager, H.N., van Kleffens, H.J., van der Laarse, R., Venselaar, J.L.M. and Westermann, C.F. A 3-gaussian fit of phantom scatter correction data. Accepted Phys. Med. Biol., 1997.

[67] van Gasteren, J.J.M., Heukelom, S., Jager, H.N., van Kleffens, H.J., van der Laarse, R., Venselaar, J.L.M. and Westermann, C.F. On the parameterization of headscatter correction factors S_c of rectangular fields of photon beams. I. Symmetrical and asymmetrical open beams. Submitted in revised form to Phys. Med. Biol., 1998.

[68] van Gasteren, J.J.M., Heukelom, S., Jager, H.N., van Kleffens, H.J., van der Laarse, R., Venselaar, J.L.M. and Westermann, C.F. On the parameterization of headscatter correction factors S_c of rectangular fields of photon beams. II. (a)symmetrical wedged beams. Submitted in revised form to Phys. Med. Biol., 1998.

[69] van Kleffens, H.J., van Gasteren, J.J.M., Heukelom, S., Jager, H.N., van der Laarse, R., Mijnheer, B.J., Venselaar, J.L.M. and Westermann, C.F. Dependence of the tray transmission factor on the collimator setting in high-energy photon beams. Proc. XII ICCR (Intern. Conf. on the Use of Computers in Radiation Therapy), Salt Lake City, USA, 1997 (Abstract).

[70] Venselaar, J.L.M., Heukelom S., Jager H.N., Mijnheer B.J., van Gasteren, J.J.M., van Kleffens H.J., van der Laarse R. and Westermann C.F. Is there a need for a revised table of equivalent square fields for the determination of phantom scatter correction factors? Phys. Med. Biol. 42: 2369-2381, 1997.

[71] Venselaar, J.L.M., van Gasteren, J.J.M., Heukelom S., Jager H.N., Mijnheer B.J., van der Laarse R., van Kleffens, H.J. and Westermann C.F. A consistent formalism for the application of phantom and collimator scatter factors. Phys. Med. Biol. Submitted for publication, 1998.

[72] Venselaar, J.L.M., Heukelom S., Jager H.N., Mijnheer B.J., van der Laarse R., van Gasteren, J.J.M., van Kleffens, H.J. and Westermann C.F. The relation between scatter correction factors defined at dose maximum and at a reference depth of 10 cm. Phys. Med. Biol. Submitted for publication, 1998.

[73] Weber, L., Nilsson, P. and Ahnesjö, A. Build-up cap materials for measurement of photon head-scatter factors. Phys. Med. Biol. 42: 1875-1886, 1997.

[74] Yu, M.K. and Sloboda, R. Analytical representation of head scatter factors for shaped photon beams using a two-component x-ray source model. Med. Phys. 22: 2045-2055, 1995.

[75] Zhu, T.C. and Bjärngard, B.E. Scattered photons from wedges in high-energy x-ray beams. Med. Phys. 22: 1339-1342, 1995.

Publications of the Netherlands Commission on Radiation Dosimetry

Radiation dosimetry activities in the Netherlands. Inventory compiled under the auspices of the Netherlands Commission for Radiation Dosimetry. NCS Report 1, July 1986.	n.a.
Code of practice for the dosimetry of high-energy photon beams. NCS Report 2, December 1986.	f20,-
Proceedings of the Symposium on Thermoluminescence Dosimetry. NCS Report 3, October 1988.	f20,-
Aanbevelingen voor dosimetrie en kwaliteitscontrole van radioactieve bronnen bij brachytherapie NCS Report 4, Februari 1989 (in Dutch).	f20,-
Recommendations for dosimetry and quality control of radioactive sources used in brachytherapy. Synopsis (in English) of NCS Report 4, February 1991.	f20,-
Code of practice for the dosimetry of high-energy electron beams. NCS Report 5, December 1989.	f20,-
Dosimetric aspects of Mammography. NCS Report 6, March 1993.	f25,-
Recommendations for the calibration of Iridium-192 high dose rate sources. NCS Report 7, December 1994.	f25,-
Kwaliteitscontrole van Medische Lineaire Versnellers, methoden voor kwaliteitscontrole, wenselijke toleranties en frequenties. NCS Report 8, December 1995 (in Dutch).	f25,-
Quality Control of Medical Linear Accelerators, current practice and minimum requirements. NCS Report 9, August 1996.	f25,-
Dosimetry of low and medium energy x-rays, a code of practice for use in radiotherapy and radiobiology. NCS Report 10, July 1997.	f25,-
Quality Control of Simulators and CT scanners and some basic QC methods for Treatment Planning Systems, current practice and minimum requirements. NCS Report 11, September 1997.	f25,-
Determination and use of scatter correction factors of megavoltage photon beams, measurement and use of collimator and phantom scatter correction factors of arbitrarily shaped fields with a symmetrical collimator setting. NCS Report 12, March 1998.	f30,-

From within The Netherlands, reports can be ordered by paying the amount into ABN-AMRO account nr. 51.70.64.332 to the credit of "Nederlandse Commissie voor Stralingsdosimetrie", stating the report number(s). Please add f5,- for postage and packing.

From outside The Netherlands, please complete the order form below.

ORDER FORM

Please send this completed order form to:
NCS secretary, P.O.Box 654, 2600 AR DELFT, The Netherlands

QTY	REPORT NUMBER AND TITLE	COST
.....	.....	.....
.....	.....	.....
.....	.....	.....
.....	.....	.....

Subtotal .....

Add postage and packing (Europe ƒ10,-, outside Europe ƒ20,-) .....

Total .....

Payment by:
- ☐ Cheque/postal order* made payable to Netherlands Commission on Radiation Dosimetry (add ƒ15,- for banking costs)
- ☐ Please charge my Eurocard/Mastercard
  Credit card No.
  Expiry date .....

Name:
.....

Address:
.....
.....

Date: .....

Signature:
.....

* please delete as applicable

NCS report 12